
Theses

Dissertations and Theses

9-2018

The Design, Test and Evaluation of a Sensing System for Process Analytical Technology (PAT)

Trevor Murphy

Department of Engineering, Institute of Technology, Tralee, Kerry, Ireland

Follow this and additional works at: <https://sword.cit.ie/allthe>



Part of the [Materials Science and Engineering Commons](#), and the [Operations and Supply Chain Management Commons](#)

Recommended Citation

Murphy, Trevor, "The Design, Test and Evaluation of a Sensing System for Process Analytical Technology (PAT)" (2018). *Theses* [online].

Available at: <https://sword.cit.ie/allthe/811>

This Master Thesis is brought to you for free and open access by the Dissertations and Theses at SWORD - South West Open Research Deposit. It has been accepted for inclusion in Theses by an authorized administrator of SWORD - South West Open Research Deposit. For more information, please contact sword@cit.ie.

The Design, Test and Evaluation of a Sensing System for Process Analytical Technology (PAT)

A Thesis Submitted for Fulfilment of Degree of

“Master of Engineering by Research.”

September 2018

By

Trevor Murphy B.Sc (Hons), B.Eng

Supervisors:

Dr Joseph Walsh (I.T Tralee)

Dr Daniel Riordan (I.T Tralee)



Institiúid Teicneolaíochta, TráLí

Institute of Technology Tralee

School of Science, Technology, Engineering and Mathematics (STEM)

“Submitted to Quality and Qualifications Ireland, September 2018.”

Abstract

Increased globalisation and competitiveness has given rise to a more dynamic and diverse global market that has begun to place incredible strain on manufacturing supply chains. Conventional manufacturing methods such as the batch manufacturing methods employed largely by the materials processing industries i.e. pharmaceuticals, polymers and magnesium processing plants are ill-suited to cope with the demands of today. As products evolve with technological advancements they become more complex to produce and require alternative approaches to manufacturing to ensure product quality while reducing costs and increasing manufacturing efficiencies.

A potential solution to the growing demands on today's supply chain is process analytical technology (PAT). PAT is a system to continuously monitor and control process parameters that affect the quality of a product through multivariate analytics of in-process data in real-time. This allows for the real-time adjustments of process parameters to maintain a predetermined level of quality while significantly increasing quality, reducing costs and downtime. PAT utilises the latest in sensory technologies to monitor in process material through continuous sampling, reducing the need for manual sampling and analytics. The data acquired from integrated sensors is analysed in real time using multivariate analytics that generate a corrective response to plant equipment.

This research provides an in-depth study of the key drivers of process analytical technology in the manufacturing industry and the design and development of a Modular Prototype Sensing Unit (MPSU) with integrated process analysers and smart sensors. Development of the MPSU and selection of suitable sensors and process analysers was undertaken as part of a Horizon 2020 Spire initiative project titled "ProPAT" and was aimed at developing a modular PAT system for the materials processing industry. This research focused on the development of PAT systems for end users, namely GlaxoSmithKline and MBM Nanotmaterialia, and included an assessment of end user current states and project requirements prior to sensor selection and development of the MPSU.

Rapid Prototyping techniques were employed to develop suitable prototype components for the MPSU systems prior to assembly of the unit. The MPSU accommodated the integration of smart sensors and process analysers that monitored a blend of material conveyed through the unit. The data acquired from the integrated hardware was then analysed using a multivariate analysis software package where a statistical model was generated using partial least squares regression techniques, thus providing the required response to potentially control plant equipment. This thesis presents the results and analysis of the MPSU under a variety of test conditions

Declaration

I declare that this thesis, submitted in fulfilment of the requirements for the award of Master of Engineering by Research in the Institute of Technology, Tralee, encompasses primary research carried out by me and that all secondary research is appropriately referenced, as per Institute regulations, and acknowledged.

.....

Mr. Trevor Murphy

Acknowledgements

I would like to express my gratitude to all the staff at the Institute of Tralee for the opportunity to complete this Masters through research and thesis and for their continued support throughout my academic career. I would like to thank everyone involved in the H2020 ProPat project for the chance to work so closely such prestigious academic and industrial world leaders on such an innovative and important collaborative project. I would also like to thank my principle supervisor Dr Joseph Walsh and my Co-supervisor Dr Daniel Riordan for the guidance they have provided me throughout the course of this research and the ProPAT project. I am immensely proud and honoured to have worked with them on this project. I would also like to thank my Colleague Niall O'Mahony for his contributions to this thesis and the ProPat project, it was a pleasure to have worked with him.

I would also like to express my immense gratitude to my parents for their unconditional support throughout my life and their belief in my abilities academically, professionally and personally. I would also like to thank my sisters for believing in me throughout my entire life and driving me to continuously improve myself in every aspect of life.

Lastly, I would like to reserve my sincerest appreciation and thanks to my Partner of 14 years and mother of my 3 beautiful children, without whom this thesis would not be possible. I thank you from the bottom of my heart for having the patience with me on my return to education.

Dedication

This thesis is dedicated to my partner Laura O'Sullivan and my three children Darragh, Keelin and Ryan O'Sullivan who provided me with the motivation and drive to continually better myself. Without their support this thesis and many other of my achievements would not be possible.

Table of Contents

Abstract.....	i
Declaration.....	ii
Acknowledgements.....	iii
Dedication.....	iv
Table of Contents.....	v
List of Figures.....	ix
List of Tables.....	xii
List of Equations.....	xiii
Definitions.....	xiv
Chapter One – Introduction.....	1
1.1 Project Motivation.....	2
1.2 Purpose of Research.....	2
1.2.1 ProPAT Aims & Objectives.....	3
1.3 Thesis Aims & Objectives.....	3
1.3.1 Investigate Key Aspects of PAT & Conventional Process Monitoring Techniques.....	4
1.3.2 Assessment & Selection of Sensory Options Available for PAT Systems.....	4
1.3.3 Development of a Modular Prototype Sensing Unit (MPSU) for a PAT system.....	4
1.3.4 Assessment of NIR Technology for the Measurement of Chemical Composition of a Bulk Solid.....	4
1.4 Thesis Layout.....	5
Chapter Two - Review of Process Analytical Technology (PAT), Quality by Design (QBD) and Conventional Material Sampling Techniques.....	7
2.1 Introduction.....	8
2.2 Introduction to Process Analytical Technology (PAT).....	8
2.3 Quality by Design (QBD) Framework.....	10
2.4 Process Monitoring.....	12
2.4.1 Off-line Process Monitoring.....	13
2.4.2 On/In/At-line Process Monitoring.....	14
2.5 Sampling Techniques.....	15
2.5.1 Scooping.....	17
2.5.2 Thieving.....	18
2.5.3 Cone and Quartering.....	19
2.5.4 Automatic Samplers.....	20
2.6. Segregation.....	20

2.6.1 Sifting	21
2.7 Conclusion.....	24
Chapter Three – Review of Smart Sensors, Process Analysers and the Application of Chemometrics	26
3.1 Introduction	27
3.2 Fiber Optic Sensors	27
3.3 Smart Sensors	30
3.4 Colour Sensors	31
3.5 Mass Flow Sensors/Meters.....	34
3.6 IR Temperature Sensor	39
3.7 Spectroscopic Sensors.....	41
3.8 Chemometrics	46
3.9 Data Fusion	47
3.10 Conclusion.....	48
Chapter Four – Active ProPAT Case Study Review of PAT Implementation	49
4.1 Introduction	50
4.2 GlaxoSmithKline (GSK) Continuous Tableting Line (CTL)	50
4.2.1 CTL Process Overview	55
4.3 MBN Nanomaterialia & PAT.....	57
4.3.1 Tungsten Carbide Cobalt (WCCo) Milling Process (MBN).....	57
4.4 Improvements Through PAT Implementation	60
4.4.1 GSK Process.....	60
4.4.2 MBN Nanomaterialia Process	62
4.4.3 Summary of Both GSK and MBN Process.....	64
4.5 Conclusion.....	65
Chapter Five – ProPAT Sensor Suite Calibration	66
5.1 Introduction	67
5.2 Selection and Calibration of Sensor Types for Sensing Unit	67
5.2.1 Microwave Mass Flow Sensor.....	73
5.2.2 NIR Spectrometer.....	79
5.2.3 IR Temperature Sensor	86
5.3 Sensing Unit Mechanical Interface	90
5.3.1 Modular Prototype Sensing Unit (MPSU) Design	91
5.4 Conclusion.....	105
Chapter Six – ProPAT Sensing Unit Testing & Results.....	106
6.1 Introduction	107
6.2 NIR Analysis of Powder Blends using Collimating Lenses	107

6.2.1 Introduction	107
6.2.2 Aim	107
6.2.3 Equipment & Materials Used	108
6.2.4 Methodology.....	108
6.2.5 Results and Conclusions.....	111
6.3 Temperature Measurement Using The Modular Prototype Sensing Unit (MPSU)	114
6.3.1 Introduction	114
6.3.2 Aim	114
6.3.3 Equipment & Materials Used	114
6.3.4 Methodology.....	114
6.3.5 Results and Conclusions.....	115
6.4 MPSU & Sensor Suite Measurement of Chemical Composition	117
6.4.1 Introduction	117
6.4.2 Aim	117
6.4.3 Equipment & Materials Used	117
6.4.4 Methodology.....	118
6.4.5 Results and Conclusions.....	119
6.5 Real-Time Process Control	120
6.6.1 Introduction	120
6.5.2 Aim	121
6.5.3 Equipment & Materials Used	121
6.5.4 Methodology.....	121
6.5.5 Results and Conclusions.....	122
6.6 Conclusions	123
Chapter 7 – Conclusion of Research & Future Work	125
7.1 Introduction	126
7.1 Research, Methodology & Implementation Summary	126
7.2 Major Contributions.....	127
7.2.1 Comparison of Conventional Material Processing vs PAT systems	127
7.2.2 Assessment & Selection of Measurement Solutions & Design of MPSU for ProPAT	128
7.2.3 Near Infrared Spectroscopy for Real-Time Measurement of Chemical Composition	128
7.2.4 Summary	129
7.2.5 Publications.....	129
7.3 Discussion.....	130
7.4 Future Work	131
7.4.1. Regulatory Barriers	131

7.4.2 Lens Fouling	131
7.4.3 Development of Mass Flow Sensor.....	131
7.4.4 Assessment of spectroscopic techniques	131
Appendix	132
A-1 Analysis of the Effects of Granulation on Blend Uniformity and PSD Using NIR.....	133
A-1-1 Introduction.....	133
A-1-2 Aim	133
A-1-3 Equipment & Materials Used	133
A-1-4 Methodology.....	134
A-1-5 Results and Conclusions	135
B-1 Appendix PLSR results from material sampling chamber testing.....	136
B-2 Appendix PLSR results from material sampling chamber testing.....	137
B-3 Appendix PLSR results from material sampling chamber testing.....	138
B-4 Appendix PLSR results from material sampling chamber testing.....	139
B-5 Appendix PLSR results from material sampling chamber testing.....	140
C-1 Appendix NIR reference spectra.....	141
D-1 Appendix raw data from NIR.....	142
D-2 Appendix PLS model	143
References	144

List of Figures

Figure 2.1 Batch Manufacturing Process, Continuous PAT Comparison(GMPUA, 2017)	9
Figure 2.2 Batch Manufacturing Process, Continuous PAT Comparison(Надлежащая производственная практика Process Analytical Technology (PAT), 2017)	12
Figure 2.3 Workflow Diagram of Off-line Sample Analysis (Majors, 2013)	13
Figure 2.4 Agilent Technologies survey on time allocation of typical offline analysis (Majors, 2013) .	14
Figure 2.5 Key Components of Representative Sampling	17
Figure 2.6 Key Components of Representative Sampling (Sampling.UK, 2018)	18
Figure 2.7 Multi-thief sampling rod (Sampling Systems News June 2010 - Multi Volume Powder Sampler, 2010)	18
Figure 2.8 Implementing the Sampling Plan (Chemistry LibreTexts, 2016)	19
Figure 2.9 Automatic auger sampler (Powder sampler / for solids / for granule / automatic - HPR - Sentry Equipment Corp, 2017)	20
Figure 2.10 Particle behaviour during sifting (Johnson, 2016)	22
Figure 2.11 Results of experiments on the effects of particle diameter ratio and mean particle diameter respectively on the segregation of binary mixtures (Purutyan and Carson, 2006)	23
Figure 3.1 Conveyance of optical signal through fiber (Keyence, 2017a)	29
Figure 3.2 Comparison of Extrinsic Fiber Optic Sensor and Intrinsic Fiber Optic Sensor (extrinsic fiber optic sensor Archives - Optical Cables on Fiberstore, 2017)	30
Figure 3.3 CEI 1931 chromaticity diagram with colour space values (Shingala and Natesan, 2017) ...	32
Figure 3.4 Pharmaceutical tableting process and the effect of a deviation in ingredient concentration on the colour of the product (Colour measurement of tablets in pharmaceutical production Micro- Epsilon Measurement, 2017)	33
Figure 3.5 In-line photometer for the measurement of colour of in-process material (Kemtrak DCP007 Photometer (UV-VIS-NIR) - Industrial in-line analyzer for concentration and color control, 2017)	34
Figure 3.6 Hopper fed gravimetric flow meter (Solids Flow Meters, Feeders and Fillers - El Mass Flow Meters, 2017)	35
Figure 3.7 Volumetric feeding system using rotating auger system (Thayer Powder Feeder™ Model PF-S-4 – Thayer Scale, 2017)	36
Figure 3.8 MIC Flow Meter (Type ‘MIC- Flow Meter’ for Solids MIC-Flowmeter Solid Flow Measurement Products Hense Wägetechnik GmbH, n.d.)	38
Figure 3.9 Integration of a microwave mass flow sensor in a stainless steel pipe(Flow, n.d.)	39
Figure 3.10 Typical components of a NIR spectrometer (Liu et al., 2017)	42
Figure 3.11 Suitability of sample types to NIR and/or Raman applications. Sample types closer to the left are better suited to NIR, while samples closer to the right are more suitable to Raman spectroscopy (Strother and Scientific, 2009)	45
Figure 4.1 Process flow diagram – GSK (Opitz, 2014a)	51
Figure 4.2 Schematic of a gravimetric feeding system (How to Troubleshoot Your Feeder to Achieve Optimal Performance : Plastics Technology, 2017).	51
Figure 4.3 The granulation process and the formulation of a multi-particle granulated mixture through agglomeration (Granulation & Particle-Bonding Mechanism Process Production, 2017).	52
Figure 4.4 Comil inlet with milling apparatus (Quadro, 2017)	53
Figure 4.5 Blending chamber with helix agitator (Ribbon Blender and vertical single-shaft mixer - amixon GmbH, 2017)	54

Figure 4.6 Depicts a rotary tableting machine similar to that of GSKs, that compresses a blended powder mixture into solid dose oral tablets (The Theory and Practice of Pharmaceutical Technology Digital Textbook Library, 2017).....	55
Figure 4.7 Block Diagram of GSK Tableting Process and Pipe System (Opitz, 2016)(Opitz, 2014a).	56
Figure 4.8 MBN Process Flow of WCCo Milling Process	58
Figure 4.9 Agitated steel bearings impacting on material for particle size reduction through pulverisation (Opitz, 2014b)	58
Figure 4.10 MBN Particle Size Distribution Off-Line Analysis of WCCo Powder (Opitz, 2014a).....	60
Figure 4.11 ProPat schematic of upgraded CTL with integrated ProPat system (Digby, 2014).....	61
Figure 4.12 Malvern Mastersizer 2000 for off-line particle size analysis (Malvern Mastersizer 2000 particle size analyzer, 2017).....	63
Figure 4.13 MBN WCCo Process with Integrated PAT system (Opitz, 2014a)	63
Figure 5.1 IMKO Sono-Vario Radiowave Moisture Sensor (Tecdass, 2018).....	72
Figure 5. 2 Microwave mass flow sensor (Hense, 2018c).....	74
Figure 5.3 Microwave mass flow sensor calibrated for course and fine sand in vertical and freefall conditions (mass flow rate g/min vs sensor readout(mV)).....	76
Figure 5.4 Linear relationship between supply voltage and peak amplitude voltage.....	79
Figure 5.5 Ocean Optics NIRQuest Spectrometer (Spectrometers, Optics, Nirquest and Bus, n.d.)....	79
Figure 5.6 Raw NIR spectra from initial testing (Absorbance (AU) on Y axis, Wavelength (nm) on X axis)	81
Figure 5.7 Pre-Processed Spectra of Coffee and Sugar NIR Data (Absorbance (Y) vs Wavelength (X).82	82
Figure 5.8 Graphical representation of Explained Variance	83
Figure 5.9 Scores – Hotelling T2 Plot	84
Figure 5.10 X-Y Loadings Plot.....	84
Figure 5.11 Predicted vs. Reference Plot.....	85
Figure 5.12 Micro-Epsilom (Micro-Epsilon, 2016)	88
Figure 5.13 Granulated blend of 50% Coffee, 50% Sugar in baking tray after removal from oven	89
Figure 5.14 Analysis of Particle Attrition During Repetitive Cycling of Dextrose in a Pneumatically Conveyed System (Arakaki and Tel-tek, 2008)	90
Figure 5.15 Schematic of Material Build-Up on Protruding Sensors	91
Figure 5.16 Sensing Unit Mechanical Interface Design.....	92
Figure 5.17 Dimensions for Calculation the Area of Round and Flat Oval Section.....	93
Figure 5.18 schematic of MPSU detailing initial air velocity at inlet	93
Figure 5.19 Equation of Continuity(Continuity Equation Fluid Dynamics & amp; Examples, 2018) .94	94
Figure 5.20 250mm, 50mm Diameter Pipe Section.....	98
Figure 5.21 CFD Simulated Velocity Profile of the Sensing Unit Pipe System	99
Figure 5.22 XY Plot of CFD Velocity Analysis.....	99
Figure 5.23 3D Printed Transition Couplings	100
Figure 5.24 transition Pieces After Polishing process.....	101
Figure 5.25 Sensor Location Points.....	102
Figure 5.26 Modified NPT Coupling	102
Figure 5.27 Welded Transition Couplings	103
Figure 5.28 Sensors Mounted on Sensing Unit.....	103
Figure 5.29 Sensor Locations	104
Figure 5.30 MPSU Test Rig.....	104
Figure 6.1 Experimental Set-Up of Collimating Lenses Mounted on Sensing Unit	108
Figure 6.2 Dark NIR Data Acquisition.....	109
Figure 6.3 Experimental Set-up of NIR Spectrometer, Collimating Lenses and Sensing Unit	110

Figure 6.4 Air Supply Hose Inserted Into & Beyond the Bend	111
Figure 6.5 Multi-Variate Data Analysis Results of NIR Spectrometer with Collimating Lenses Mounted on the Sensing unit	112
Figure 6.6 Effects of Lens Fouling on the intensity of the NIR data.....	113
Figure 6.7 Access point for lens purging during testing.....	113
Figure 6.8 Granulated Material heated to 70°C.....	115
Figure 6.9 PLS Results from Temperature Measurement of Dynamic Powder Blend	115
Figure 6.10 PLS Model Overview of IR Temperature Sensor Test	116
Figure 6.11 MPSU with Integrated Sensors and Feeding System	118
Figure 6.12 Raw Data from Test 1.....	119
Figure 6.13 Raw Data from Test 6.....	119
Figure 6.14 Results from PLS Model of MPSU and Sensor Suite	120
Figure 6.15 Auger Feeder Response Signals	122
Figure 6.16 PID Control of Chemical Composition in Real time.....	123
Figure A-1.1 Experimental Set-Up of Collimating Lenses Mounted on Sensing Unit	133
Figure A-1.2 Experimental Set-Up of Collimating Lenses Mounted on Sensing Unit	134
Figure A-1.3 Hamamatsu Spectrometer (left) & Ocean Optics Light Source (right).....	134
Figure A-1.4 Configuration of NIR/Light Source on Coupling	135
Figure B-1.1 Results from test 1 PLSR of coffee and sugar	136
Figure B-1.2 Results from test 2 PLSR of coffee and sugar	136
Figure B-1.3 Explained variance graph from test 2 PLSR of coffee and sugar	136
Figure B-2.1 Figure B-4 Results from test 3 PLSR of coffee and sugar	137
Figure B-2.2 Figure A-2.2 Explained variance graph from test 3 PLSR of coffee and sugar.....	137
Figure B-3.1 Results from test 4 PLSR of coffee and sugar	138
Figure B-3.2 Explained variance graph from test 4 PLSR of coffee and sugar	138
Figure B-4.1 Figure A-4.1 Results from test 5 PLSR of coffee and sugar	139
Figure B-4.2 Figure A-4.2 Results from test 6 PLSR of coffee and sugar.....	139
Figure B-5.1 Results from test 7 PLSR of coffee and sugar	140
Figure B-5.2 Results from test 8 PLSR of coffee and sugar	140
Figure C-1.1 Reference spectral data from NIR sensor for coffee	141
Figure C-1.2 Reference spectral data from NIR sensor for sugar	141
Figure D.1.1 Raw NIR data from NIR spectrometer	142
Figure D.2.1 Highlights the number of PLS tests conducted during the generation of PLS model	143

List of Tables

Table 3. 1 List of Fiber Optic Measurement Capabilities (Krohn, MacDougall and Mendez, 2014).....	28
Table 3.2 Advantages of Fiber Optic Sensing (Krohn, MacDougall and Mendez, 2014)(Optics, 2013)	28
Table 3.3 Types of Colour Sensor (Jensis, 2013)	33
Table 3.4 Volumetric concentration and velocity measurement techniques for bulk solid mass flow (Zheng and Liu, 2011).....	37
Table 3.5 Categorisation based on Sensor Configuration (Sensor Fusion in Time-Triggered Systems, n.d.)	47
Table 4.1 Sampling points, method and measurements taken from GSK CTL	56
Table 5.2 GSK & MBN CQA's and measurement solutions	68
Table 5.3 Pugh chart with weighted criteria for selection of material flow based sensors	69
Table 5.4 Pugh chart with weighted criteria for selection of process analysers	70
Table 5.5 Pugh chart with weighted criteria for selection of physical measurement based sensors ..	71
Table 5.6 Final selection of sensors for MPSU	72
Table 5.7 Hense Mic-Flow Meter Specifications (Hense, 2014)	75
Table 5.8 Actual mass vs. Recorded Mass using coarse sand.....	77
Table 5.9 Results from WCCo testing.....	78
Table 5.10 Physical properties of test material	80
Table 5.11 Ocean Optics NIR Specifications (NirQuest Near Infrared Spectrometers Spectrecology - Spectroscopy & Optical Sensing Solutions, 2018)	80
Table 5.12 IR Temperature Sensor Specifications (Micro-Epsilon, 2016).....	87
Table 5.13 Table 5.12 IR Temperature Sensor Calibration Results.....	89
Table 5.14 Sensor Mechanical Interface Requirements.....	101
Table 6.1 Blend Ratios of Test Material Through the Sensing Unit	109
Table 6.2 Temperature Change During Testing	116
Table 6.3 Test Material Blend Ratios	118

List of Equations

1. Multiplicative Scatter Correction	83
2. Bernoulli Equation	96
3. Equation of Continuity	96
4. Darcy-Weisbach Formula	97
5. Colebrook Equation	97

Definitions

Process Analytical Technology (PAT) defined by the United States Food and Drug Administration (FDA) as a mechanism to analyze, monitor and control the critical process parameters (CPP) that affect the critical to quality attributes (CQA) of a product (Willis, 2004).

Food and Drug Administration (FDA) is a federal agency of the United States department of health and human services and is responsible for the regulation and control of food, tobacco and pharmaceutical products (Broadcast, 2006)

Critical Quality Attributes (CQA) are the chemical, physical, biological and microbiological attributes that can be defined, measured, and continually monitored to maintain predetermined levels of quality (Maguire and Peng, 2015).

Critical process parameters (CPP) are the manufacturing parameters such as temperature, feed rate, machine speed or any other variable affecting the production process (Demand-Solutions, 2017).

Non-Value Add (NVA) is an activity that generates a zero or negative return on the investment of resources and usually can be eliminated without impairing a process (Lean-Manufacturing-Tools, 2017).

Active Pharmaceutical Ingredient (API) is the ingredient in a pharmaceutical drug that is biologically active (Stone, 2018).

Continuous Tableting Line (CTL) A tableting manufacturing line that produces pharmaceutical oral dose tablets continuously as opposed to the batch manufacturing technique.

Chemometrics is a technique employed in extracting, analyzing and interpreting chemical information of a material.

Chapter One – Introduction

1.1 Project Motivation

Increasing demands in the materials processing industry, in conjunction with new developments in sensor technology and computational power, have provided a platform for the emergence of new manufacturing techniques such as Process Analytical Technology (PAT). PAT utilises advancements in areas such as smart sensor technology, process analytics and process understanding to optimise manufacturing processes, particularly in the solid bulk processing industries through analysis of in-process data.

This thesis focuses on the acquisition of in-process data using embedded smart sensors integrated into manufacturing processes and the analysis of in-process data for the purposes of achieving real-time measurement and control of process parameters.

1.2 Purpose of Research

This research was conducted as part of a multinational project titled “ProPAT” and was funded under the Horizon 2020 SPIRE (Sustainable Process Industry through Resource and Energy Efficiency) Initiative. The ProPAT project (ProPAT, 2017) is comprised of 16 academic and industry based partners across 8 European countries (Ireland, Germany, Spain, Finland, Greece, Italy, UK, Switzerland) tasked with developing a modular system for providing closed loop process control and real-time data acquisition of manufacturing processes.

The ProPAT project team consists of the following organisations

1. IMaR (Institute of Technology Tralee research centre)
2. GlaxoSmithKline (GSK)
3. University of Barcelona
4. University of Leeds
5. Innovation I Recerca Industrial I Sostenible (IRIS)
6. Spectral Engines
7. Institute of Photonic Science
8. VTT Research Centre of Finland
9. Grecian Magnesite
10. MBN Nanomaterialia
11. Megara Resins
12. Universitat Rovira I Virgili
13. Zurich University of Applied Sciences
14. Technische Universitaet Dresden
15. VTT Memfab Ltd
16. Dechema E.V.

1.2.1 ProPAT Aims & Objectives

ProPAT aims to develop a suite of low cost sensors and process analysers for the measurement of material characteristics such as chemical composition and particle size as well as utilising smart sensor technology for the measurement of Critical Process Parameters (CPPs) such as temperature, mass flow rate, moisture content, colour and viscosity. Selected sensors and process analysers will be integrated into a versatile global control platform to enable data acquisition, processing and mining of real-time data on in-process material.

The platform aims to provide closed loop, self-learning and predictive capabilities based on in-process data analysed using chemometric multivariate analytics for the purpose of reducing overheads caused by slight deviations from the optimum process.

A series of modular systems will be developed as a pilot system for end user processes in GSK, MBN, Grecian Magnesite and Megara Resins facilities (GSK, 2018; MBN, 2018b; Magnesite, 2018b; Megara, 2018b). The outcome of the pilot systems will contribute towards advancements in the materials processing industries in terms of efficiencies, process understanding and sustainable manufacturing technologies.

As a member of the ProPAT project team, the role of this author within the project, is to identify, source and validate, suitable low cost sensors capable of accurately measuring process parameters dictated by ProPAT end user manufacturing processes. Selected sensors must be capable of providing real-time process information to ProPAT global control platforms for processing and analysis. Technical support on the operation of chosen sensors must also be provided throughout the project duration in conjunction with contribution towards project direction and attendance in teleconference and annual ProPAT team design review meetings.

1.3 Thesis Aims & Objectives

The principle aims of this authors research and thesis is to investigate the benefits of a PAT system over conventional process monitoring techniques relating to the powder processing industries. This research will be based on information obtained through this authors involvement in the ProPAT project i.e. source, selection and validation of smart sensors, as outlined in section 1.2.1.

One of the primary aims of this thesis is to integrate selected sensors into a housing unit with a view to developing a “scaled down” PAT system capable of measuring the physical, chemical and material flow characteristics of a bulk solid mixture.

A Modular Prototype Sensing Unit (MPSU) will be developed to house selected sensors. The MPSU will be designed with the capability to provide accurate, real-time data acquisition of in-process material

and process parameters to allow for a high level of process monitoring and control. The MPSU will be designed with ProPAT end users GlaxoSmithKline (GSK) and MBN Nanomaterialia sensory requirements and process parameters in mind.

A series of experimental tests will be conducted to assess the performance of sensors individually and collectively with a view to generating a predictive model on the process via the real-time data provided. The predictive model will be employed to generate an electrical response to control the process parameters of the MPSU.

1.3.1 Investigate Key Aspects of PAT & Conventional Process Monitoring Techniques

This thesis will outline the key aspects of PAT in conjunction with an assessment of the various process monitoring techniques i.e. On/In/At-line process monitoring, associated with a PAT system. Conventional process monitoring techniques such as Off-line process monitoring and manual material sampling methods are also investigated along with their associated issues such as the segregation effect of a bulk solid.

1.3.2 Assessment & Selection of Sensory Options Available for PAT Systems

Investigations on spectroscopic techniques, non-contact, optical and smart sensors are conducted to aid in the selection of suitable measurement options for integration into the MPSU. Sensors and process analysers are selected based on their suitability to ProPAT end users (GlaxoSmithKline (GSK) and MBN Nanomaterialia) applications. Selected sensors will be sourced, calibrated and tested prior to integration into the MPSU.

1.3.3 Development of a Modular Prototype Sensing Unit (MPSU) for a PAT system

A MPSU will be developed to house selected sensors and provide the ability for seamless integration of PAT hardware into existing plant equipment. This will be achieved through analysing ProPAT end user applications, sensory requirements and material conveyance techniques in order to produce a suitable “scaled down” PAT system for proof of concept. Selected sensors and process analysers will be integrated into the MPSU to undergo a series of production simulations (based on end user process parameters) in order to accurately capture and assess in-process data for the purpose of real time control of production/plant equipment.

1.3.4 Assessment of NIR Technology for the Measurement of Chemical Composition of a Bulk Solid

Advancements in NIR spectroscopic techniques and equipment lend themselves to applications requiring continuous process monitoring and control of a bulk solid. This research focuses on the suitability of in-line NIR spectrometers for the real-time measurement of chemical composition of a

granulated powder blend. Chemometric tools such as multivariate data analysis will be employed to analyse NIR data sets to determine the accuracy of NIR spectrometers in determining the chemical composition of a powder blend of varying ratios.

1.4 Thesis Layout

Chapter 2 describes the emergence of PAT in the pharmaceutical industry and outlines some of its key benefits in comparison with conventional process monitoring techniques. Also discussed in this chapter is the Quality by Design framework and its relationship with PAT systems. Various process monitoring techniques relating to both PAT and conventional batch manufacturing methods are defined and manual material sampling techniques (and associated issues) currently employed within the materials processing industries are discussed.

Chapter 3 examines the various sensory options and process analysers available to PAT systems for the real-time measurement and control of manufacturing processes. Non-contact optical sensors and their benefits over conventional contact sensors are discussed in conjunction with the advantages of smart sensor technology. Process analysers such as NIR and Raman spectroscopy are also discussed in detail in this chapter and their respective applications are outlined in detail and compared to determine their suitability to end user applications.

Chapter 4 investigates the potential benefits of PAT implementation through an active case study assessment of ProPAT end user applications. GlaxoSmithKline (GSK) and MBN processes are evaluated in their current state prior to PAT implementation and in their future state after PAT implementation.

Chapter 5 provides a summary of end user sensor requirements to aid in the selection of suitable sensors and process analysers. Sensors are evaluated and selected based on the predetermined requirements prior to calibration and initial testing. NIR spectral data analysis techniques are outlined during instrument calibration and set-up and includes the generation of predictive modelling based on in-process NIR data. Details of the design of the MPSU are also detailed in this chapter including a series of calculations to determine potential issues surrounding integration of the MPSU into existing conveyance systems.

Chapter 6 details the testing and results of sensors and process analysers both individually and collectively i.e. incorporated into the MPSU. NIR spectrometers are used to determine the chemical composition of a granulated blend through multivariate data analysis and PLS modelling. Smart sensors are tested individually for their respective real-time measurement of mass flow and temperature prior to their inclusion with the NIR spectrometer into the MPSU for further testing of chemical composition. Amalgamated data from all measurement equipment is then used to generate

a Partial Least Squares (PLS) predictive model and determine the accuracy of the MPSU and integrated sensors.

Chapter 7 provides a summary of the body of work contained in this thesis and outlines the major contributions to the field along with recommendations of future work and advancements in the area of PAT. This chapter also lists the publications based on the research carried out during the course of this Masters.

Chapter Two - Review of Process Analytical Technology (PAT), Quality by Design (QBD) and Conventional Material Sampling Techniques

2.1 Introduction

This chapter will give an overview of the mechanisms and principles of Process Analytical Technology (PAT) and gives information on the key benefits of adopting this system over conventional manufacturing techniques. The Quality By Design (QBD) framework is also discussed in detail to provide an overview of the recommended FDA strategy for implementing manufacturing process improvements in a highly regulated industry such as the pharmaceutical industry.

Process monitoring techniques are evaluated and discussed in terms of their suitability to PAT systems and real-time process monitoring and control. Conventional process monitoring techniques can largely consist of manually based sample extraction in conjunction with laboratory-based material analysis to gauge the Critical to Quality Attributes (CQA) of a powder blend. The varying techniques widely practised in the powder processing industries for the manual sampling of powder-based material are reviewed in conjunction with the effects of particle segregation, segregation mechanisms and their potential impact on the quality of the product.

2.2 Introduction to Process Analytical Technology (PAT)

Process Analytical Technology (PAT) was defined in 2004 by the Food and Drug Administration (FDA) as a mechanism for designing, analysing and controlling the Critical Process Parameters (CPP) of a manufacturing process that can affect the Critical to Quality Attributes (CQA) of raw or in-process materials and processes (FDA, 2004b). The use of PAT systems for continuous process monitoring and control in the pharmaceutical industry is steadily increasing with a number of prominent pharmaceutical manufacturers investing heavily in continuous manufacturing facilities (Palmer, 2014, 2016). The increasing use of PAT is largely driven by enhancing the quality of pharmaceutical manufacturing through use of increased technological capabilities that provide improvements in process monitoring and control, and the FDA's directives for good manufacturing practices (Particle-Sciences, 2012; FDA, 2004b; a)(Murphy et al., 2016b).

The goal of PAT, is to consistently generate products with a predetermined level of quality (Kinjal G and Ketan V, 2014). PAT enables pharmaceutical manufacturers to transition away from the tedious and empirical methods of batch manufacturing, consisting of time and labour intensive off-line sampling and analysis (Majors, 2013), to a more continuous and dynamic method of manufacturing pharmaceuticals. In a PAT system, process sensors and analysers, integrated into new and existing production equipment, perform continuous timely measurements of critical process parameters (figure 2.1) increasing end product levels (Particle-Sciences, 2012) (Murphy, O' Mahony et al., 2016b).

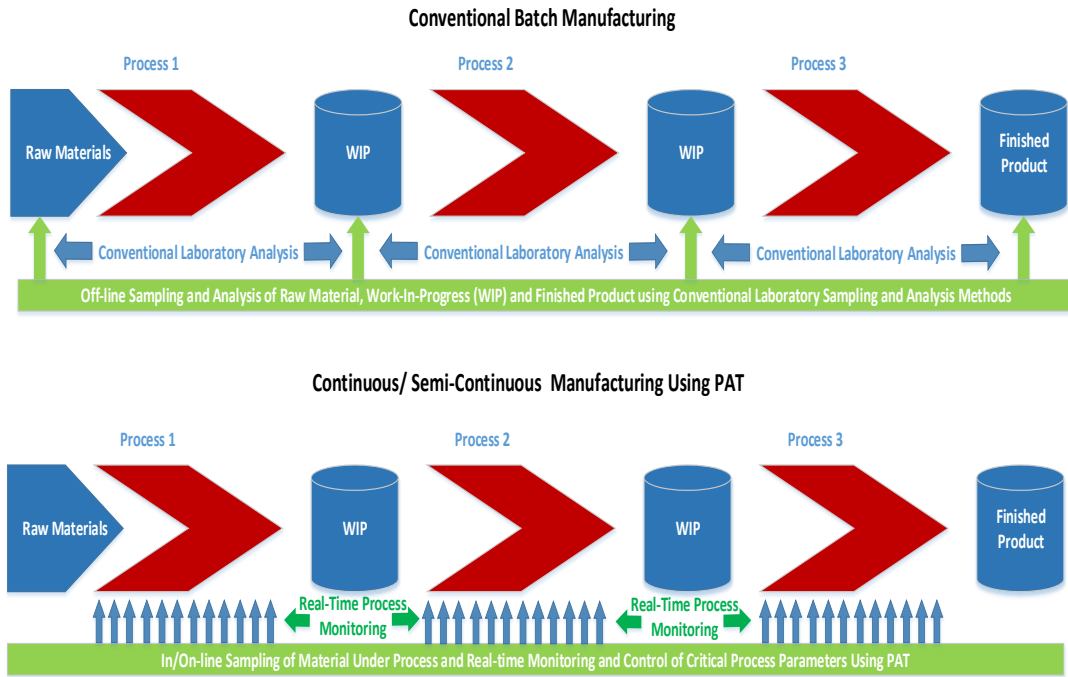


Figure 2.1 Batch Manufacturing Process, Continuous PAT Comparison (GMPUA, 2017)

The key to ensuring product quality is through the identification and management of the many variables that exist within a manufacturing process. In-process variables exist in raw-materials, mechanical performance of processing equipment and process parameters. Scientific understanding of how these variables interrelate, lead to an enhanced level of process monitoring and control (Willis, 2004) (Murphy, O' Mahony et al., 2016b).

PAT develops process understanding through the identification and real-time monitoring and control of each of these variables using specific technological tools such as sensors, analysers, probes and optical equipment located at predetermined critical measurement points that accumulate large data sets. The resulting data is then analysed and evaluated using multivariate analysis tools and converted into an electrical signal used to control or adjust plant equipment to compensate for variability in raw materials and equipment to produce a consistent product. Analysed data can also be utilised in continuous improvement strategies on manufacturing processes through simulations and process modelling that identify key areas within the process that are critical to quality. Identification and control of these key areas allow for the precise adjustment of plant equipment and raw materials. This allows for the optimisation and automation of the entire process stream (Shrestha, Basnett and Raj, 2009) and reducing the dependency on off-line analytics (Murphy et al., 2016b).

2.3 Quality by Design (QBD) Framework

Similarly to PAT, the Quality by Design (QBD) framework promotes a systematic approach to process understanding and development and is used extensively in the pharmaceutical industry as a quality risk management tool (Friend, Arlington, Marshall and Bailey, 2011)

In 2009 the International Conference on Harmonisation (ICH) pharmaceutical development guideline Q8 (R2) defined the QBD framework as a *“systematic approach to development that begins with predefined objectives and emphasises product and process understanding and process control, based on sound science and quality risk management”* (ICH Expert Working Group, 2009). Fundamental to the QBD framework is the understanding of the raw material attributes and process parameters, their effect on the Critical to Quality Attributes (CQA) and the identification and control of sources of variables within the process (Wu, White and Khan, 2011). This enables quality to be built into manufacturing processes rather than testing for quality in finished products, as during development stage, quality issues can be analysed for root cause and corrective procedures can be implemented accordingly to ensure product end quality (Murphy et al., 2016b).

The QBD framework is based on 6 fundamental components that must be considered prior to the implementation of this strategy (DPT, 2013)(Status, Guidelines, Tech- and Space, 2012);

- Defining the product design goal
- Determining the CQA
- Risk assessment
- Developing design space
- Control strategy
- Product life cycle management

Defining the product design goal is the first step in implementing QBD and involves evaluating the requirements for the products design and performance. These requirements are found in the quality target product profile (QTPP) which are a set of target specifications set for each individual product. The QTPP is used to define the product design and can also be used to establish the CQA's of a product and can serve as a guideline throughout the development stage to ensure target specifications are achieved (WestPharma, 2016) (Murphy, O' Mahony et al., 2016b).

Determining the CQA is achieved through evaluation of the QTPP and is vital to ensure QBD as the CQA's are the characteristics that directly affect the quality of the final product. The framework for the products design and process understanding is achieved through the identification of the CQA's.

CQA's can be utilised in the developmental risk assessment stage to evaluate root causes of quality issues (Murphy, O' Mahony et al., 2016b).

Risk assessments must be carried out when implementing QBD to evaluate the risks associated with manufacturing a product. The most influential factors that affect the product quality such as process parameters and CQA's must be scrutinised along with all quality control and process control systems (Status et al., 2012) (Murphy, O' Mahony et al., 2016b).

Developing design space involves the understanding of how the combination and interaction of process variables such as raw material characteristics and process parameters effect the CQA's. Identification of critical process parameters is imperative to ensure process optimisation (DPT, 2013)

Control Strategy is a planned set of goals derived from current product and process understanding, that assures process performance and product quality, allowing for identification of which material attributes and process parameters should be controlled in order to achieve the pre-determined goal of product end quality (Piriou, Elissondo, Hertschuh and Ollivier, 2012) (Murphy, O' Mahony et al., 2016b).

Product life cycle management involves implementing measures to maintain, improve and control product quality through a variety of strong quality control systems that provide feedback on product performance such as;

- Change management and control procedures and systems
- Validation
- Trending and analysis
- Training
- Six Sigma lean manufacturing
- Quality risk management

Product life cycle management is driven largely by data (both qualitative and quantitative), that can be used to highlight potential issues in quality, supply chain, material attributes and process parameters while also providing information and guidance on continuous improvement strategies to enhance product quality and performance (Murphy, O' Mahony et al., 2016b).

Improper product development strategies and manufacturing control systems can have a serious impact on product quality and system efficiencies that ultimately affect the financial success and performance of a product. The QBD framework offers several benefits that not only improve process understanding, quality and control, but also provides a rapid response to manufacturing deviations, improves the developmental stage through reducing time and costs and reduces FDA approval times.

The QBD model is an ideal approach for implementing PAT due to its systematic data driven approach to pharmaceutical development and manufacturing (Murphy et al., 2016b).

2.4 Process Monitoring

This section outlines the various techniques involved in the monitoring of a manufacturing process. There are many techniques available that are suited to a range of applications across all industries to monitor the condition of in-process material. This is achieved through dedicated equipment such as sensors immersed into the process stream or analytical lab-based equipment.

During the manufacturing process of a given product, regardless of industry, it is necessary to implement some form of process monitoring to assess the progress of the product in terms of quality, cost and efficiency as it travels through the value stream. This provides vital information as to the current state of the product and the performance of the manufacturing process. This information can then be utilised to implement a variety of improvements targeting the product directly through improving quality or cost of the product or through implementing process improvements to reduce machine downtime, cycle time or wastes associated with manufacturing the product.

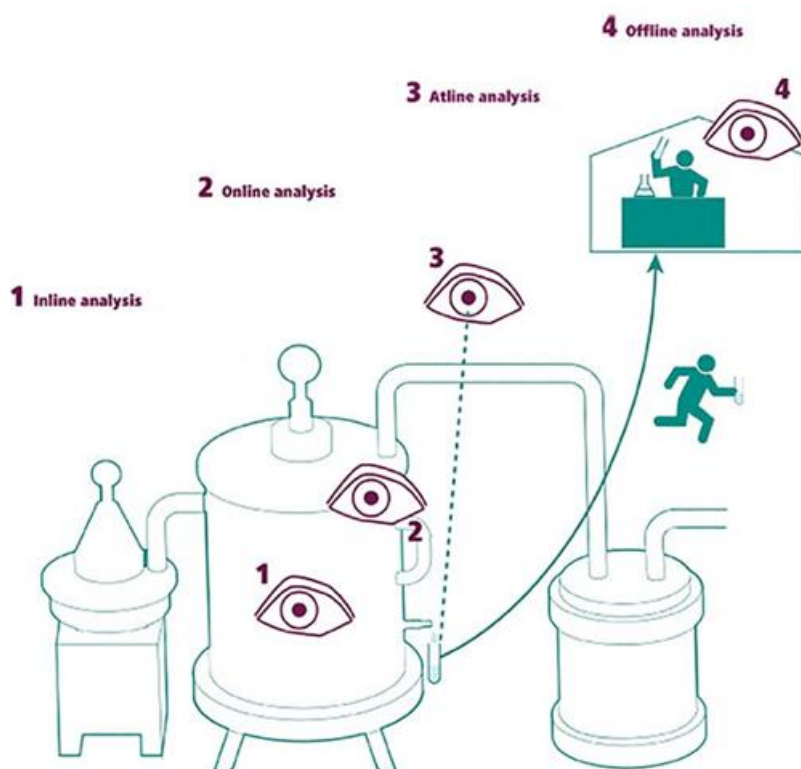


Figure 2.2 Batch Manufacturing Process, Continuous PAT Comparison (Надлежащая производственная практика Process Analytical Technology (PAT), 2017)

There are four main categories of process monitoring as shown in figure 2.2, offline, atline, online and inline. The following defines each category of process monitoring and evaluates their suitability to PAT applications.

2.4.1 Off-line Process Monitoring

Many of the variables within a process can be measured using off-line process monitoring techniques. Off-line process monitoring generally consist of the manual sampling of material from the process for analysis in laboratory conditions using several off-line analytical techniques like high performance liquid chromatography (HPLC) Spectroscopy. Off-line process monitoring has been used extensively in the pharmaceutical industry and involves rigorous quality control (QC) procedures that must be constantly repeated for each individual process such as sample collection, transport, preparation and analysis of samples, prior to documentation and archiving of generated report documents as depicted below in figure 2.3 (Murphy et al., 2016b).

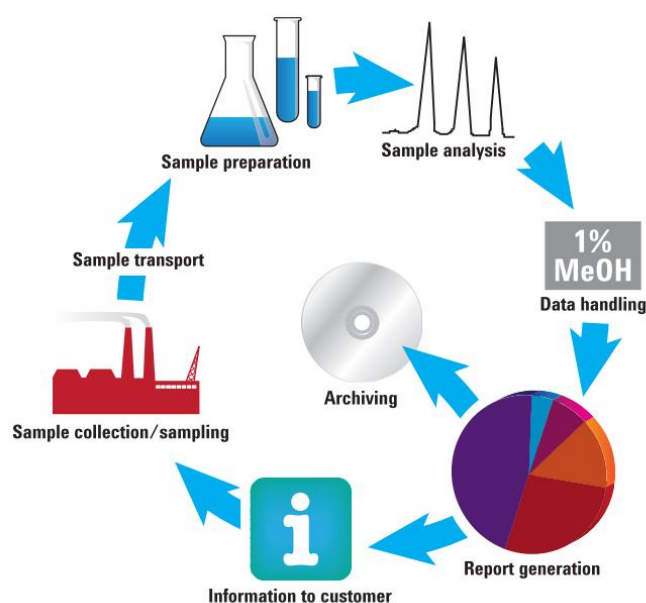
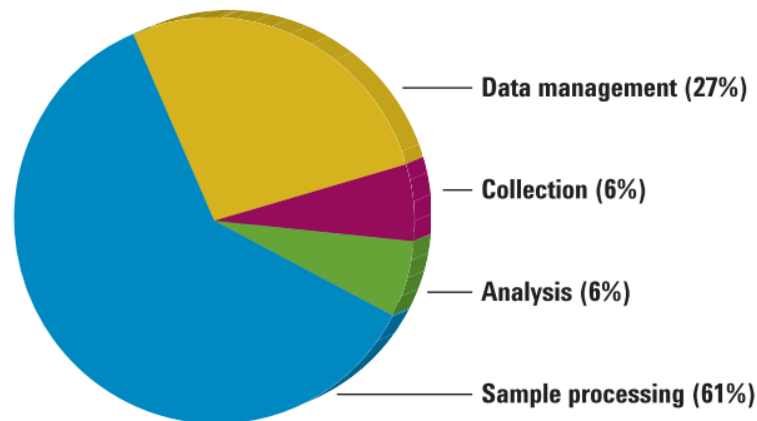


Figure 2.3 Workflow Diagram of Off-line Sample Analysis (Majors, 2013)

Laboratories are a critical component of current drug manufacturing and require complex, dynamic scheduling and skilled personnel to cope with the demands of the supply chain, and they can have a major impact on the overall supply chain service level through their influence on cycle times, delivery times and quality levels (Maslaton, 2012). The time and labour-intensive nature of offline laboratory analysis (however necessary) can also be inefficient and a waste of valuable resources due to lengthy process time frames from sample collection to results of analysis. The process of off-line analysis also contains a large portion of non-value added (NVA) process steps as depicted below (figure 2.4), and according to a 2013 Agilent Technologies survey (Majors, 2013), only 6% of the off-line analysis

process cycle time is spent on analysis with 27% of the time spent on data management and 61% of the time spent on sample processing (Murphy et al., 2016b).



Data taken from Agilent Technologies survey

Figure 2.4 Agilent Technologies survey on time allocation of typical offline analysis (Majors, 2013)

The manual aspect of this method of sampling and analysis can also be prone to a variety of errors, ranging from human error in sample preparation to administrative errors in documentation and reporting that can further effect the supply chains service level (Majors, 2013), (Hayes, 2009). A reduction in the source of these errors can be achieved through the implementation of PAT systems in manufacturing processes resulting in real-time release testing, improved cycle times and product end quality while also reducing labour hours for laboratory analysts through the reduction in the need for manual sampling. NVA laboratory processes such as data management and administrative duties (e.g. documentation and reporting) can also be significantly reduced through on/in/at-line monitoring and control of critical process parameters which can reduce the complexity of lab scheduling and improve lab performance (Murphy et al., 2016b).

2.4.2 On/In/At-line Process Monitoring

A fundamental component to PAT is the generation of product quality information in real time and the use of that information to control the CPP's of a manufacturing process. Methods of obtaining this information generally depend on the process in question and its suitability to various process monitoring solutions such as on/in/at-line process monitoring. Evaluation of the CQA and identification of key measurement points within the process generally dictate the suitability of on/in/at-line process monitoring critical measurement points within the process (Murphy et al., 2016b).

At-Line Process Monitoring

At-line process monitoring consists of installing process specific testing equipment at the production line. The proximity of the test equipment to the process reduces the time lag resulting from the

transport and documentation of samples from the process to the laboratory. This allows for a reduction in the reaction time to perform the necessary counter measures to ensure product end quality. It is generally observed that at-line process monitoring equipment, is significantly more robust and insensitive towards process environments, however in general it is less precise than off-line laboratory test equipment (Tuchin, Chiou and Heinemann, 2012) (Murphy et al., 2016b).

In-Line Process Monitoring

In-line process monitoring requires no sampling and takes timely measurements of material in the process stream through use of a variety of either invasive sensors, such as immersive probes or non-invasive sensors such as optical sensors. Advances in fibre optic sensor technology has improved the performance of optical sensors for industrial operations and is replacing the need for more traditional sensors for process monitoring with the ability to measure almost all physical measurands of interest (Ahuja and Parande, 2012) (Murphy et al., 2016b).

The wide dynamic range of measurands and remote sensing capabilities of fibre optics allow for the removal of expensive sensory equipment from or near hazardous environments generated within manufacturing processes through use of optical fibres embedded at critical process measurement points or through immersive fibre optic probes. This allows for precise measurement solutions in previously unobtainable process locations such as areas of extreme temperatures, pressures or the measurement of corrosive or hazardous materials, resulting in accurate real time data on critical to quality attributes to process analysers (Murphy et al., 2016b).

On-line Process Monitoring

On-line process monitoring involves the redirection of a sample of material through automatic extraction systems, bypass lines or recirculation loops, where the sampled material is conveyed to the sensor locations and either returned to the process stream or safely disposed of. This method is generally used in instances where modification required for the integration of in-line process monitoring is either too costly, impractical or where a higher degree of precision is required, as on-line process monitoring *“offers an opportunity to condition the sample before analysis to achieve higher quality results”* (Tuchin, Chiou and Heinemann, 2012), (Murphy et al., 2016b).

2.5 Sampling Techniques

The sampling of powders is generally undertaken to determine whether a solid bulk mixture has been blended correctly and is in line with specifications. In the pharmaceutical industry, a powder mixture can consist of a mixture of active pharmaceutical ingredients (API's) which is the active drug ingredient and excipients or inactive ingredients such as anti-caking agents, sugar and starch etc.

Together these blended ingredients form a tablet or capsuled solid dose for human consumption so care must be taken during the processing of these products, from raw material input to production operations, to ensure batch to batch homogeneity. Granular mixtures have the potential to un-mix or segregate during processing, however complications can arise as the material is often fed from the side into containers or belt conveyors which can result in both horizontal and vertical segregation. (T. Allen, 2003)

Assessment of the effectiveness of the blending process or the homogeneity of the product throughout the process stream, requires a representative sample of the material to be obtained for analyses either manually or automatically at various and pre-determined locations along the process stream.

The material attributes that are most critical to quality are then analysed off-line or on/in/at-line dependant on the capabilities of the process line. The information gained from the analyses is used to clear the processed material for further processing or return the material to the previous processing stage where the critical process parameters are adjusted in accordance to the information obtained from the results of the analyses, resulting in the achievement of the accepted quality level.

All techniques for determination of parameters such as particle size *“have absolutely no value unless the composition of analysed samples is representative of the bulk from which they were removed”* (Brittain, 2002) and so several factors should be considered when developing a sampling scheme.

These factors (shown in figure 2.5) include:

- Sample Size
- Sample Frequency
- Sampling Location
- Sampling Technique

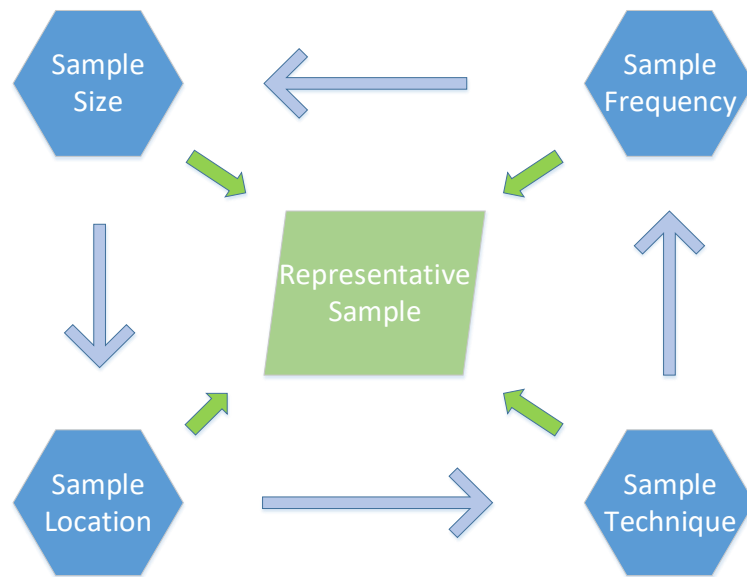


Figure 2.5 Key Components of Representative Sampling

Consideration must also be given to Powder Researcher Terence Allen's "2 Golden Rules of Sampling" (Allen, 2003a)

1. "A Powder should always be sampled when in motion"
2. "The whole of the stream of powder should be taken for many short increments of time in preference to part of the stream being taken for the whole of the time" (Allen, 2003a)

It is not always possible to strictly adhere to these rules as occasionally sampling from static material may be the only option available that is both practical and cost effective, however methods not adhering to both rules would be liable to sampling errors in excess of 6.81% relative standard deviation (Particle Sciences, 2011). In cases where the Active Pharmaceutical Ingredient (API) of a product is toxic at high doses, tighter controls on API uniformity are required to allow for safe consumption of certain products.

Where static sampling must be performed, there are 3 main methods of obtaining a manual sample from a static bulk of material widely practiced in the pharmaceutical industry and are as follows:

- Scooping
- Thieving
- Cone and Quartering

2.5.1 Scooping

Scooping (as shown in figure 2.6) is a widely-used method of sampling powders and consists of an operator manually scooping material from the top layer of a powder or granular material. While this method is by far the easiest and most cost-effective method in obtaining samples, it is also extremely

ineffective for non-homogeneous materials as segregation effects can result in a concentration of coarse particles at the top layer of a bulk solid resulting in a bias towards the larger particles. For this reason, scoop sampling is only suitable for homogenous materials with poor flow characteristics. (Escubed, 2015).



Figure 2.6 Key Components of Representative Sampling (Sampling.UK, 2018)

2.5.2 Thieving

Thief sampling is common practice in industry and is an improvement in comparison to scoop sampling with regards to accuracy or representative sampling. Thief sampling is performed using a metal tool that is plunged into the bulk of material to extract sample material for analysis. The sampling thief consists of a metal rod with one or more cavities that is inserted into a tube with corresponding slots allowing it to freely rotate within the tube (see figure 2.7). Prior to sampling the rod is rotated to ensure the cavities within the rod do not align with the slots of the tube to prevent material entering the cavities during insertion.

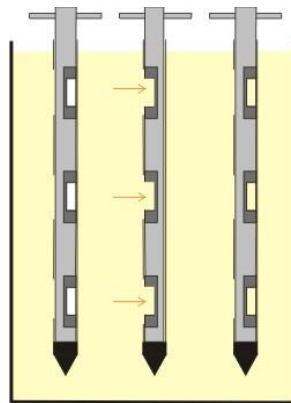


Figure 2.7 Multi-thief sampling rod (Sampling Systems News June 2010 - Multi Volume Powder Sampler, 2010)

The tool is then inserted into the bulk of material to a predetermined depth and the rod is then rotated 360°. This full rotation ensures that when submerged to the correct depth, the cavities of the rod are exposed to the material which flows into the cavity. Once the full rotation is complete, the cavities are then shut, trapping the material inside. The rod is then removed from the material and the samples are then collected for analysis.

Although an improvement on scoop sampling, this method is not without its flaws. The very act of sampling the material introduces a bias in the results particularly in blends of varying particles sizes. Coarse particles will flow more freely than fine particles and the introduction of the tool into material introduces an agitation to the material that causes a higher concentration of coarse particles into the tools cavities (Brittain, 2002).

2.5.3 Cone and Quartering

It has been shown that sampling from static bulk solids is ineffective (Particle Sciences, 2011) and dynamic sampling is a more representative sampling method. Cone and quartering was a technique developed to overcome the static element of manual sampling through introducing conveyance of the material prior to sampling. This is achieved through pouring a portion of the material onto a flat surface where it forms a conical pile. This pile is immediately flattened and divided into quarters. 2 sections are removed and the remaining 2 sections are then gathered and poured onto the flat surface for the process to be repeated until the desired sample size is achieved.

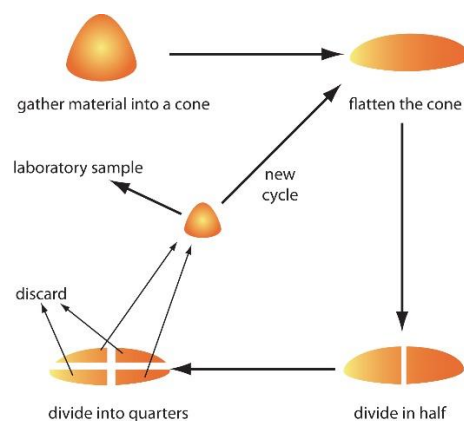


Figure 2.8 Implementing the Sampling Plan (Chemistry LibreTexts, 2016)

Cone and quartering (figure 2.8), as a sampling method can be quite effective (for a static mode of manual sampling) when implemented correctly, however there exists many opportunities for error during the sampling process. When the initial volume of material is poured onto the flat surface, the material undergoes a range of segregation mechanisms that cause the coarse particles to gravitate to the outer perimeter of the cone while the fine particles are located centrally. During the process of flattening the cone, there is potential for large sections of the fine particles to be concentrated in one particular section, essentially skewing the results of any analysis on the material (Brittain, 2002). Furthermore, the results of any analysis of the material is highly influenced by the method of obtaining the original volume of material. This fact in conjunction with the variations introduced through the manual handling of the material can be attributed to the large portion of error and variation in the

results of cone and quartering sampling techniques (typically 6.81% relative standard deviation) (Particle Sciences, 2011) and can be improved upon using automatic samplers.

2.5.4 Automatic Samplers

Automatic samplers (as shown in figure 2.9) are devices or units that are integrated into a process stream for obtaining sample material to be used to analyse material in process. The frequency and volume of the sampling varies from process to process and is dependent on the level of accuracy required and the powder flow characteristics. Automatic sampling units are situated within the process equipment and obtain a fixed volume of material from a point within the powder stream (Sentry, 2017a). This material can then be diverted to at-line process monitoring equipment for analysis or to a container for collection (Prosys.ie, 2017). The material extracted from the process is generally disposed of after analysis and is not fed back into the process stream. Thus, sample volumes and frequencies must be predetermined to prevent excessive waste of material.



Figure 2.9 Automatic auger sampler (Powder sampler / for solids / for granule / automatic - HPR - Sentry Equipment Corp, 2017)

The principle of operation of automatic samplers varies between manufacturers (Prosys.ie, 2017; Sentry, 2017a; b; Sampling-Systems, 2017), however most automatic samplers are pneumatically based units or mechanically based units such as auger samplers. Automatic samplers eliminate the risk of chemical exposure and sample contamination during the sampling process and can be designed to sample the entire stream of powder during transit, thus improving the accuracy of the results of off-line/at-line process monitoring. This method of powder sampling is not suited to PAT systems as automatic samplers are designed to extract samples for analysis or at best divert samples to at-line process analysers intermittently rather than continuously.

2.6. Segregation

This section outlines particle segregation and the various mechanisms of segregation that can severely affect the results of analysed samples extracted from in process material. Segregation is the separation of a mixture or blend of material occurring either during processing, transportation or sampling.

Segregation in bulk solid production refers to the unfavourable effect of “un-mixing” of the material during normal processing and/or storage conditions and represents one of the biggest challenges to overcome in many industries dealing with granular material mixtures. The severity of the effects of segregation on a product can vary within each industry application and as a result the level of control required to correct any occurring segregation varies with it (Purutyan and Carson, 2006).

For any bulk solid production, segregation of a mixture can lead to several undesirable outcomes for both manufacturer and consumer, such as product to product variation, poor sampling of the material or samples not representative of the bulk material. This can lead to high rejection rates of a material if the sample has been collected from segregated mixtures with a higher concentration of a particular particle or particle size in the sample than that of the entire bulk (Johanson, 1988).

The opposite is also true, sampling from a segregated mixture can yield samples within the approved tolerance, however if the mixture is segregated it may not be a true representation of the bulk and could lead to the manufacture and sale of faulty products. Any products released to the consumer found to be faulty, particularly in the pharmaceutical industry, could result in a full product recall costing the manufacturer millions in revenue and pose a serious health and safety risk for the consumer. The following sections will highlight the various mechanisms of segregation that occurs to a granular material during normal processing and/or conveyance conditions.

Segregation occurs through many different mechanisms. The severity of segregation in a bulk solid depends on the physical characteristics of the material in question and handling method used (Purutyan and Carson, 2006). Particle size, shape, density, coefficients of friction and inadequate or incorrect processing methods are all factors in a bulk material mixtures tendency to segregate via segregation mechanisms such as sifting, fluidisation, dusting and angle of repose.

2.6.1 Sifting

Sifting is the most common form of segregation and is the result of the movement of fine particles (known as fines), into the interstitial spaces created from the contact of coarse particles. This type of segregation can occur in storage as well as during processing if the storage container is exposed to excessive levels of vibrational or mechanical energies. The vibrational energies cause movement of the particles within the container creating space between the coarse particles, which is then filled with the fines. This causes the fine particles to eventually locate to the centre of the container pushing the coarse particles outwards as illustrated in figure 2.10. The severity of sifting within a bulk solid is proportional to the amount of fines available in the mixture (Johanson, 1988) i.e. the more fines available, the greater the potential for sifting.

It must be noted that particle size differences are not the sole cause of sifting and must be accompanied by several conditions for sifting to occur.

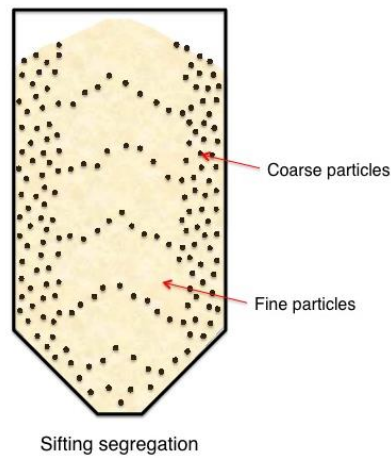


Figure 2.10 Particle behaviour during sifting (Johnson, 2016)

2.6.1.1 Varying Particle Sizes

Particle size differences within a bulk mixture can lead to segregation even in chemically homogenous mixtures. Experiments undertaken on binary mixtures have indicated that segregation through sifting can occur in bulk solids with a particle size ratio of as low as 1.3:1 (Barnam and Prescott, 2011) if the ratio of particle size increases within a bulk solid, so does the tendency for that bulk solid to segregate.

2.6.1.2 Mean Particle Size

The mean particle size of the bulk solid mixture must also be considered when analysing the segregation potential of a material, as experiments on binary mixtures have shown (Purutyan and Carson, 2006) that below 500 microns the tendency of a material to segregate due to sifting, drops substantially (figure 2.11) since cohesion of particles and resistance to flow increase dramatically as particle size decreases. If the material becomes cohesive and does not flow freely, the bulk mixture will not be as easy to segregate through sifting unless the particle size ratio is increased. Sifting can still occur in bulk solids where the mean particle diameter is below 200 microns (Barnam and Prescott, 2011) and when the particle size ratio is as low as 2:1.

Results of sifting segregation experiments

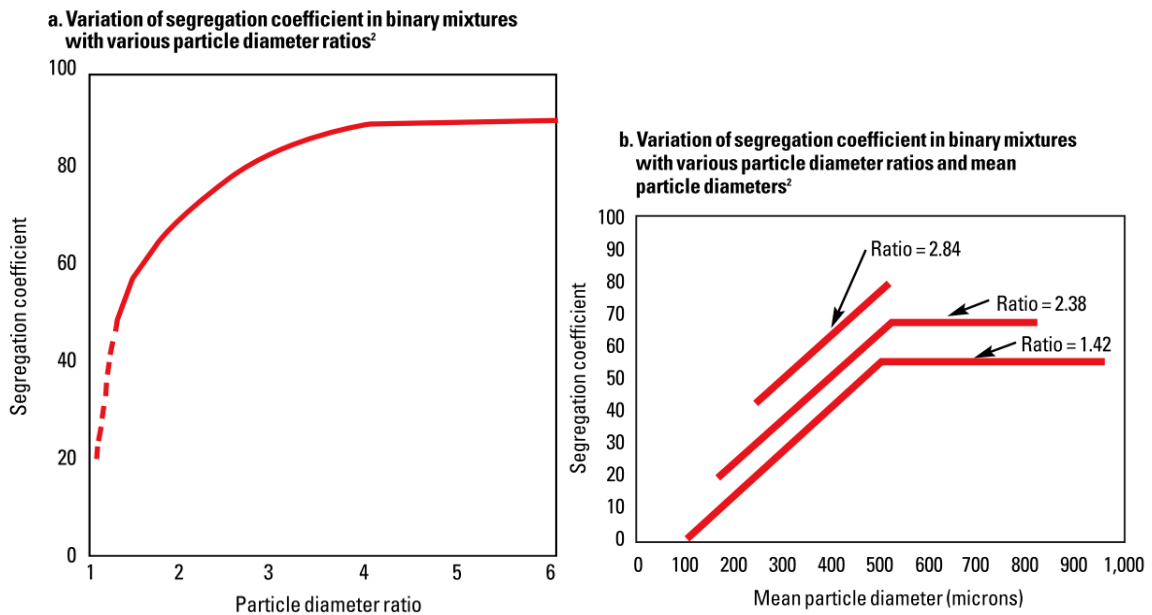


Figure 2.11 Results of experiments on the effects of particle diameter ratio and mean particle diameter respectively on the segregation of binary mixtures (Purutyan and Carson, 2006)

2.6.1.3 Inter-particle motion

For sifting to occur within a bulk solid mixture, the particles within the mixture must not flow at uniform velocities. For mixtures with particles of varying sizes and chemical compositions (non-homogeneous), it is highly unlikely that particles within the mixture will exhibit the same co-efficient of friction, density and flow properties and thus would have an increased potential for segregation. For instance, if the material is under process or in motion, the particles with a higher co-efficient of friction (typically fines) would have an increased resistance to flow and its velocity within the mixture would be restricted. For particles with a lower co-efficient of friction (typically dry coarse particles), the particles would be more free flowing thus the velocities would vary and segregation could occur.

2.6.1.4 Material Flow

For segregation through sifting to occur, the particles of the bulk solid mixture must be able to flow freely within the process or in storage. Moisture content within the mixture can cause agglomeration of the particles which is the increase in particle size due to the bonding of particles and creates a “snowballing” effect within the mixture.

The material properties of the mixture will also dictate its tendency to flow freely or form agglomerates i.e. particle shape, particle size, density and co-efficient of friction of the material. Particles that exhibit high forces of adhesion or cohesion will reduce or eliminate the materials tendency to segregate through sifting.

Decreasing particle sizes inhibits the ability of the material to flow freely as smaller particles are more susceptible to external forces acting on the material which increases its cohesive properties and causes deformation of the particles in contact resulting in the bonding or agglomeration of the material.

For segregation through sifting to occur in a bulk solid, all four of the previously stated conditions must be present within the materials environment (Purutyan and Carson, 2006).

2.7 Conclusion

This chapter outlined the characteristics of PAT and provided an overview of the advantages of continuous manufacturing in relation to process monitoring and material sampling over conventional batch manufacturing techniques. The hesitancy among manufacturers to adopt PAT, regulatory FDA barriers and a lack of incentives, in conjunction with the initial time and financial investments have been off-putting to some manufacturers. Uncertainty over validation and regulations surrounding the PAT issue within the pharmaceutical industry can be overcome through adoption of the QBD framework during PAT implementation. QBD offers a risk management-based approach to process improvements and/or control and can be utilised as a best practice guide for PAT implementation where uncertainty exists.

The benefits associated with this level of process control are many. The elimination or reduction in manual sampling and off-line analytics provides many advantages such as an increase in speed to market of new products, reduced cycle times, improved efficiencies and quality of the product. In-house chemical analysts would no longer be burdened with the rigors of off-line analytics such as sample collection, sample preparation, sample analysis and reporting and could focus more on the development of new products or improving existing products.

Manufacturing process parameters, raw materials, plant equipment and end product quality should be carefully evaluated prior to selecting the most suitable process monitoring techniques to ensure accurate measurements are achieved. At-line process monitoring offers a solution to the time lag created through sample transportation and laboratory queuing however it lacks both the accuracy and real-time process monitoring and control provided through in-line and on-line methods. The manual sampling aspect and inability of at-line process monitoring to capture information at key measurement locations can be a source of the inaccuracies in comparison with other methods while manual sampling of material also contributes to excessive downtime as the results of the process time for analysis.

The effects of segregation discussed in this chapter, have been a continued area of concern for several solid bulk manufacturers producing products to a very specific tolerance. The tendency of a material to segregate under normal processing conditions can severely affect the results of sample analysis and could potentially provide false information regarding the composition of a material through non-representative sampling. This can happen at both ends of the spectrum i.e. sample results can indicate conformance falsely or non-conformance falsely. There are many procedures and processes in place that can reduce the potential for this occurrence, ensuring representative sampling is achieved. However, as segregation has many mechanisms, these procedures involve frequent manual sampling and off-line analysis of in process material. This highlights the advantages of a PAT system over processes dependent on manual sampling and off-line analytics. PAT systems eliminate the need for sampling and laboratory analysis of powders through use of integrated sensors and process analysers. PAT monitors the conditions of the material and provide a real-time data of the material process parameters. This data is then used to correct any deviations from pre-determined quality levels. This is particularly useful for the pharmaceutical industry as it provides a more accurate analysis of a pharmaceutical blend to ensure the correct levels of Active Pharmaceutical Ingredient (API) are present in a particular mixture.

Chapter Three – Review of Smart Sensors, Process Analysers and the Application of Chemometrics

3.1 Introduction

This Chapter is based on previously published work (by this author) on Process Analytical Technology (PAT) systems and its application in the pharmaceutical industry (Murphy et al., 2016b), (O'Mahony et al, 2016). A major driving force behind the emergence of PAT, is the integration of state-of-the-art smart sensors, optical sensors and process analysers to provide reliable in-process data to control-platforms and statistical models. As PAT is a completely data driven system, fundamental to its effectiveness is that data obtained from in-process sensors and analysers is accurate, repeatable and reliable. Careful consideration must be given during the selection of the hardware, such as the sensors which will interface with the processing equipment and material, as the process environmental conditions can in some instances damage sensors due to abrasion of conveyed material, excessive temperatures and corrosive substances.

A vast array of sensors can exist in a single PAT system with each one monitoring the Critical Quality Attributes (CQA) of a Critical Process Parameter (CPP) through streaming large data sets back to control platforms in real-time. The ability to handle large data sets from a multitude of sensors, amalgamate each data set and generate a real-time response to deviations from pre-determined levels of quality, is achieved by utilising data fusion techniques and statistical modelling such as chemometrics.

This chapter presents a review of some of the sensory options available for applications involving the continuous monitoring and control of a manufacturing process. PAT systems and the methods employed to interpret the data from an array of sensors into a response signal to adjust plant/processing equipment accordingly are also discussed.

3.2 Fiber Optic Sensors

Over the last 25 years there has been a dramatic increase in the use of fiber optics. High volume demand, driven by the telecommunications industry, has both driven the cost of fiber optic systems down and prompted heavy investment in Research and Development (R&D). This level of R&D in fiber optics has advanced the technology to such a level that it can now be adopted as a suitable solution to the measurement of a host of physical and chemical attributes of a process, product or system (Yu and Yin, 2002) as shown in table 3.1.

Fiber Optic Measurands
Rotation
Acceleration
Temperature
Pressure
Acoustics
Vibration
Linear and Angular Position
Strain
Humidity
Viscosity
Chemical Measurements

Table 3. 1 List of Fiber Optic Measurement Capabilities (Krohn, MacDougall and Mendez, 2014)

The use of fiber optic sensors in manufacturing processes for real time measurement of process parameters is increasing with advances in both manufacturing and optical technologies (Luna, n.d.; Harun, S.W.; Yasin, M.; Yang, H.Z.; Ahmad, 2010; Sensuron, 2016). Fiber optic sensors provide many benefits over conventional sensory options as shown in table 3.2.

Advantages of Fiber Optic Sensors
Small Size
Light Weight
Immunity to Electromagnetic Interference
High Temperature Performance
Large Bandwidth
High Sensitivity
Environmental Ruggedness
Distributed Sensing

Table 3.2 Advantages of Fiber Optic Sensing (Krohn, MacDougall and Mendez, 2014) (Optics, 2013)

Fiber optic sensors generally consist of a light source, optical fibers, sensing unit or transducer and a detector (Optics, 2013). Optical sensors are primarily based on the principle of the detection or absence of light or infra-red (Iso, 1999). The optical fiber itself consists of a glass or plastic core surrounded by a layer of cladding. The difference in the index of refraction of the two materials allows the fiber to act in accordance with the principle of total internal reflection (LLC, 2017) i.e. light is trapped within the core and travels through the fiber by bouncing off the cladding due to the lower index of refraction of the cladding (Nave, 2017) as can be seen in figure 3.1.

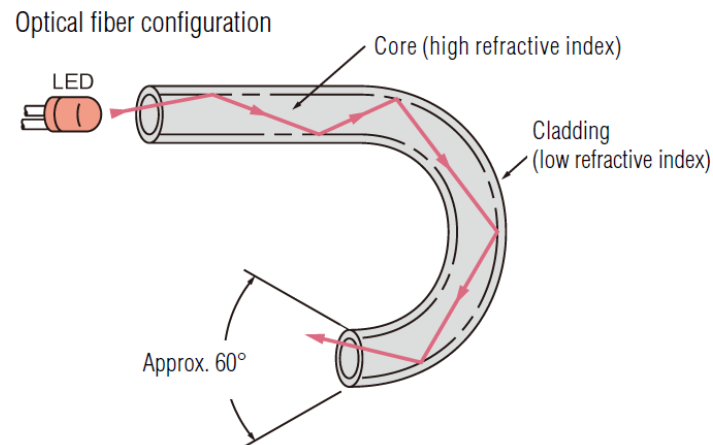


Figure 3.1 Conveyance of optical signal through fiber (Keyence, 2017a)

By introducing a light source at the point or process that is required to be measured, it is possible to detect changes in state of a point or process etc, due to the changes in the lights amplitude, frequency, phase or polarisation. This optical information is then converted into an electrical signal correlating to the physical or chemical properties of a given parameter.

Most optical sensors can be broadly categorised as extrinsic or intrinsic sensors. Extrinsic optical sensors use fiber optics to transport the light or infra-red signal from the point of occurrence to the sensing region or transducer where the signal can be processed and analysed (see figure 3.2) i.e. modulation of the signal is performed by the transducer (Yu and Yin, 2002). Typical extrinsic type sensors would include encoders for the measurement of angular and linear positioning, spectroscopy such as Near Infrared (NIR). Mid Infrared (MIR) spectroscopic sensors are widely used in the pharmaceutical industry for chemical composition and blend uniformity measurements and colour sensors are used in the polymer resin industry as indication of the status of polymer resins in reactor units (Extrinsic vs Intrinsic Fiber Optic Sensors - Sensuron, 2016).

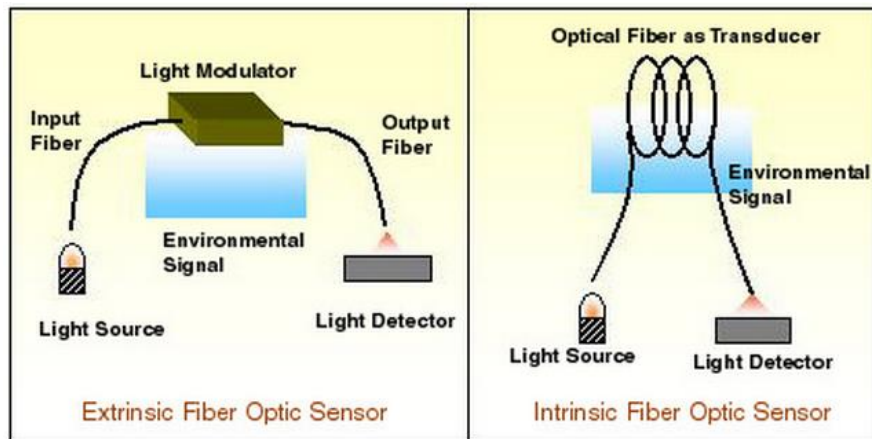


Figure 3.2 Comparison of Extrinsic Fiber Optic Sensor and Intrinsic Fiber Optic Sensor (extrinsic fiber optic sensor Archives - Optical Cables on Fiberstore, 2017)

In intrinsic fiber optic sensing, the modulation of the signal takes place within the fiber itself. When perturbations act on the fiber, the fiber alters some characteristic of the light i.e. amplitude, phase, frequency. The light within the intrinsic fiber optic sensor remains in the fiber so the optical signal can be measured using a variety of techniques such as Fiber Bragg Grating (FBG) or natural backscattering of light as the signal travels through the fiber. Measurements can be obtained for temperature, strain and load (among others) through observing the magnitude of changes in the characteristics of the light as it is conveyed through the fiber (Extrinsic vs Intrinsic Fiber Optic Sensors - Sensuron, 2016; Yu and Yin, 2002; Krohn, MacDougall and Mendez, 2014).

3.3 Smart Sensors

According to Malar and Kamaraj “20% of the total cost of a data acquisition system belongs to the hardware configuration and calibration of sensors” (Malar and Kamaraj, 2014).

A smart sensor is a sensor with additional functionality with the inclusion of a microprocessor (Frank, 2013). An increase in cost is introduced by the addition of a microcontroller, however, the advantages in most applications offset costs such as those incurred from incorrect calibration arising from the manual entry of important parameters. The resultant inaccuracy leads to a deviation from optimum process control.

Wei et al. detail how to conform a sensor to the IEEE 1451 standard (a smart sensor family of standards aimed at enabling plug and play capability) provides signal conditioning and processing, self-recognition and self-documentation easing system integration. As a result, the time taken to setup a sensor network is drastically reduced along with the related costs (Wei et al., 2005), (Mahony et al., 2016a). Smart sensors enable remote/automatic calibration so that the sensor’s parameters can be corrected promptly without the need for manual intervention and process downtime. Thus,

maintenance costs are reduced as are costs associated with poor product quality (Breede, 2015), (Mahony et al., 2016a).

Ongoing development in Micro-Electro-Mechanical Systems (MEMS) has brought many improvements to the smart sensor industry. MEMS sensors are serially manufactured by means of mature technologies derived from the semiconductor industry. With such mass production, comes reduced cost. MEMS are now a mature industry where a lot of the research has been done in the area of the engineering process (Bourgeois and Goldstein, 2015), co-fabricating sensors with electronics (CMOS-MEMS) (Fedder, Howe, Liu and Quevy, 2008), reducing production time (Fukui, Osanai, Mizoroke and Khorram, 2015), improving yields (Nestler et al., 2011) and developing new manufacturing technologies (Luo and Pan, 2007)(Mahony et al., 2016a).

Smart sensors process the signal from the sensor element, to eliminate non-linearity due to sensor imperfections, and communicate the information digitally (Gaura and Newman, 2004) They also define two further degrees of intelligence; Intelligent and cogent sensors. Intelligent sensors is a term, although sometimes interchangeable with 'smart sensors', to define sensors that go a processing step further and provide a measurement relevant to the sensors application. Data processing features may include multivariate analysis to produce correlated measurements (e.g. temperature/pressure compensation). The reduction of data to 'real world' measurements means that the central control platform needs only to be concerned with the process information and not the specific protocols and conversion ratios of each sensor in its network. Cogent sensors reduce the data down to information the application requires using data fusion techniques, trend recognition and decision-making (Bhuyan, 2010). Deviations from normal operation or natural stages in product development can be identified and transmitted. Unnecessary data is not passed on which reduces network traffic and makes the sensor very suitable for use in very large distributed control systems (Mahony et al., 2016a).

3.4 Colour Sensors

Colourimetry is "*the science and technology used to quantify and describe physically the human colour perception*" (Schanda, Eppeldauer and Sauter, n.d.). An object's colour information is determined by the spectral distribution of the electromagnetic waveform (light beam) emitted/reflected by that object. Monitoring colour can be used in quality control to determine if a product's appearance is acceptable or in process control where the colour of the product changes as the process develops.

Colour sensors implement the tristimulus method (i.e. use of varying proportions of the three primary colours to generate all other colours) of colour measurement where three light sources of different wavelengths (red, green and blue light or just a white light source) are shone on the object and the light reflected is measured using filtered photo sensors (if white light is used, some basic sensors shine

the red, green and blue light independently and measure the reflected light for each). Photo sensors, include photodiodes, phototransistors, and light dependant resistors that convert light into current. With a photodiode, when a photon strikes the P-N junction of the diode (in the depletion region), it creates an electron-hole pair which is a current carrier that increases current flow as in a regular diode (holes are swept to anode and electrons to cathode) (Mohankumar, 2017).

Each of the photosensors have spectral filters which defines their spectral sensitivity (basically which of the tri-stimuli they're sensitive to - red, green or blue light) and these spectral sensitivities define the colour space the sensor measures.

Colour spaces as shown in figure 3.3, give a numerical representation of the way colour is defined as a mixture of colours. The colours 'mixed' are the red, green and blue which were standardised as the primary colours by CIE, The International Commission on Illumination (Cie, 2004). The accuracy of a colour measurement is the perceived colour difference between the actual colour and the measured colour. The difference between two colours is measured by ΔE . Colour sensors may sometimes communicate the colour change from the last reading before the colour space values. The performance of a colour sensor may be represented by the minimum colour difference it can detect.

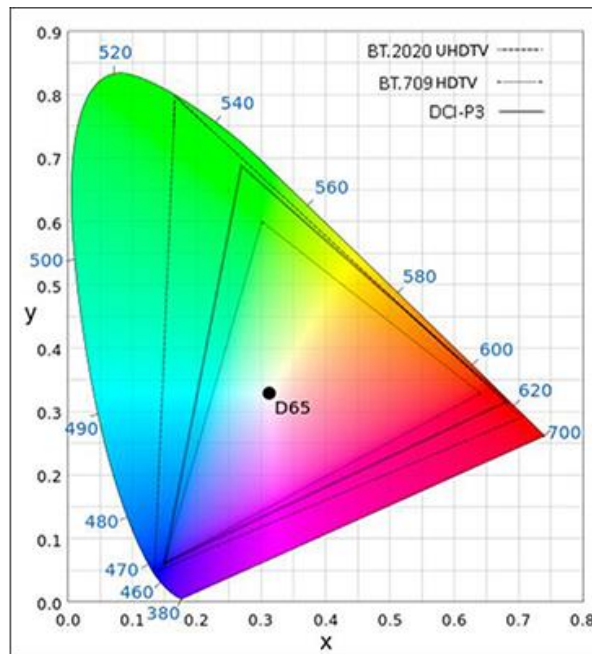


Figure 3.3 CIE 1931 chromaticity diagram with colour space values (Shingala and Natesan, 2017)

Multispectral sensors also exist in which the filters' spectral sensitivities overlap thus light is measured across an entire spectrum and metamerism effects (when colours are perceived to match when in fact they don't) can be compensated (Jensis, 2013). Table 3.3 summarises the types of colour sensor available.

Fiber Amplifiers	<ul style="list-style-type: none"> • Measure light intensity on one wavelength.
RGB Colour Sensors	<ul style="list-style-type: none"> • Measure light on red, green and blue wavelengths. • Use absorption filters with spectral sensitivities often uniformly spaced for general purpose use. • Have limited accuracy and are not used for precise colourimetric measurement.
True Colour Sensors	<ul style="list-style-type: none"> • Similar to RGB type but with better accuracy. • Use interference filters which are manufactured to implement a standard colour space. • Used to make colourimetric measurements with better accuracy than the human eye.
Spectroscopic Methods	<ul style="list-style-type: none"> • Multispectral sensors, mini-spectrometers and spectrometers provide spectral information. • More expensive and not as fast compared to colour sensors.
Vision Systems	<ul style="list-style-type: none"> • Camera's photosensor arrays are covered in a pattern of spectral filters enabling colour measurement. • There are twice as much green filters to make colour perception closer to human perception. • A noteworthy upcoming technology in diffractive filter arrays so that cameras can be used in low light situations as less light is absorbed compared to absorption filters.

Table 3.3 Types of Colour Sensor (Jensis, 2013)

Typical applications of colour sensors include monitoring the colour of metals during heat treatment, in the food industry, the colour of a polymer during polymerisation and in the formulation of pharmaceutical products. These examples typically have extreme temperatures involved, far greater than electronic circuits can withstand, making the use of fiber-optics with heat resistant cables an effective solution (O'Mahony et al., 2016b).

In the pharmaceutical industry, the final colour of a tablet can be affected by the concentration of certain ingredients within the formulation (Micro-Epsilon, 2017a). Figure 3.4 depicts a colour gradient varying from white to yellow as a result of deviations within the blended material and/or non-uniformity of the blend.



Figure 3.4 Pharmaceutical tableting process and the effect of a deviation in ingredient concentration on the colour of the product (Colour measurement of tablets in pharmaceutical production | Micro-Epsilon Measurement, 2017)

It is possible that an ingredient within a pharmaceutical formulation that significantly impacts the final colour of the product can be the Active Pharmaceutical Ingredient (API) of that product. Excessive

quantities of an API within a formulation can pose serious health hazards if consumed. Colour sensors offer a solution to early identification of both individual defective tablets and defective formulations prior to tableting through measuring in-process material and comparing it to pre-determined accepted colour gradients. Sensors can also be integrated in-line to ensure real time measurements and control of in-process material. Figure 3.5 shows a typical in-line sensor system that can easily be adapted to production conveyance pipes (Kemtrak DCP007 Photometer (UV-VIS-NIR) - Industrial in-line analyser for concentration and color control, 2017).



Figure 3.5 In-line photometer for the measurement of colour of in-process material (Kemtrak DCP007 Photometer (UV-VIS-NIR) - Industrial in-line analyzer for concentration and color control, 2017)

3.5 Mass Flow Sensors/Meters

A fundamental parameter in the production of bulk solids, is the measurement of mass flow which is generally either pneumatically conveyed or transported in free falling or belt driven systems. There exists a wide variety of conventional methods for the metering of the mass flow of a bulk solid (Lewis, D, 2016; Engineering360, 2017) and many can incur heavy financial costs, depending on the complexity of design, accuracy required and general performance characteristics of the system. Recent studies in the field of mass flow metering attempt to identify more cost effective alternatives than that of more established methods of the mass flow sensing of a solid bulk mixture (Murphy et al., 2016a; O'Mahony et al., 2016a) such as inertia sensing of a bulk solid mixtures mass flow and mass flow metering using acoustics. More conventional methods currently used within the bulk solids industries consist of gravimetric and volumetric flow metres and feeding systems while advances in sensory technology has led to the development of smart sensors that can monitor the flow of a bulk solid based on the amplitude and frequency shift of a microwave signal (Hense, 2014; MIC, 2015).

Gravimetric flow meters as shown in figure 3.6, are commonly used in the powder processing industry for accurate metering of a bulk solids mass and consist of a gravimetric feeding system such as a hopper and a weighing system, generally in the form of a pan or plate with integrated load cells.

Gravimetric flow meters operating on the “loss in weight” measurements of material within a hopper or feeding system (Gea, 2017). Material is fed from the hopper or gravimetric feeding system onto the weighing system until a pre-determined mass of material has been recorded on the scales (PSG, 2017). The measurements taken, independent from density and particle size (Easternn-Instruments, 2017), are primarily mass per unit time measurements.



Figure 3.6 Hopper fed gravimetric flow meter (Solids Flow Meters, Feeders and Fillers - El Mass Flow Meters, 2017)

This system allows for the controlled weight/unit time discharge of powder that constantly monitors the feed rate of bulk solids into the production process with typical accuracies ranging from 2% - 0.25% (Easternn-Instruments, 2017; Eastern-Instruments, 2017). The accuracies of gravimetric feeding systems are driven by the accuracies of the weighing systems load cells and the response times of mechanical, electrical or pneumatical shut off valves. In instances where accuracies of 0.25% are required, such as in pharmaceutical manufacturing, load cell systems with increased sensitivity are incorporated into weighing systems for closed loop control of material feed rates into manufacturing processes.

Volumetric flow metres are used to provide a controlled feed of a powder based material into a manufacturing process from a hopper through use of an auger or rotating screw with a known diameter and pitch (Liptrott, 2017) enclosed in a tube rotating at a uniform speed (Liptrott, 2017). The material escapes the hopper and fills the flights of the auger and is then conveyed though the tube as the auger is rotated. To ensure uniform volume within each flight, the material is generally conditioned in terms of moisture content and density while within the hopper, agitation or vibration prevents any material bridging, agglomeration or starvation of the auger flights as shown in figure 3.7 (Thayer, 2017; Gea, 2017).

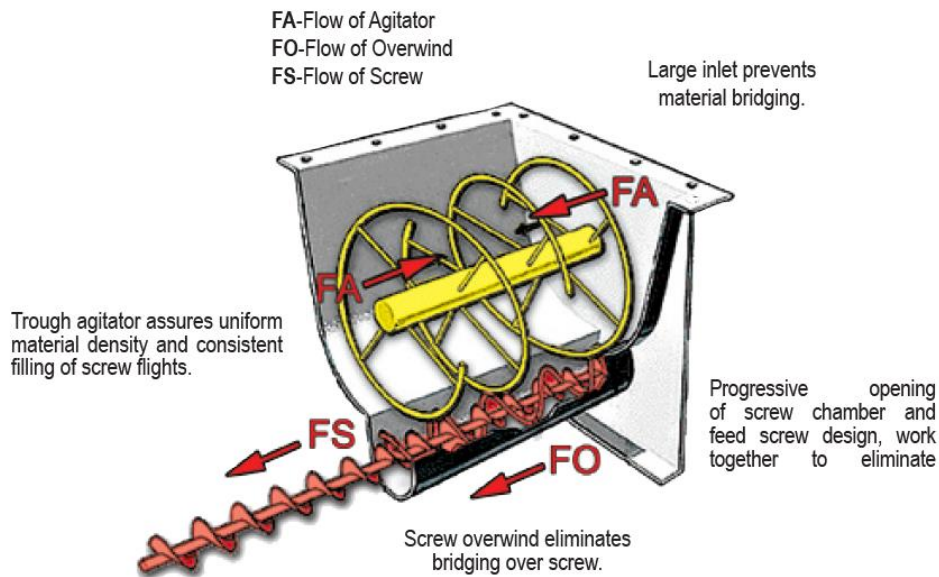


Figure 3.7 Volumetric feeding system using rotating auger system (Thayer Powder Feeder™ Model PF-S-4 – Thayer Scale, 2017)

Typical accuracies of a volumetric feeding system range between $\pm 1\%$ and $\pm 2\%$ (Gea, 2017) provided the material is preconditioned through agitation or other means and operated at the correct speed. The flow characteristics of a bulk solid can vary from material to material due to particle size, particle shape, moisture content and co-efficient of friction of the material, among others. Each material, because of the variations in flow characteristics, require the volumetric feeder to operate at a uniform speed suited to the flow behaviours of that material. Identifying the optimum running speed of the volumetric feeder is generally achieved through trial and error until steady state feeding or “straight line graphs” have been achieved (Liptrott, 2017).

What both gravimetric and volumetric systems offer by way of accurate solutions to mass flow metering, they lack in flexibility and adaptability. Slight variations in material through changing suppliers or variations within the process environment can be a source of errors for both systems resulting in inaccuracies (Wilson, 2001) as they are assumed to be constant in both gravimetric and volumetric systems (Lewis, D, 2016).

Incorporating mass flow sensors into gravimetric or volumetric metering systems can improve the accuracy of the feed rate through closed loop control while also validating the accuracy of the machine through cross validation of data from the metering system to data from the mass flow sensors. Sensors can operate independent of particle size, pressure, temperature and material densities (MIC, 2017) making them ideal solutions for the enhancement and control of material feed rates in manufacturing processes.

There are many sensory options available for the measurement of mass flow of a bulk solid material (see table 3.4). One of the more emerging techniques in this area is the use of microwave technology to accurately measure the mass flow of a powder/granular material.

Volumetric concentration and velocity measurements of solids.		
Category	Method	Sensing Technique
Concentration Measurement	Electric Methods	Capacitive
		Electrostatic
	Attenuation & Scattering	γ Ray
		Microwave
		Optical
		Acoustic/Ultrasonic
	Resonance	Magnetic
		Microwave
		Acoustic
	Flow Tomography	Capacitance/Resistance
Optical		
γ Ray		
Digital Imaging	Laser sheet and CCD Camera	
Velocity Measurement	Cross Correlation	Optical
		Electrostatic
		Capacitive
		γ Ray
	Electric Sensors & New Signal Processing Methods	Electrostatic Sensor & Wavelet Analysis
		Capacitive Sensor & Fourier Transform
	Doppler	Laser Doppler
		Microwave Doppler
	Spatial Filtering	Capacitive/Electrostatic
		Microwave
Optical		

Table 3.4 Volumetric concentration and velocity measurement techniques for bulk solid mass flow (Zheng and Liu, 2011)

For the purposes of this research the commercial microwave mass flow sensor “MIC Flow Meter” (figure 3.8) is discussed which measures both the amplitude and frequency shift of the microwave signal to infer mass flowrate (Hense, n.d.). This particular sensor was chosen over alternative methods as it provided a non-contact form of measurement while recording only moving particles. Set-up times due to sensor calibration are also significantly reduced due to the in-built microprocessor that conditions the signal and self-calibrates the unit periodically while providing a moderate level of accuracy at a low cost (Hense, 2017a). The sensor can achieve a typical accuracy of 2% when calibrated for a specific flowrate range for a homogenous material of fixed particle size.



Figure 3.8 MIC Flow Meter (Type 'MIC- Flow Meter' for Solids | MIC-Flowmeter | Solid Flow Measurement | Products | Hense Wägetechnik GmbH, n.d.)

Microwave sensors are a popular method for non-intrusive measurement of mass flowrate for the following reasons:

- Moderate accuracy (3-5% typical).
- Easy installation, calibration and maintenance (Morrissey, n.d.).
- Wide range (multiple microwave sensors can be spread around the perimeter of large pipes to increase the field of measurement).
- Ability to handle any type of powder material in gas/solid multi-phase flow (has been used for pharmaceutical powder, pulverized coal (Meier et al., 2016) and agricultural grain (King, King and Woo, 1992)).
- Can be used in both lean and dense phase applications (Happel, 2015).
- Ability to handle particle agglomeration.
- Immunity to vibration.

Microwave sensors perform inferential measurement of solids mass flow by:

1. Sensing particle concentration by:

- a. Measuring the attenuation of electromagnetic radiation from a microwave source due to absorbance by the particulate stream. Attenuation varies significantly with changes in moisture content, particle size and density (Yan, 1996).
- b. Measuring the Doppler shift in frequency of microwave radiation due to Rayleigh scattering by the solids. An advantage of this method include immunity to solids

deposition in the sensing zone. Limitations include insensitivity to particulates of size greater than 1 μm and sensitivity to particle size, chemical composition of solids and solids velocity (Yan, 1996)

2. Sensing particle velocity by measuring the Doppler shift in frequency of microwave radiation. According to the well-known Doppler-shift principle, the difference in frequency between the transmitted and received signals is directly proportional to the solids velocity (Penirschke et al., 2009).

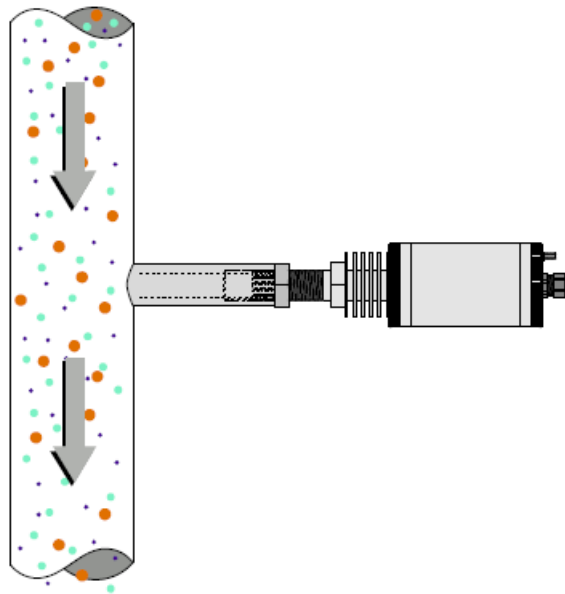


Figure 3.9 Integration of a microwave mass flow sensor in a stainless-steel pipe (Flow, n.d.)

Microwave mass flow sensors are a highly adaptable and flexible solution for monitoring particulate materials within the range of 1nm – 2cm of a pneumatic or free fall system. Installation of the sensor is a simple and cost-effective process and provides a non-contact, real-time measurement sensing solution. The microwave mass flow sensors are also designed to be flush mounted with the internal wall of the metallic pipe ensuring minimal intrusion of the material flow is achieved (figure 3.9).

3.6 IR Temperature Sensor

In solid bulk processing industries such as pharmaceutical manufacturing, the measurement and control of temperature of a material or process is considered as one of the most critical parameters within the production of quality pharmaceutical products (Wirth, Berlenbach, Zimmer and Brudel, 2009). Processing equipment such as fluidised beds and the tablet compression process rely heavily on the effects of temperature on a powder blend (Macri et al., 2017; Lettieri and Macri, 2016; Weber, 2012). Fluidised bed reactors are used in the pharmaceutical industry for rapid solids mixing and for inducing chemical reactions reliant on accurate temperature control while the effects of temperature

on the tablet compression process has a direct impact on a tablets tensile strength and compressibility (Lettieri and Macri, 2016; Weber, 2012). Therefore, the ability to accurately measure the temperature of an environment, material or process and react to deviations of temperature set points in real time, provides many benefits with respect to process control.

Temperature measurement techniques can be broken down into two main categories i.e. contact and non-contact. Contact temperature measurement techniques such as thermocouples, thermometers and immersive probes must have physical contact with the object to be measured (Barron, 1992). Contact temperature sensors rely on the process of thermal transfer to the sensing element of the temperature sensor from the object or material to be measured making them unsuitable for some pharmaceutical manufacturing processes. In instances where accurate temperature measurement of a dynamic powder stream is required, non-contact temperature measurement solutions such as infrared (IR) thermometry have become industry standard (Carillo, 2002).

IR thermometry is a highly advantageous method of in-process temperature measurement due to its ability to accurately measure the temperature of a dynamic material. Infrared thermometry measures the infrared radiation that is emitted from an object and calibrates the intensity of the emitted radiation in terms of degrees Celsius. The IR temperature sensor is an optoelectronic sensor that is non-contact in nature. This enables the sensor to be integrated into harsh environments to measure the temperature of material such as a bulk solid.

IR Temperature sensors are commonly used for noncontact measurement of the surface temperature of the objects. They average the infrared radiation emitted by surfaces in their field of view, so an average reading of a stream of powder and pipe wall in the background can be produced. IR sensors can be configured to measure substances of a particular emissivity (DeWitt and Nutter, 1988) thus allowing only the powder (which will have a higher emissivity than the reflective surface of the internal pipe wall) to be measured and the reflective background of the process (in this case a stainless steel pipe system) to be ignored (Mahony et al., 2016c). The emissivity of stainless steel falls within a large range, typically between 0.1 and 0.9. The actual emissivity value of a given sample of stainless steel is dependent on a number of key factors such as (Evitherm, 2018);

- Surface Condition - oxidation and surface roughness increase the emissivity of stainless steel, while clean, polished & oxide free surfaces have a low emissivity
- Temperature – increasing material temperatures result in increased emissivity

The internally polished and reflective surface of the stainless-steel pipe system, provides clear contrast to the powder stream in terms of emissivity, thus allowing for the accurate determination of

temperature of the conveyed material through the pipe system. This is shown in later experiments in section 5.3.3.4 where the IR temperature sensor is calibrated using a temperature probe as validation of sensor readout.

Several different optical configurations are available to adjust the spot size dependent on the distance between the powder stream and the sensor. The main issue to address for IR and any other optical sensors would be keeping the lens clean as powder build up will mean the sensor will only measure the surface temperature of the coating that sits on the lens itself. A number of solutions are available including situating the probe clear of the powder, using pneumatics (either built into the probe (Narayanan, Product and Spectroscopy, n.d.) or from the process) to clean the lens periodically and using a sight glass with particular shape/material properties such as a Fresnel lens (Edmund-Optics, 2017) that prevent the powder build-up (Portoghese, Berruti and Briens, 2008), (Mahony et al., 2016c) without impeding the optical signal to the sensor.

3.7 Spectroscopic Sensors

In the past few decades, the discipline of process analytical chemistry has grown significantly due to the increasing use and appreciation for the value of collecting process data (Jagtap and Karekar, 2016) coupled with the technological advances in computing large data sets (Department of Energy Office of Science, 2000). As a result, the accuracy, variety and flexibility of analytical techniques used in the pharmaceutical industry has steadily improved. The most commonly used analytical techniques in pharmaceutical manufacturing, development and analytical chemistry are spectroscopy and chromatography. There is a wide variety of both spectroscopy and chromatography techniques in use in industry such as NIR, MIR and Raman spectroscopy and high-performance liquid chromatography (HPLC). For this research, the focus will be on NIR spectroscopy and Raman spectroscopy due to their non-contact, non-destructive and remote sensing capabilities that can provide real-time data on a wide range of physical, chemical and biological properties in a manufacturing process and their suitability for integration into PAT systems. MIR is not investigated as transmitting materials such as optical fibers are more expensive than that of NIR and are also difficult to manipulate. MIR is also best suited to applications involving reaction monitoring of liquids through use of the Attenuated Total Reflection (ATR) method (Wilks, 2007).

3.7.1 NIR Spectroscopy

NIR spectroscopy is a simple non-contact, non-destructive analytical technique that can provide multi-variate analysis on in-process material while providing levels of accuracy comparable to that of primary reference methods (Spectroscopy, 2013). NIR Spectroscopy is used to monitor and record the absorption, transmittance or reflectance of light (within wavelengths of 600 – 2500nm) as it interacts with the material under test. The low absorption co-efficient of NIR's allows for deep penetration of the radiation in the sample that can provide information on both sample thickness and volume parameters (Polytech, 2007), (Reich, 2005) while providing real time, precise and repeatable measurements requiring no sample preparation. Other advantages of the penetration depth of NIR's is the increased volume of material that is analysed and reduces sampling error in the system (Strother, 2009).

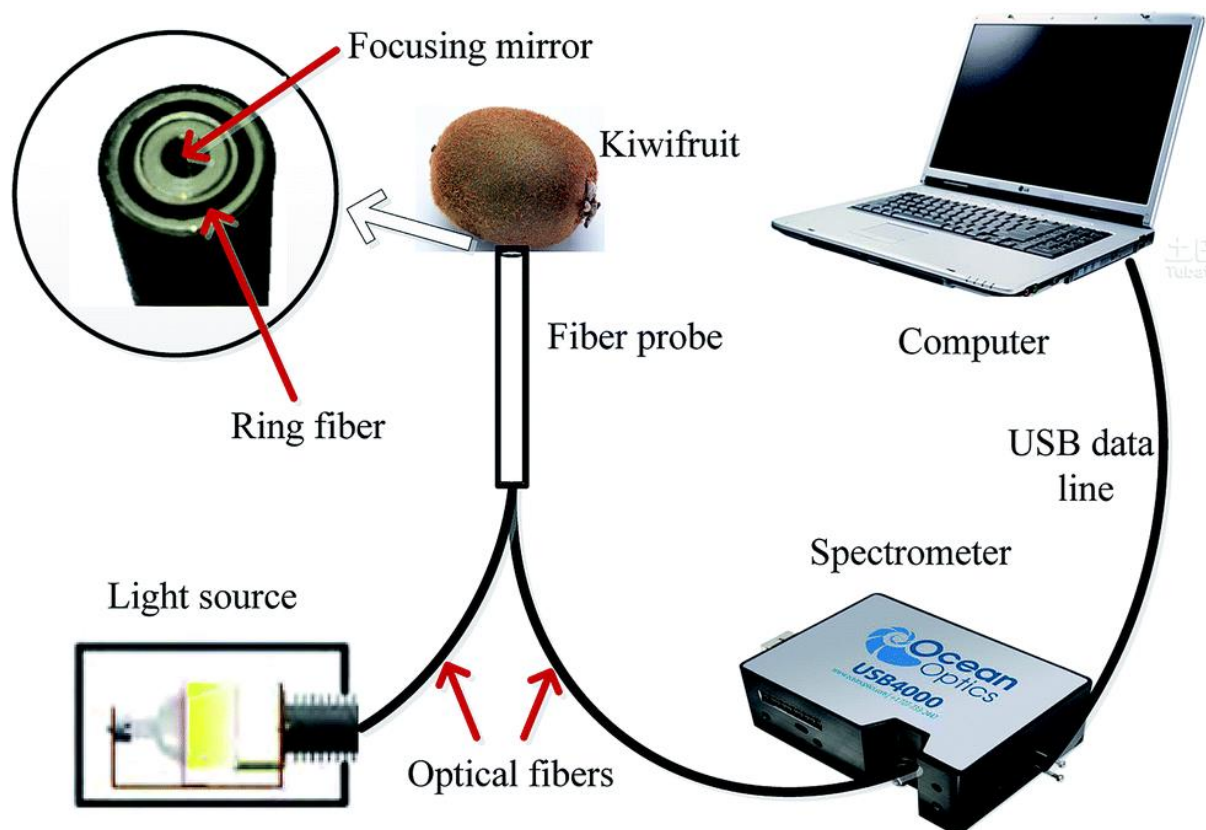


Figure 3.10 Typical components of a NIR spectrometer (Liu et al., 2017)

An NIR spectrometer consists of a light source in the form of a tungsten -halogen or LED lamp, a detector or sensing region (i.e. spectrometer) and optical fibers to transport the light to and from the sample material or sensing region as depicted in figure 3.10. The NIR detector operates in a variety of modes such as;

- Transmission, where the attenuation of light is measured at varying wavelengths as it is passed through the sample material. Transmission can be used for the measurement of liquids, solids

and gasses. Light is passed through the sample material and the results are then compared to light that has not passed through the sample. There are many variables to consider when analysing the resulting spectrum such as the sample thickness, sample reflectivity and sample co-efficient of absorption (Andor, 2017).

- Transflectance, where the light is passed through the sample, and reflects off a highly reflective substrate before passing back through the sample, effectively doubling the path length. This mode is generally used for the measurement of transparent or partly transparent samples. The term “transflectance” is derived from transmission/reflectance, in that both the light absorbed and reflected by the sample is considered (Ritchie, 2017).
- Diffuse Reflectance is the most commonly used method in the pharmaceutical industry for the measurement and analysis of a pharmaceutical compound (Mccarthy, Magnuson, Nicolet and Solutions, n.d.). Diffuse reflectance measures the amplitude of reflected light of solid granular samples at different wavelengths that are affected by scattering and absorbance (Pasquini, 2003).

Selection of the correct mode of measurement of NIR spectroscopy is dependent on the characteristics of the material to be tested. For the accurate measurement of a bulk solid, reflectance techniques are generally used, while transmission and transflectance are more suitable for the measurement of gasses and liquids (Pasquini, 2003)

NIR spectra can often be complex due to the overlapping NIR absorption bands and require mathematical procedures such as chemometric data processing for data for analysis (Murphy, O' Mahony et al., 2016b). NIR spectroscopy techniques are becoming the most widely used analytical technique due to their ability to be placed off-line or on/in/at-line (Bakeev, 2004) using optical couplings that allow for easy integration into manufacturing process streams. For continuous monitoring of manufacturing processes, NIR spectroscopy has been successfully deployed online to monitor a number of processes in the pharmaceutical industry (Tollifson, n.d.)(Li, 2007) such as;

- **Reaction monitoring**, monitoring the chemical reactions of liquids and solids
- **Powder blending**, measuring blend homogeneity in a bulk solid
- **Solvent monitoring**, monitoring the mixture of solvents in a solvent recovery process
- **Moisture measurements**, measuring the amount of moisture during granulation, drying, and purification stages of solids (Murphy et al., 2016b).

NIR is an important PAT tool for continuous monitoring when utilised in conjunction with multivariate and statistical analysis tools and can provide both qualitative and quantitative assessments of

materials composition and chemical reactions. The data acquired from NIR spectroscopic techniques can then be utilised for continuous improvement and optimisation of both process control and product quality (Murphy et al., 2016b).

3.7.2 Raman Spectroscopy

Raman spectroscopy has been an established analytical method in pharmaceutical development and general analytical chemistry for many years used to provide a fingerprint by which molecules can be identified. Similar to NIR, Raman spectroscopy is a non-contact, non-destructive analytical technique with remote sensing capabilities that utilises fiber optics to integrate into process streams and hazardous environments (Murphy et al., 2016b).

The principle of operation of Raman spectroscopy is based on the inelastic scattering of monochromatic light from a laser that interacts with molecular vibrations, phonons or other excitation systems (Ahlawat, 2014). When light interacts with a material, the light energy is altered and the frequency changes, the resulting Raman effect is weak and requires highly sensitive spectrometers to analyse the effect and produce data (Murphy et al., 2016b).

Raman spectroscopy is the most widely used analytical technique in pharmaceutical development. Raman spectroscopy is generally employed to rapidly characterize the chemical composition and structure of materials such as solids, liquids, gases, gels, slurries or bulk materials such as powders through providing detailed characteristics of their vibrational transitions. The interpretation of data is also easier than that of NIR spectroscopy and does not compulsorily call for multivariate modelling as simple modelling of the peak heights or ratios can often achieve the desired goals (Misra, Sullivan and Cullen, 2015), (Murphy et al., 2016b).

Raman spectroscopy is ideally suited for application in PAT systems due to the flexibility of the technique to operate online or inline whilst providing accurate and repeatable real-time measurements of materials under process and providing both quantitative and qualitative data to enhance process monitoring and control. Typical applications of Raman spectroscopy in the pharmaceutical include (Horiba, 2016b),(Murphy et al., 2016b);

- Blend uniformity
- Active pharmaceutical ingredient (API) concentration measurements
- Raw material verification
- Contamination & impurity measurements

Recent advances in Raman spectroscopy has increased the versatility and suitability of this technique for application in continuous process monitoring systems such as PAT. The proven accuracy and

precision of these instruments allow them to be utilised in highly regulated industries such as pharmaceutical development and analytical chemistry to provide real time data on key characteristics of materials for continuous process monitoring and continuous process improvement strategies.

3.7.3 Summary of Spectroscopic Sensors

While similarities exist with NIR and Raman spectroscopy there are some fundamental differences between the two methods that effect their suitability to certain applications, however the complimentary nature of NIR and Raman spectroscopy ensures that most measurement applications would be suitable to at least one of the two techniques as depicted in figure 3.11. This is due to the fact that strong bands in the IR spectrum correspond to weak bands in the Raman spectrum and vice versa (Peeran, 2005).

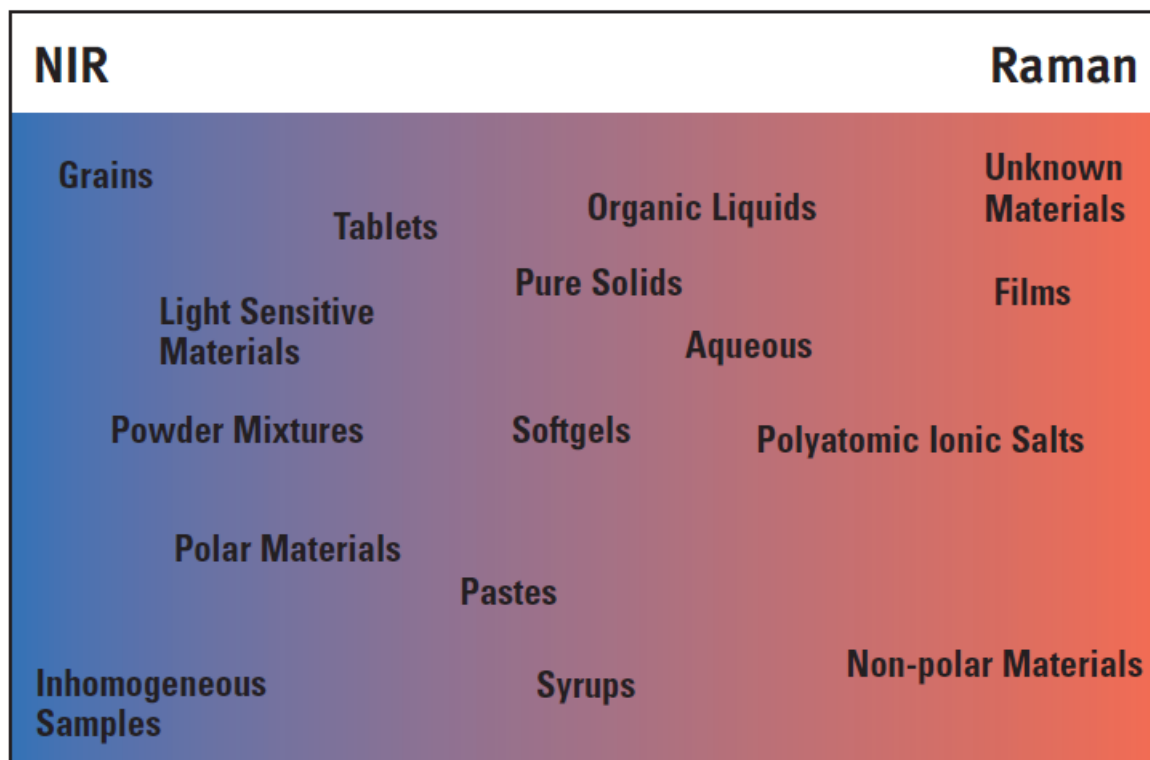


Figure 3.11 Suitability of sample types to NIR and/or Raman applications. Sample types closer to the left are better suited to NIR, while samples closer to the right are more suitable to Raman spectroscopy (Strother and Scientific, 2009).

Raman spectroscopy is used for highly specific analyses of materials and for analysis of liquids and as the Raman effect is weak, it requires expensive and highly accurate equipment for detection. Fluorescence from impurities and heating of the sample from laser radiation can obstruct the Raman spectrum and equipment must be carefully tuned and calibrated to counteract these effects (Dippel, 2016)(Murphy et al., 2016b).

NIR spectroscopy is used in the pharmaceutical industry to provide rapid measurements in areas such as raw material identification and classification (providing that reference spectra/material has been

obtained), blend homogeneity and particle sizing and requires multivariate statistical analysis techniques to interpret the data collected from in process materials. NIR spectroscopic instrumentation, in comparison to that of Raman is relatively simplistic and inexpensive while maintaining a high level of precision, repeatability and accuracy. Its penetration depth into sampled material can also reduce percentage error as a larger portion of the material can be analysed (Murphy et al., 2016b).

There are several key factors to consider prior to selecting the correct spectroscopic technique for integration in PAT systems, such as;

- The application in terms of the sample type (i.e. measurement of unknown material (Raman) or uniformity of a powder blend (NIR))
- Level of understanding of Statistical Modelling or Chemometrics
- Cost of the system

Understanding these key factors allows for selection of the correct technique to ensure optimum levels of performance in an integrated PAT system (Romero-Torres, Huang and Hernandez-Abad, 2009)(Murphy et al., 2016b).

3.8 Chemometrics

Chemometrics is one of the most critical aspects to PAT systems and is used to extract, analyse and interpret chemical information from materials under process through use of mathematical and statistical methods and is driven primarily from physical and spectral data. The data, acquired from sensors and analyser located at key measurement points within the process, is computationally analysed using a variety of mathematical and statistical tools and simulations. This allows for a more in-depth understanding of chemical information and the correlation of quality parameters or physical properties of materials to instrument data (Bu, 2007)(Murphy et al., 2016b).

Analysis of the data is achieved using specialised software packages such as Camo Unscrambler X multivariate analysis software (Camo, 2018) (employed in sections 5.3, 6.3, 6.4, 6.5 & 6.6). Camo is comprised of a variety of multivariate, univariate and statistical analysis tools that are suited to a variety of applications in materials processing such as (Camo, 2016)(Murphy et al., 2016b);

- Identification of CQAs of a CPP
- Identification of multifactorial relationships between process variables
- Spectroscopic calibration solutions
- Statistical modelling for process optimisation
- Multivariate statistical process control

- Process modelling for continuous monitoring and fault detection

This allows for a previously unachievable level of process understanding and control, and drives innovation in pharmaceutical development and manufacturing (Murphy et al., 2016b).

3.9 Data Fusion

Data fusion, or Sensor fusion, refers to the analysis of multiple sensor outputs to achieve better process understanding than that which would have been possible when considering the sensor outputs independently (Elmenreich, 2002), (Mahony et al., 2016b).

Sensor fusion is implemented on a basic level in sensors with temperature compensation (or pressure compensation, etc.). Sensor fusion can be used to create virtual or ‘soft sensors’. Soft sensors or virtual sensors can be used to boost process understanding achievable from available hardware. For one reason or another, the sensors used in a process control approach have limitations such as poor accuracy, poor field of measurement, or perhaps the parameter we want to measure cannot be measured due to a limited budget, extreme process conditions or nonexistence of sensor technology. To give some examples of data fusion, mass flow can be better calculated using outputs from both a microwave sensor and a Particle Size Scatterometer. Also, an NIR sensor can be calibrated in real-time against the supporting sensors. Larger scale data fusion is often implemented with neural networks (Gaura and Newman, 2004) and other machine learning approaches. A number of fusion algorithms have been developed to perform tasks such as deciding on what sensors to fuse based on their reliability (Cohen and Edan, 2008) and performing distributed sensor fusion (Jeon and Eun, 2014; Xi, He and Liu, 2010). Data fusion can be categorised in a number of ways, e.g. based on inputs and outputs or on configuration, as in table 3.5 (Mahony et al., 2016b).

Category	Competitive	Complementary	cooperative
Fused Sensors Measure:	The same phenomenon	Different phenomena	Multiple phenomena
Fusion Achieves	Better reliability, accuracy & robustness	A more complete view of the process	Data unavailable from individual sensors
Aspects	Redundant configuration	Sensors are not interdependent - offers a more complete view	Difficult - accuracy & reliability are reduced
Example	Sensor arrays	NIRS calibration	E-nose (MCB University Press., 1981)

Table 3.5 Categorisation based on Sensor Configuration (Sensor Fusion in Time-Triggered Systems, n.d.)

3.10 Conclusion

This chapter details the technological and analytical aspects to PAT in terms of the available measurement solutions (i.e. fiber optics, smart sensor and spectroscopic analysers) and their applications, in conjunction with the methods employed to fuse and interpret the data from these measurement solutions into an appropriate corrective response from plant machinery to maintain optimum processing conditions.

The significant advances in the areas of fiber optics, sensory technology and spectroscopy play a major role in the emergence of PAT in the solid bulk processing industries such as pharmaceutical manufacturing. A significant reduction in the cost of optical fiber based sensors, their ability to transmit optical signals to and from key measurement locations and their immunity from electromagnetic interference allow optical fiber based sensors to integrate seamlessly into manufacturing systems and processes. Expensive detection and sensing units can be situated away from hazardous processing environments allowing for previously unobtainable levels of measurement due to potential risk to expensive hardware.

The evolution of smart sensors and their application in PAT systems for providing real-time data can significantly reduce set-up times due to their in-built microprocessors and ability to automatically perform “self-calibrations” compared to conventional sensors that require signal conditioning and manual scheduled calibrations.

Spectroscopic equipment, once confined as fixed units in a laboratory environment are now manufactured similar in size to conventional smart sensors. Although interpretation of NIR data can be, in some cases complex, the ability to continuously monitor the uniformity of a powder blend provides more advantages than the disadvantages associated with complex data interpretation.

The ability of a PAT system to fuse the data from smart sensors, optical sensors and spectrometers into one or many response signals allows for a previously unknown level of process understanding when used in conjunction with chemometrics and statistical tools such as Partial Least Squares (PLS) regression techniques etc. PAT systems incorporate the latest in sensory and spectroscopic technology and in conjunction with multivariate analytics can generate predictive modelling programs to provide optimum levels of process control.

Chapter Four – Active ProPAT Case Study Review of PAT
Implementation

4.1 Introduction

This chapter contains a case study based review of two end users from the ongoing “Horizon 2020 (H2020) SPIRE”, “ProPAT Project” (ProPAT – INTEGRATED PROCESS CONTROL, 2017). The ProPAT project is comprised of 16 European partners from academia and industry with a goal to developing a modular PAT system for the materials processing industries. Within the ProPAT project team there are 4 designated end users of the pilot PAT system consisting of GlaxoSmithKline (GSK), MBN Nanomaterialia, Grecian Magnesite and Megara Resins (GSK, 2017; MBN, 2017a; Megara, 2017a; Magnesite, 2017a). For the purposes of this chapter, GSKs and MBN Nanomaterialias manufacturing processes and their end user requirements for the pilot PAT system will be discussed.

This chapter will give an overview of each end users “current state” and identify how PAT, through an implementation using suitable sensors and process analysers, can provide benefits to powder processing industries in terms of quality, cost, efficiency and improved process understanding.

4.2 GlaxoSmithKline (GSK) Continuous Tableting Line (CTL)

GSKs tableting process consists of a Continuous Tableting Line (CTL) arrangement that involves the blending of several powdered ingredients together through wet granulation and milling techniques before compressing the material into tablets. The entire process consists of a series of unit operations such as material input (feeding), granulation, drying, milling, blending and compression, that transform a mixture of powders i.e. Active Pharmaceutical Ingredients (API’s) and excipients, into pressed solid dose tablets ready for human consumption. The products produced on this line are variable, depending on particular runs.

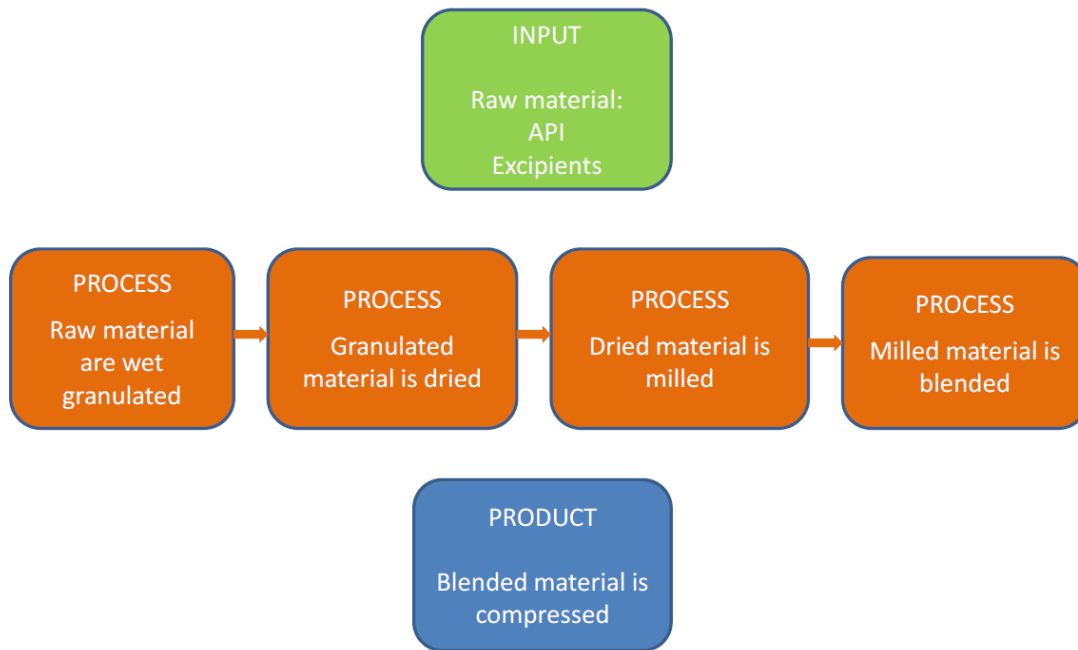


Figure 4.1 Process flow diagram – GSK (Opitz, 2014a)

Figure 4.1 depicts the process flow of the GSK tableting process. Raw material in the form of API and excipients such as binders and disintegrants are inputted into the CTL via three loss-in-weight gravimetric feeding systems. Integrated load cells within the feeders are used to provide a control signal to the feeder control unit that in turn, adjusts the feed rate of the material into the process through altering the speed of rotation of the screw driven metering zone. The material from the gravimetric feeding system (figure 4.2) is then conveyed directly to the wet granulation stage.

Loss-in-Weight Feeder Principle

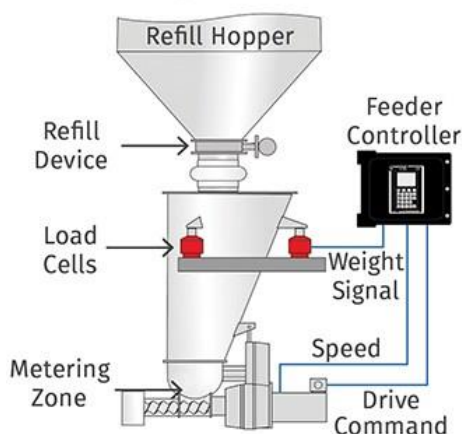


Figure 4.2 Schematic of a gravimetric feeding system (How to Troubleshoot Your Feeder to Achieve Optimal Performance: Plastics Technology, 2017).

The wet granulation of the raw material is achieved by twin screw granulation using a 25mm twin screw granulator with a Length/Diameter (L/D) ratio of 40:1 and a capacity of 25kg/hr. As the material is fed into the granulator, small amounts of binder in the form of a liquid is added to the material creating physical bonds between the raw material (Kaminska and Danko, 2011) as depicted in figure 4.3.

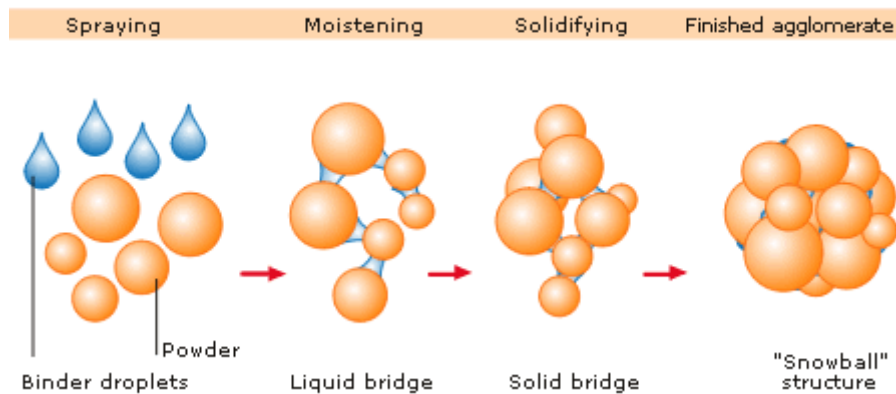


Figure 4.3 The granulation process and the formulation of a multi-particle granulated mixture through agglomeration (Granulation & Particle-Bonding Mechanism Process | Production, 2017).

The granulated material is conveyed by the rotation of the twin screw to the outlet of the granulator where it is gravity fed to the drying operation. Based on off-line analytics, particle size of wet granulated samples is controlled by screw speed, feed rate and liquid to solid ratio. Typical analytical results of particle sizing show granulated particles <4mm with the majority of particles being <1mm.

Removing moisture from the wet granulated material is achieved through use of a gravity fed rotary dryer with inlet temperature and humidity control. Material is passed through the 6 rotary cells where it is exposed to heated air as it cascades within the chambers of each cell. The exposure time of the material within the dryer is set automatically through timers in accordance to product specifications.

Vacuum transfer is used to convey the material from the drying operation to the milling operation. The milling operation, achieved using a Comil conical milling machine (Quadro, 2017), this breaks up agglomerates created during the drying operation while also providing size reduction of particles and increasing surface area that improves the dissolution properties, absorption and content uniformity of the blend (Horiba, 2016a). The Comil conical milling machine consists of an inlet chamber with a rotating impeller and perforated milling screen and is shown in figure 4.4 below.

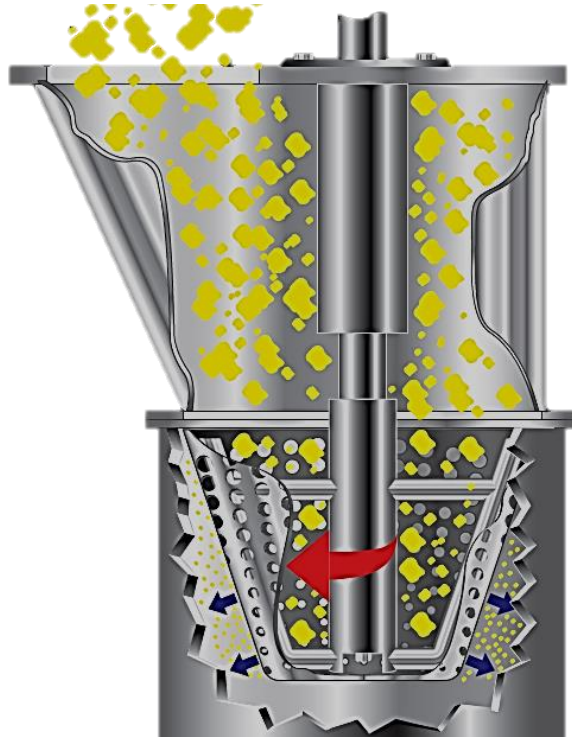


Figure 4.4 Comil inlet with milling apparatus (Quadro, 2017)

Centrifugal forces created through the rotating impeller, force the material through the perforated milling screen where the dried granulated material is uniformly sized before it is conveyed through gravity to the blending operation. The purpose of blending is fundamentally to reduce tablet to tablet variation, this is achieved through mixing the powder blend to such a degree that each ingredient within the mixture is distributed evenly throughout the bulk of material.

A helical blending machine is used to mix the milled material through agitation using a rotating helix located within the blending chamber as shown in figure 4.5 which also displays the agitation pattern of the milled material within the chamber. Material enters the chamber and is thoroughly mixed through the rotating helical agitator for set period of time.

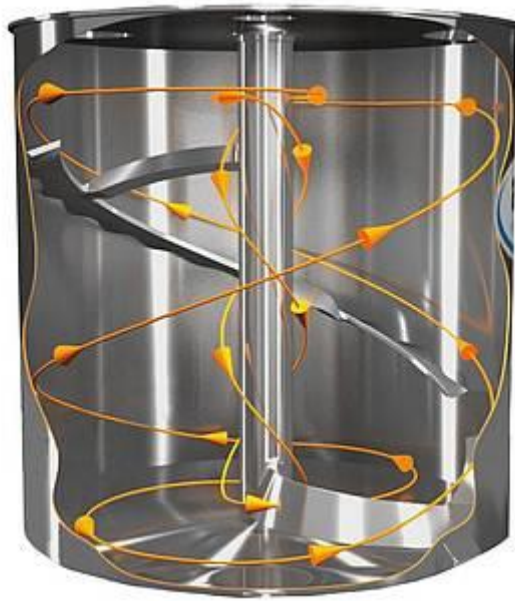


Figure 4.5 Blending chamber with helix agitator (Ribbon Blender and vertical single-shaft mixer - amixon GmbH, 2017)

Several feeder inlets are located around the blending chamber to allow for the input of lubricants to reduce the shear forces on the material and the input of milled material to keep the blender primed with product. The blended material is then conveyed by gravity to the tablet compression stage. No sampling of material occurs between the blending stage and the compression stage.

The compression stage of the tableting operation involves the transformation of the granulation mixture into solid dose oral tablets using tableting machinery. The tableting machine consists of a series of cavities or dies and punches (upper punch and lower punch) that come together using Compression rollers to compress a volume of powder into a tablet as shown in figure 4.6.

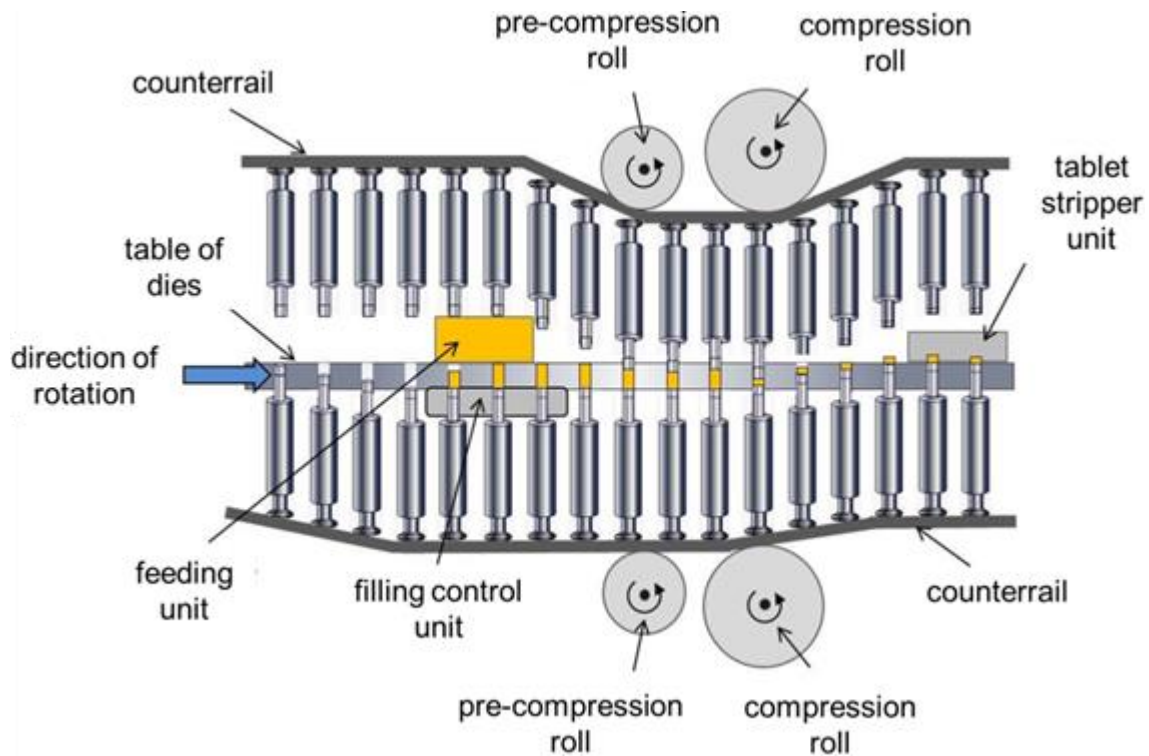


Figure 4.6 Depicts a rotary tableting machine similar to that of GSKs, that compresses a blended powder mixture into solid dose oral tablets (The Theory and Practice of Pharmaceutical Technology | Digital Textbook Library, 2017).

Material is fed into the cavities that are calibrated to contain the correct volume of material to produce a single tablet. The lower punch is located at the base of the cavity while the upper punch is suspended above. Once the correct volume of material is present in the cavity, the upper and lower punch come together through compression rollers to compress the powder within the cavity. A predetermined pressure is applied to the material so that when released the material has formed to a solid at which point the lower punch is then initiated via a counter-rail, to expel the tablet from the cavity for collection (Choudhary, 2011).

4.2.1 CTL Process Overview

GSKs CTL is currently operating in semi-batch/semi-continuous mode as it does not possess any closed loop control feedback to enable real time adjustment of CTL equipment such as granulators, dryers and milling machines. The process is controlled through a mixture of manual adjustments based on the results of off-line analytics in between unit operations or automatic pre-set values such as drying timer programmes. Each unit operation is connected through a system of pipes used to convey the material to and from each unit operation automatically through vacuum or gravity conveyance techniques as depicted below in figure 4.7. Material sampling ports are located in between each unit operation to allow for the manual extraction of material samples to monitor the material as it is conveyed through the process stream, however material is only sampled at the unit operations listed in table 4.1.

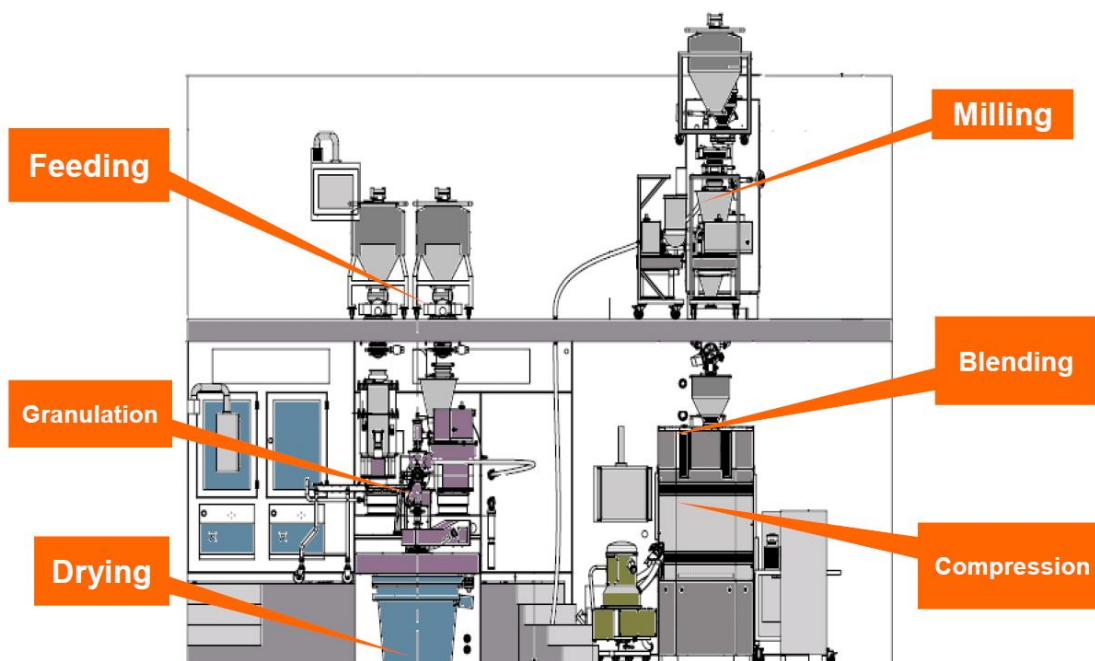


Figure 4.7 Block Diagram of GSK Tableting Process and Pipe System (Opitz, 2016) (Opitz, 2014a).

Table 4.1 lists each unit operation, the sampling method used and the Critical to Quality Attributes (CQAs) measured for each operation. During Raw material input into the granulator a sample of the powder blend is obtained to measure the chemical composition of the mixture to ensure ingredient ratios conform with predetermined values. No material samples are extracted from the granulation or dryer stage as the process is controlled through the pre-set parameters of the twin screw (i.e. screw feed, feed rate and liquid/solid ratio) and pre-set timers respectively.

Unit Operation	Sampling	Measurement
Raw Material Hoppers	Blend Sample	Chemical Composition
Granulator	N/A	
Dryer	N/A	
Mill	Thief Sampler	Particle Size Distribution
Blender	N/A	
Press	Manual Sample	Tablet Content Uniformity

Table 4.1 Sampling points, method and measurements taken from GSK CTL

A thief sampler is used to manually extract a sample of material from the outlet of the milling machine for off-line Particle Size Distribution (PSD) testing. Typically, 50% of the material passes through a 500µm mesh which is extracted and analysed, while the remaining particles (ranging between >500µm – 2mm) are diverted back into the milling machine to be milled.

The cycle time of the blending process, similarly to the drying process is controlled through a pre-set timer programme specific to each product and is not sampled after completion of this unit operation. After the tablet compression operation, several tablets are manually extracted from the tableting machine outlet and analysed off-line for content uniformity which must be between 85% - 115% nominal.

4.3 MBN Nanomaterialia & PAT

MBN Nanomaterialia are an Italian based manufacturer of ultrafine ceramic, metal and polymeric powders that are used in a variety of applications such as cutting tool coatings for heat, wear and corrosion resistance, raw materials for direct laser sintering and thermal spray powder coating applications. MBN offer innovative nanometric materials and solutions that are a direct outcome of technological research initiatives with a host of universities, research institutes and industries through Europe (MBN, 2017a).

MBNs involvement in the H2020 SPIRE ProPAT project is to accommodate the integration of the modular PAT system into their manufacturing process. MBNs processing of a Cermet composite material (tungsten carbide cobalt (WCCo)) was selected as the most suitable pilot operation to investigate the potential benefits of PAT systems. WCCo powder is used to deposit a thick coating using high velocity oxygen fuel spraying (HVOF), onto surfaces such as cutting tools to provide protection against erosion, rapid wear, corrosion and hostile environmental conditions (Opitz, 2014a). The particle size range of WCCo powder used in thermal spraying applications must be within the range of 10 – 38 μ m. Particles in the <10 μ m range exhibit poor flow characteristic and a reduction in surface hardness (Fauchais, Montavon and Bertrand, 2010) thus rendering them unsuitable for some thermal spray applications while particles above the 38 μ m range have a poor deposit efficiency and surface finish (Fauchais, Montavon and Bertrand, 2010).

The following section provides a detailed description of MBNs particulate material and production processes.

4.3.1 Tungsten Carbide Cobalt (WCCo) Milling Process (MBN)

MBNs milling process of the CerMet composite material (WCCo) in its current state, involves the pulverisation and milling of recycled WCCo tool-tips. WCCo must be processed under a dry and inert atmosphere as cobalt is prone to oxidation when exposed to oxygen and moisture. This is achieved through High Energy Ball Milling (HEBM), sieving and air classification of particles.

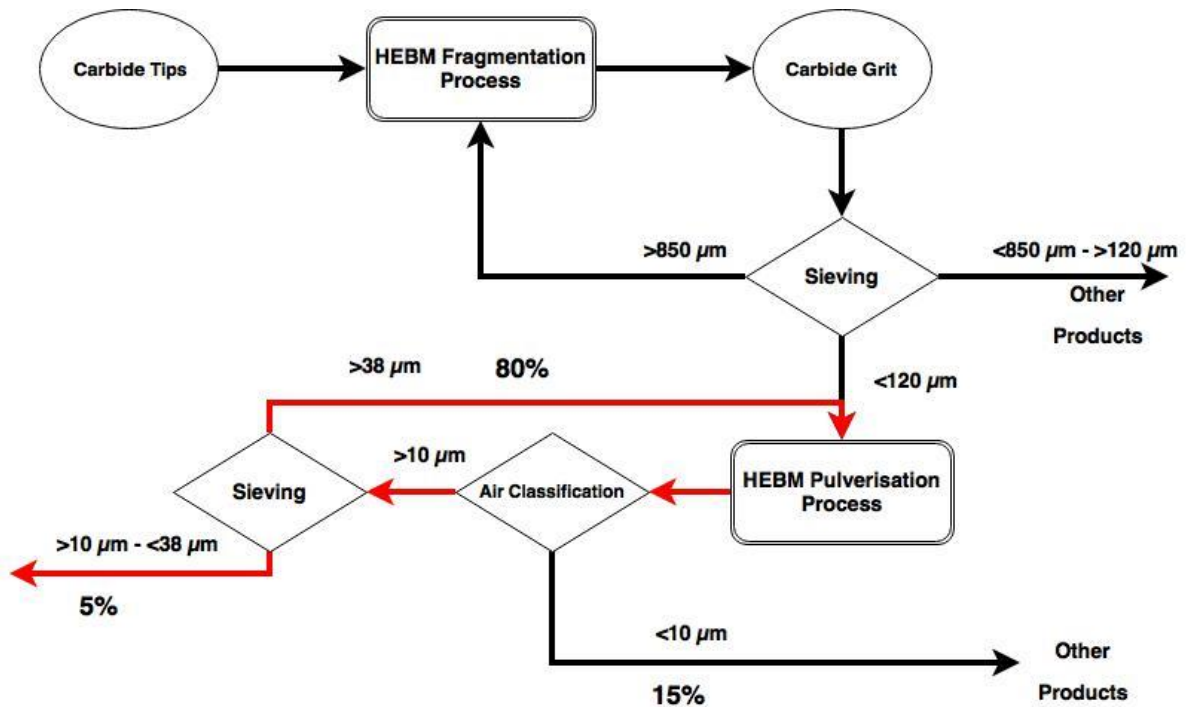


Figure 4.8 MBN Process Flow of WCCo Milling Process

Figure 4.8 details the WCCo milling process at MBNs manufacturing facility. The process flow denoted in red represents the area of the process selected for PAT integration. MBN manufacture their WCCo powder from recycled carbide tips using a series of HEBMs, sieves and air classification units. Carbide tips are loaded into the first HEBM where a WCCo grit, having a coarse distribution of particle sizes up to some mm, is produced. HEBMs fragment particles using the impact of steel ball bearings within the mill on the material to reduce the particle size of the material as depicted in figure 4.9.

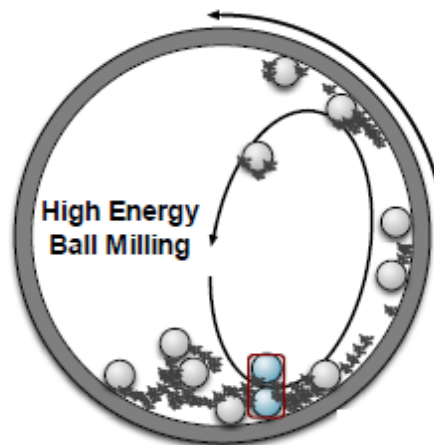


Figure 4.9 Agitated steel bearings impacting on material for particle size reduction through pulverisation (Opitz, 2014b)

The material is then classified using a series of sieves that separate the material to different areas within the process stream according to their respective particle sizes. Particles $>850\mu\text{m}$ are conveyed

back to the HEBM for further fragmentation, particles within the range of 120 - 850 μm are harvested for other applications and particles <120 μm are collected for further processing. For the purposes of this case study and the ProPAT project, the process relating to particles <120 μm will be discussed.

As previously stated, HVOF spraying requires WCCo particles within the range of 10 – 38 μm to ensure product quality. This is achieved through running several batch cycles through the HEBM pulverisation process. The material must be repeatedly sieved and/or redirected to the pulverisation process, according to particle size, as the main parameter affecting particle size is cycle time. The greater the cycle time of the HEBM, the greater the number of particle <10 μm , resulting in a low yield of 10 - 38 μm particles. Conversely, the lesser the cycle time, the greater the number of cycles required to mill the product to the specified range of 10 – 38 μm .

As the material exits the HEDM pulverisation process, an air classification unit separates the material into the predetermined particle size ranges, where it is then redirected to areas within the process according to respective particle sizes. Particles <10 μm are sorted by the air classifier and collected for other application while the remaining material is passed through a 38 μm mesh and collected for HVOF applications. Particles too large to pass through the mesh are redirected for pulverisation in the HEBM. For each complete cycle, 5% of the total mass of material loaded into the HEBM pulverisation process produces particles <38 μm , with the remaining 95% of the material is conveyed to the HEBM for re-work.

As the 38 μm mesh expands in 2D, particles with a larger 3D structure i.e. rods, can pass through the mesh which results in larger particle size measurements that can affect the product quality. Samples of milled material within the expected range of 10 - 38 μm , when analysed off-line have shown that particle size distribution of the material can be recorded as high as 10 - 100 μm approx. as shown in figure 4.10.

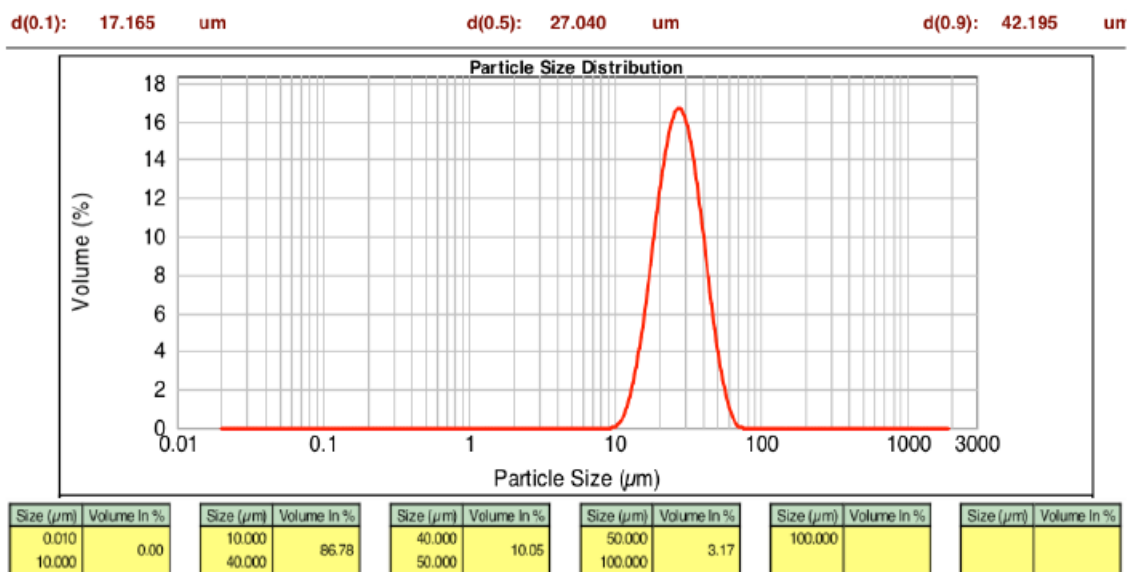


Figure 4.10 MBN Particle Size Distribution Off-Line Analysis of WCCo Powder (Opitz, 2014a)

Figure 4.10 also outlines the effectiveness of the air classification unit in comparison with the 38µm mesh. 0% of particles within the sample are shown to be <10 µm, while approx. 13% of particles passing through the 38µm mesh exceed the 10 - 38µm predetermined particle size range, resulting in an accuracy of approx. 87%.

4.4 Improvements Through PAT Implementation

This section focuses on the potential improvements offered by an embedded PAT system through careful determination of key measurement locations and the selection of suitable measurement systems, sensors and process analysers in both GSK and MBN processes. The information on sensor type and location will then be employed to develop a MPSU capable of analysing and controlling the physical and chemical properties of a bulk material in real-time. A number of sensors will be chosen from both case study applications and integrated into the sensing unit for proof of concept. Instances where sensors are integrated directly to plant equipment will not be considered due to access issues and availability of plant equipment. Therefore, sensors located within conveyance lines i.e. pneumatic pipelines between processing equipment, will be selected for proof of concept as this can be more accurately replicated using the sensing unit in a laboratory test environment.

4.4.1 GSK Process

GSKs main requirement from the ProPAT project is the implementation of in-line sensors for assessing the physical and chemical properties of pharmaceutical blends in their continuous tableting line (CTL) with a view to providing real-time control of CQAs. Particle Size Distribution (PSD), particle shape, moisture content and chemical composition provide information on the quality of the final product and the ability to achieve automatic in-process control of product quality. Automatic in-process

control of CPPs will enable the transition of GSKs CTL from semi-batch/semi-continuous to continuous closed loop production of pharmaceutical solid dose products.

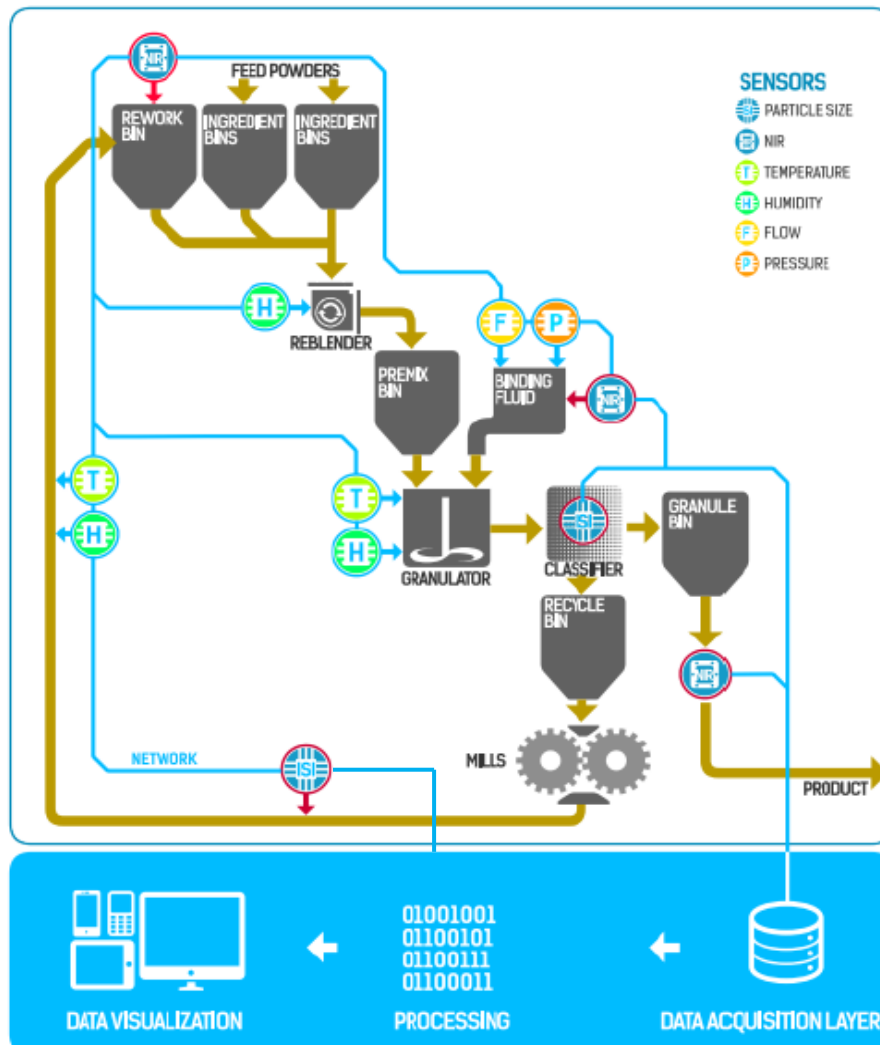


Figure 4.11 ProPat schematic of upgraded CTL with integrated ProPat system (Digby, 2014)

Figure 4.11 details the suggested locations of PAT sensors (determined through collaborative ProPAT team meetings) along the CTL process and the information flow from plant equipment to data visualisation systems and control-platforms using on/in/at-line analytical techniques. As shown in figure 4.11, raw material is fed into the blender along with reworked material extracted from the milling process and conveyed back to feeding hoppers via 50mm stainless steel pipe networks. The reworked material is analysed for chemical composition via an NIR spectrometer and the data stream is used to control the input of raw materials into the blend stage, thus compensating for the ingredient ratios in the reworked materials to ensure a homogeneous blend.

During granulation and drying, the materials drying end point can be determined through embedded humidity and temperature sensors. The residual moisture of the powder can be determined in key

process locations that can provide real-time control feedback to spray dryer parameters. GSK expect significant cost savings after ProPAT implementation, particularly through minimisation of drying times through the detection of the drying end point of the material. This can be achieved through incorporating temperature and humidity sensors in key locations throughout the process.

Reworked material recirculated through the process is monitored for temperature and moisture prior to reintroduction to the blending process where additional raw materials are added. The subsequent blended materials moisture content is then closely analysed and monitored through granulation and finally controlled during the drying stage based on the data from humidity and temperature sensing.

Particle size analysers integrated into air classification systems can then be employed to sort material according to particle size and convey material to its respective process location i.e. for re-working operations or for collection as final product. In addition, the inline access to physical/chemical information of powder blends allows immediate corrective adjustments of plant equipment through closed loop systems.

With respect to particle size detection, optimisation of the process through reduced energy consumption, increased product quality and increased speed to market through elimination of off-line analytics, are expected to significantly contribute to a reduction in the costs associated with this manufacturing line.

4.4.2 MBN Nanomaterialia Process

MBN require their WCCo process to be 97% accurate in producing ultrafine powders for HVOF thermal spray applications. ProPAT aims to achieve this level of accuracy in conjunction with a reduction in cycle time through the integration of its PAT system into their process.

MBNs current process is monitored off line through particle size analysis which can take up to 2 hours and through manually weighing output to determine each batches yield percentage. Particle size analysis involves manually extracting a sample of product from the process and preparing the sample for analysis using laser diffraction techniques. Preparation of the sample involves the addition of 51 ml of dispersant solution (50 ml of water with 1 ml of Geospense (chemical for stabilising WCCo particles)) to 1 – 2 grams of WCCo powder. The sample is then manually stirred to agitate and blend the mixture while also removing any agglomerates that may be present. The solution is then analysed using MBNs Malvern Mastersizer 2000 as shown in figure 4.12 (Malvern-Panalytical, 2017). Each sample is measured 6 times and the average particle size range from the collective results is taken.



Figure 4.12 Malvern Mastersizer 2000 for off-line particle size analysis (Malvern Mastersizer 2000 particle size analyzer, 2017)

Consideration must also be given to the time for discharging the milling chamber and for the classification and preparation of the second batch. On-line monitoring of the process is expected to **reduce the cycle time by 30-40%** leading to considerable energy savings and increased productivity. In addition, high energy ball milling is a process that can induce different effects on the material like welding, work hardening, diffusion, heating, fracturing, flattening, alloying, mixing, etc. which affect the PSD. The on-line monitoring of the process can facilitate the prompt detection and reaction to deviations from predetermined quality levels before the process output is affected. In this application, it is estimated that the overall **process yield could be increased by 10%** through optimisation of the WCCo Process (Opitz, 2014a; Digby, 2014; Opitz, 2014b).

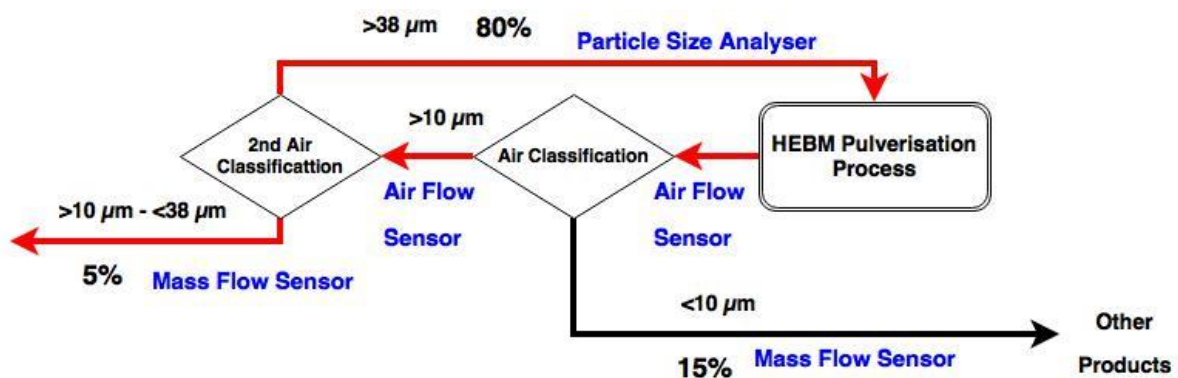


Figure 4.13 MBN WCCo Process with Integrated PAT system (Opitz, 2014a)

Figure 4.13 depicts the MBN process with integrated PAT system proposed by the ProPAT project team of which, this author was a member through IMaR. (The role of this author within the project team was to identify, source and validate measurement solutions for predetermined process parameters in the form of smart sensors and process analysers and provide support during concept generation and system design). The sieving operation has been replaced with a second air classification unit to reduce the number of large particles present in the 10-38 μm range, while a suite of integrated smart sensors (i.e. mass flow, air flow) and a particle size analyser monitor the CQAs of the product in real-time.

Material is conveyed to the High Energy Ball Mill (HEBM) for pulverisation via 50mm stainless steel pipe systems and exits the milling chamber to the first air classification unit. The first air classification unit removes particles $<10\mu\text{m}$ and conveys the material for collection. Microwave mass flow sensors will be employed to track the yield of material within the $<10\mu\text{m}$ range from the process while air flow sensors monitor the air classification unit to ensure the parameters do not deviate from pre-set values.

The remainder of the material is then conveyed to the second air classification unit where particles within the 10 - $38\mu\text{m}$ range are monitored in terms of mass flow as they are removed from the process for collection. Material with a particle size $>38\mu\text{m}$ is redirected to the HEBM via a particle size analyser that monitors the particle size of the material prior to entering the milling chamber. Milling parameters are then adjusted based on the output of the particle size analyser and microwave mass flow sensors thus providing MBN with the ability to eliminate the time and labour-intensive nature of off-line particle size analysis and the discharging of material from the milling chamber for yield determination.

4.4.3 Summary of Both GSK and MBN Process

To ensure the accuracy and effectiveness of a PAT system, correct measurement solutions and locations must be carefully selected as the system is only as accurate as the in-process data it receives. Each process step and variable must be considered prior to identification of suitable sensors, process analysers and key measurement locations. Sensors may be integrated into new or existing plant equipment, conveyance pipes (in-line) or redirected through recirculation loops (on-line) or bypass lines.

With respect to GSK and MBN processes, both processes detail the adaptability of a PAT system to integrate to existing plant equipment or material conveyance lines. In both cases, sensors are integrated directly into machinery such as blenders, dryers and air classification systems, in conjunction with sensors and process analysers integrated on the outlet pipes of machinery or conveyance lines between process steps.

Plant equipment will not be considered within the scope of this thesis due to restricted access to equipment. For the purposes of validating ProPAT designs and concepts, this thesis proposes the use of a modular sensing unit to house and validate a suite of sensors and process analysers situated on outlet pipes and within conveyance lines. Measurands from each process will be assessed and suitable sensory options will be catalogued and assessed for their suitability to their respective applications prior to the amalgamation of selected sensors into a single prototype sensing unit to monitor a dynamic stream of granulated material. Data from the material will be recorded in real time and used

to control the feed rate of material into the sensing unit to effectively simulate a powder processing operation with an embedded PAT system for real time process monitoring and control.

4.5 Conclusion

In the case of both GSK and MBN, significant improvements can be achieved through eliminating the manual sampling aspect of both processes. A significant improvement in process understanding can also be realised in both instances.

GSKs current methods of process control consist of 3 manually obtained samples analysed off-line for blend uniformity (start of the process), PSD (milling) and tablet content uniformity (end of the process). Information on the multi-factorial relationship between process variables on the quality of the final product cannot be obtained using this method as process variables are not monitored to the same degree as in a PAT system. The ProPAT system aims to incorporate smart sensors and process analysers at each unit operation for the purpose of streaming real-time production data back to PAT control platform for analysis using chemometrics. This will provide GSK with a real-time response to deviations in product quality while also offering new avenues to explore in the area of process improvement strategies.

Unlike GSK, MBNs current process does not possess any method of obtaining in-process data on materials between unit operations. Improvements from implementation of PAT systems with respect to MBNs process is therefore expected to be greater due to the lack of in-process data on MBNs part. However, the adaption of both GSK and MBN to the ProPAT platform will enable both organisations to closely monitor the slight interactions between CPP on their respective products and its effect on the CQA.

The case studies contained in this section, provide end user (GSK and MBN) sensory requirements that is used in this thesis to develop a scaled down PAT system for the purposes of concept validation. A combination of end user sensory options will be selected and integrated into a housing unit in the form of a Modular Prototype Sensing Unit (MPSU) and tested to determine if sensor output signals can be employed to provide real-time process information and closed loop control of a manufacturing process.

Chapter Five – ProPAT Sensor Suite Calibration

5.1 Introduction

This chapter focuses on the development of a “scaled down” Process Analytical Technology (PAT) system, in the form of a Modular Prototype Sensing Unit (MPSU), based on the process measurement requirements of ProPAT end users GlaxoSmithKline (GSK) and MBN Nanomaterialia. The main objective of developing this MPSU is to determine the ability of PAT to handle large multivariate data sets (from multiple smart sensors) in real time with a view to utilising this data for real-time process parameter control via production equipment. This chapter outlines the methodology behind the selection of suitable smart sensors and process analysers and techniques employed during the calibration of selected measurement solutions.

Also covered in this chapter is the design and configuration of the Prototype Modular Sensing Unit (MPSU) used to house the series of selected smart sensors and process analysers that are employed as a method of testing and evaluating the suitability of each sensor and analyser to monitor pre-defined CQAs of end user applications and the real-time control of CPPs.

End users processing conditions are then simulated using the modular sensing unit to determine the accuracy of measurement of each sensor and their ability to integrate into existing processes. This is achieved by conveying a blend of material through the sensing region pneumatically to gather real-time sensor data of in-process granulated material.

5.2 Selection and Calibration of Sensor Types for Sensing Unit

This section will look at the selection and calibration of suitable measurement solutions as outlined in chapter 3, to be incorporated into the Modular Prototype Sensing Unit (MPSU). The main objective of developing an MPSU, was to investigate the modularity of a PAT system and to determine the effectiveness of using fused data from a variety of pre-selected sensors to control the physical and chemical properties of the powder blend. This will be achieved through controlling the CPP's that affect the CQA's. Table 5.2 shows the sensor requirements and their respective applications in both GSK and MBN processes used in the selection process for the prototype sensing unit.

GSK Sensors	Applications
Raman Spectrometer	Chemical Composition
NIR Spectrometer	Blend Homogeneity
Pressure Sensor	Liquid Binder Pressure
Moisture Sensor	Humidity
Temperature Sensor	Drying End Point of Blend
Flow Meter	Liquid Binder Flow Metering
MBN Sensors	Applications
Raman Spectrometer	Particle Size Analysis
Mass Flow Sensor	Monitoring Yield %
Air Flow Sensor	Monitoring Air flow at Classifiers

Table 5.1 GSK & MBN CQA's and measurement solutions

Prior to sensor selection each sensory option was placed into one of the three following categories;

- Material Flow
- Chemical Characteristics
- Physical Characteristics

A sensor was then selected from each category to ensure a diverse range of measurands would be provided by the sensing unit, covering physical and chemical CQA's in conjunction with monitoring the flow of a dynamic medium such as a material pneumatically conveyed between processes. The sensors within each category were selected based on their respective performances within certain weighted criteria in the form of a Pugh Chart.

Material Flow					
Analysis Method		Not Applicable	On/In-line Real-Time Analysis		
Criteria	Weight	Datum	Liquid Binder Flowmeter	Airflow Sensor	Massflow Sensor
Cost	3	0	-	+	+
Calibration	2	0	0	+	+
Functionality	4	0	-	+	+
Accuracy	4	0	+	+	+
Efficacy of Data	2	0	0	0	+
Real-time measurement	3	0	+	+	+
Mechanical Interface	1	0	-	+	+
+		0	7	17	19
0		7	4	2	0
-		0	8	0	0
Net Score		0	-1	17	19

Table 5.2 Pugh chart with weighted criteria for selection of material flow-based sensors

Table 5.3 shows the results from a Pugh chart analysis of the sensors placed into the material flow category and consists of a liquid flow meter for GSK's liquid binder solution, an airflow sensor for monitoring the air flow of MBN's pneumatic conveyance of particles through its process and a mass flow sensor for the yield determination of MBN's pulverisation process. Application specific criteria were selected and weighted in order of importance for the purpose of assessing each measurement option in terms of suitability.

Of the 3 sensors listed in table 5.3, the mass flow sensor performed the strongest based on the criteria listed in table 5.3 and outperformed the liquid binder flowmeter in every criterion with exception to accuracy and real-time measurement capabilities. Furthermore, the application of the liquid binder flow meter is more suited to integration into milling and granulation equipment which falls outside the remit of this thesis.

With respect to the airflow sensor, the value of the data that could be obtained from real-time measurement of in-process air flow would not compliment or enhance the data from integrated process analyser to the degree of the mass flow sensor. Increasing air flow and thus material velocities

would have little impact to the accuracy of NIR or Raman spectra as the chemical composition would remain constant, whereas higher mass flow through a pipe system or vessel could potential alter the chemical composition of a material through changes in ingredient ratios. Thus, the selection of the mass flow sensor inn this instance is justified.

Table 5.4 details the results from the weighted Pugh chart analysis of the process analysers. Similarly to table 5.3, application specific criteria were selected and weighted in order of importance and the 2 options i.e. Raman and NIR spectroscopy, are compared.

Chemical Characteristics				
Analysis Method		Off-line laboratory analysis	On/In-line Real-Time Analysis	
Criteria	Weight	Datum	Raman Spectroscopy	NIR Spectroscopy
Cost	3	0	-	+
Calibration	2	0	0	0
Functionality	4	0	+	+
Accuracy	4	0	+	+
Ease of Use	2	0	0	-
Real-time measurement	3	0	+	+
Mechanical Interface	1	0	0	+
+		0	11	15
0		7	5	2
-		0	-3	-2
Net Score		0	8	13

Table 5.3 Pugh chart with weighted criteria for selection of process analysers

Despite being used by both processes for chemical composition and particle size analysis, Raman spectroscopy was not selected for use in the MPSU due to the lack of availability and high cost associated with the instrument (typically ranging from €8,000 - €25,000) (Stellarnet, 2018). Furthermore, the main objective to ProPAT is to develop a suite of low cost sensors and process analysers, hence the exclusion of Raman from the MPSU due to the high cost. Comparatively, NIR spectrometers typically range between €2,000 and €9,000, however the trade-off is in the interpretation of data which is significantly more complex with respect to NIR. NIR spectrometer

(which will be discussed in detail) are also easier to obtain on a trial basis due to their low cost. A suitable NIR spectrometer within the required wavelength range was made available to the Institute of Technology, Tralee for trial purposes from Ocean Optics (Ocean-Optics, 2018), allowing for the inclusion of the instrument in the MPSU for the measurement of blend homogeneity of a granulated powder blend.

Physical Characteristics					
Analysis Method		Not Applicable	On/In-line Real-Time Analysis		
Criteria	Weight	Datum	Pressure Sensor	Moisture Sensor	Temperature Sensor
Cost	3	0	+	0	0
Calibration	2	0	0	+	+
Functionality	4	0	0	+	+
Accuracy	4	0	+	+	+
Efficacy of Data	2	0	0	0	+
Real-time measurement	3	0	+	+	+
Mechanical Interface	1	0	+	-	+
+		0	11	13	16
0		7	8	5	3
-		0	0	1	0
Net Score		0	11	12	16

Table 5.4 Pugh chart with weighted criteria for selection of physical measurement-based sensors

Table 5.5 details the results from the weighted Pugh chart for the physical characteristic measurement options of a granulated powder blend and highlights temperature as the chosen characteristic due to its performance relative to application specific criteria. The pressure sensor as detailed in GSK's CTL process, monitors liquid pressure of the binding agent as it is introduced into the process and would not be applicable for use in the MPSU. While the moisture sensor monitors the residual moisture of a powder blend, the selected moisture sensor was the IMKO Sono-Vario Standard Radio-wave sensor (Imko, 2018) as it was significantly lower in cost than alternative sensor options. However, with a sensor body diameter of 108mm, this particular sensor was better suited for mechanical integration into plant equipment, vessels and large ducting.



Figure 5.1 IMKO Sono-Vario Radiowave Moisture Sensor (Tecdas, 2018)

The IMKO radio-wave sensor depicted in figure 5.1, must also be in physical contact with in-process material for accurate moisture measurement of material to be achieved. As the MPSU will be required to measure the characteristics of a dynamic powder blend in a conveyance pipe system, non-contact sensory options are preferred to ensure minimal disruption to material flow during testing as this could potentially distort the sensor measurements. Non-contact IR temperature sensors are capable of accurately measuring the temperature of a dynamic stream of powder with no flow interruption from protruding sensor heads on the pipe wall as optical fibres can be used to transport the optical signal to and from the medium to be measured to the sensing unit. Temperature measurement is also an important CPP of GSK’s CTL in determining the drying end point of their material, thus the inclusion of the temperature sensor in the MPSU is justified.

Sensor Category		Measurand	Sensor Type
1	Material Flow	Mass Flow	Non-Contact Micro-wave
2	Chemical Characteristics	Blend Homogeneity	NIR Spectrometer
3	Physical Characteristics	Temperature	Non-Contact IR Temperature

Table 5.5 Final selection of sensors for MPSU

Table 5.6 details the final selection of sensor types for the prototype sensing unit. The MPSU will incorporate the chosen sensors within these categories and are as follows;

1. Hense Mic Flow Meter (as discussed in Chapter 3, Section 3.5)
2. Ocean Optics NIR Spectrometer
3. Micro-epsilon IR Temperature Sensor

Each of the chosen sensor types are available with non-contact measurement through either optical sensing or through signal emittance/reflectance of the material to a sensing head. This ensures that

there is minimal flow interruption during material conveyance that could otherwise impede or distort the accuracy of sensors further upstream on the sensing unit. In general, non-contact sensors are also easily integrated into systems and processes via optical fibres that can mechanically couple to conveyance pipes or vessel walls to provide accurate measurements of process conditions in difficult to reach or hazardous areas.

A review of alternative methods of mass flow metering was conducted and several solutions were reviewed based on non-contact measurement techniques such as electromagnetic (Measurement, 2000), ultra-sonic (Envea, 2018) and microwave techniques (Bio-Thermal-Energy, 2018; Hense, 2018b). Research and development was also carried out on a series of novel mass flow metering techniques i.e. inertia sensing and acoustic measurements that formed the basis of an academic publication at the 2016 International Control Systems Technology conference in China (Murphy et al., 2016a; O'Mahony et al., 2016a).

With respect to temperature measurement of the in-process material, consideration was given to the use of embedded thermocouples and IR imaging cameras, however these techniques were deemed unsuitable for this application. Embedded thermocouples are more suited to immersive applications as they must be in contact with the medium to be measured, while thermal imaging cameras are both high in cost and difficult to integrate into production processes. IR temperature sensors were selected as they possess the ability to accurately measure the temperature of moving particles using non-contact optical techniques, furthermore, the integrated processor of the chosen Micro-Epsilon IR Temperature Smart Sensor in conjunction with its accuracy, cost (€600) and small footprint was highly advantageous when compared to alternative sensors (Raytek, 2017)

The emergence of smart sensor technology provides many benefits through significant reduction in calibration and set-up times of sensors during installation and commissioning which will be detailed in the following section.

5.2.1 Microwave Mass Flow Sensor

The Hense Mic-Flow Meter (as discussed in Section 3.5) was selected as it provided a non-contact method of measuring only moving particles in a conveyance system such as a pipe. During powder processing, there is the potential for agglomeration of particles within the pipe that can build up over time, particularly when the granulated material is exposed to some level of moisture, such as the addition of GSK's liquid binding agent within their process.

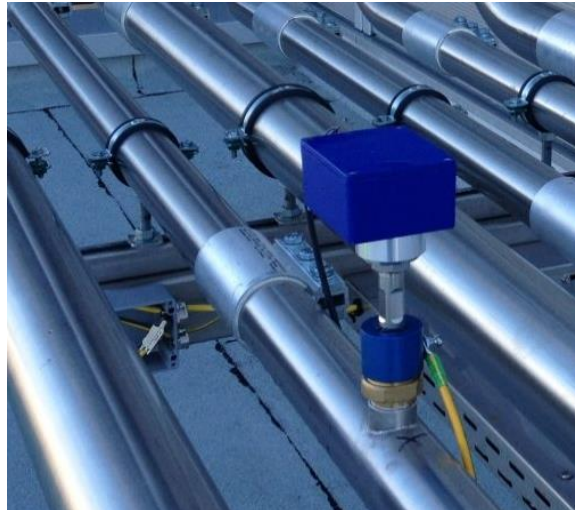


Figure 5. 2 Microwave mass flow sensor (Hense, 2018c)

The Microwave mass flow sensor as shown in figure 5.2, ignores static material and records the moving particle stream while providing a self-calibrated and conditioned signal directly to the control system. Table 5.7 details the microwave mass flow sensors specifications and shows that an Error of $\pm 2\%$ can be achieved using this sensor. Experimental testing of this sensor included the measurement of mass flow of coarse and fine sand in pneumatic and freefall flow conditions along with suitability to application testing which was achieved through use of WCCo samples obtained from MBN Nanomaterialia.

Hense Mic-Flow Meter	
Sensor Operating Principle	Microwave
Supply voltage	24 VDC
Current consumption	0,5 A
Measuring frequency	K - band (24, 125 GHz)
Output	0 - 20 mA (not standardized)
Reproducibility	+/- 2%
Operating temperature range	-10° C to 65° C / optional (optionally) 170° C
Material	
Sensor	stainless steel/ plastic or ceramic
Electronic enclosure	Aluminium
Protection class	IP 65
Mounting plug	1/2" NPT or as specified by customer
Optional	ATEX rating according to Zone 20
Electronics BW 10/40	
Line voltage	24 VDC
Output	counter pulse / kg
	4 - 20 mA / RS 232/422 / ProfiBus
Enclosure	Plastic
Protection class	IP 55
Mounting	wall mounting
Operating temperature range	0° C - 50° C
Cost (€)	3000

Table 5.6 Hense Mic-Flow Meter Specifications (Hense, 2014)

5.2.1.1 Experimental Test Conditions

The microwave mass flow sensor was calibrated for a wide range of flow rates with both coarse (0.5-2mm) and very fine sand (62.5-125um) for both freefall and pneumatic conveyance flow conditions to an error rate of approximately $\pm 10\%$. Sand was used as initial test material for assessing the microwave mass flow sensor as it was inexpensive and readily available, thus the calibration is not critical in this case as the output is only used to verify the dynamic response of the sensor in recognising changes in mass flowrates and its capabilities of monitoring mass flow in real-time. Further tests and calibration of the mass flow sensor are conducted upon completion of the test rig and integration of the mass flow sensor into the MSPSU using granulated blends of coffee and sugar (see section 6.4.4).

Calibration of the sensor, prior to experimental testing, was achieved through passing a material i.e. sand, of a known mass, passed the field of view of the sensor. The output reading of mass from the

sensor was then recorded and compared to the actual to determine the % error. The % error was then inputted into the software of the microwave mass flow sensor along with the actual value of mass. The test was then repeated using the same quantity of material and the error was reduced. This was repeated until a satisfactory level of accuracy was achieved.

The experimental tests consisted of 2 flow situations with a known particulate mass manually fed into the laboratory scale test rig for 2 flow situations: vertical free fall testing and vertical pneumatic conveyance. The particulate mass feed rate into the test rig was varied i.e. increasing over time, to evaluate the sensors accuracy over a wider range of flow conditions.

Both variances of particulate mass (coarse and very fine sand) were tested under vertical free fall and pneumatic flow situations, however due to the density of the very fine sand and the calibrated range of the sensor, this portion of the test did not provide any conclusive data thus, is not included in the tabulated results shown in table 5.8. The microwave mass flow sensor is limited in the sense that it can only be calibrated to one specific material type or a homogenous mixture. As the particle size distribution of the fine sand and coarse sand was too great i.e. $62.5\mu\text{m} - 2\text{mm}$, inaccuracies occurred during the measurement of the fine sand as the sensor was calibrated more in favour of the coarse sand. This highlighted the sensors limitations in measuring non-homogenous mixtures.

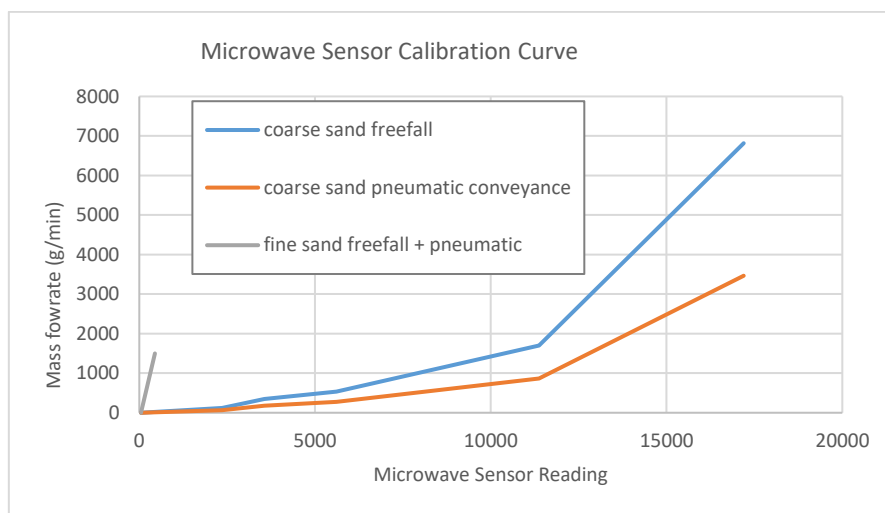


Figure 5.3 Microwave mass flow sensor calibrated for course and fine sand in vertical and freefall conditions (mass flow rate g/min vs sensor readout(mV))

Figure 5.3 shows the response from the microwave mass flow meter during calibration testing using fine and coarse sand particles at vertical free fall and pneumatically conveyed test conditions. A strong response signal is shown, particularly at higher flow rates, suggesting the sensors is best suited to applications of high mass flowrates (i.e. $>2000\text{g/min}$).

Figure 5.3 also details the effect of material velocity on the sensor output signal and must be considered during integration of the sensor onto the MPSU. In both test conditions, the velocity of the material during testing was not controlled to a high degree of precision and may have attributed to the inaccuracies of the results shown in table 5.8.

The tests P1 – P3 as shown in table 5.8, detail the results of the calibration tests carried out using the coarse sand material under pneumatic flow conditions. A quantity of sand was carefully weighed and the mass recorded before the material was conveyed through the sensing zone of the microwave mass flow sensor. As the material passed through the sensing zone, the accumulative mass flow was then recorded and displayed. Each test i.e. P1 – P3 involved a series of repeated experiments (15 tests per “P” test) where the same quantity of material was passed through field of view of the sensor. An averaging filter was applied through the sensor software to produce the average data value

Test	Actual Mass (g)	Recorded Mass (g)	Sensor Error(%)
P1	132.2	142.12	7.5
P2	103.4	95.05	-8.08
P3	130.8	130.83	0.03
Average % Error			5.2

Table 5.7 Actual mass vs. Recorded Mass using coarse sand

The results from table 5.8 show an average sensor accuracy of 95% with an average error of 5% during pneumatic conveyance testing. Despite the 5% error in the sensor output, the results were deemed favourable as they showed good dynamic response to the flow of material through the sampling chamber. Further accuracy of the sensor can be achieved through use of larger sample sizes. The microwave mass flow sensor records the average mass flow over time which can result in larger errors for smaller sample sizes.

5.2.1.2 Suitability Test (MBN)

Further testing of the microwave mass flow and its suitability to MBN’s process was carried out using sample WCCo material from MBN. 200g of 500µm WCCo and 200g of 10-38µm WCCo was provided by MBN for test purposes. The mass flow measurement range is specified by MBN at 0.50 kg/hr and the density of WCCo powder is approx. 15 g/cm³. As the material is of a high density, testing of the mass flow sensor with this material was required to ensure that accurate data could be obtained from the sensor.

The WCCo samples were tested using the microwave mass flow sensor and a variable speed auger feeder that would provide a controlled feed rate of material past the field of view of the sensor for

dynamic measurement of WCCo mass flow. 200g of 500 μ m WCCo and 200g of 10-38 μ m WCCo were introduced into the auger feeder individually to determine the capability of the sensor to measure MBN's WCCo Material. Through varying the voltage supply to the auger feeder and thus the rotational speed of the auger, it was possible to measure the sensor response at increasing feed rates. The mass flow rate for each test was then calculated by dividing the total mass (predetermined through scales measurements) and the time taken for each test.

Particle Size (μ m)	Auger Feeder Voltage Setting (V)	Total Mass (g)	Accumulated Mass (g)	Peak Amplitude (Raw Sensor Signal) (mV)
500	2	200	125	200
500	3	74	33	225
500	2	28	6	200
10 - 38	7	100	9	275
10 - 38	5	84	16	250

Table 5.8 Results from WCCo testing

Table 5.9 shows the tabulated results from the WCCo sample tests. WCCo of a known particle size and density was loaded into an auger feeding system set to a predetermined voltage and the accumulated mass as measured by the mass flow sensor was then recorded. As detailed in the above table, accumulated mass data from the sensor compared to the total mass is off by a factor of 2 for the 500 μ m sample and between 5 – 10 for the 10 - 38 μ m sample, due to the small sample sizes available. The limited sample size could not be recycled and re-circulated into the auger feeder efficiently without contaminating the sample and so the sensor could not be properly calibrated for this material. As sample testing only lasted a few seconds due to the small quantities of material available, the accuracy of the tests was affected. The accuracy of the microwave mass flow sensor can be greatly improved through adjusting the averaging filter in the sensors software, however this would require larger samples of material of repeated testing with uncontaminated samples.

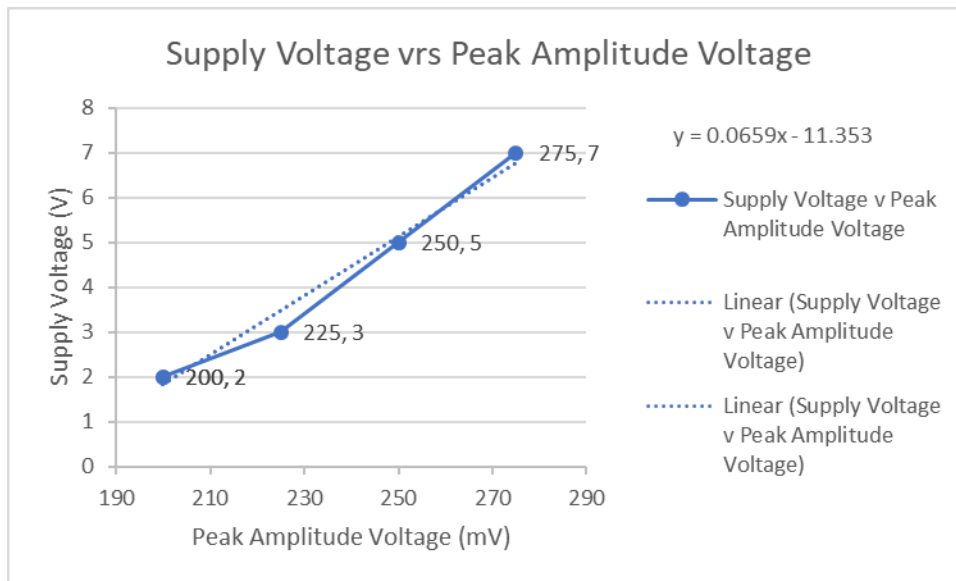


Figure 5.4 Linear relationship between supply voltage and peak amplitude voltage

However, despite the small sample size, a linear relationship (figure 5.4) can still be observed between the peak amplitude signal from the raw sensor output and the auger feeding systems supply voltage and shows the sensors suitability to the application, based on its ability to measure the test material. These results also indicate that a lack of material is the root cause of the calibration inaccuracies, which can be resolved through use of larger samples for testing and modifications to the sensors averaging filter. The tests indicated that the sensor shows a good response to varying flowrates for WCCo powder and excellent resistance to lens fouling as no material build up was present on the sensing head of the microwave mass flow sensor during this test or calibration tests involving larger material sample sizes as in section 5.3.

5.2.2 NIR Spectrometer

An Ocean Optics NIRQuest512 NIR spectrometer as shown in figure 5.5 (see table 5.11 for specifications) with wavelength range 900 – 1700 nm was used for the determination of blend homogeneity (as per the requirement of GSKs CTL in section 5.2.1).



Figure 5.5 Ocean Optics NIRQuest Spectrometer (Spectrometers, Optics, Nirquest and Bus, n.d.)

Coffee and sugar granules were used to determine the capability of the sensor to distinguish different materials based on their respective spectral wavelengths as recorded by the NIR spectrometer. These

materials were used in the testing of the NIR spectrometer, as they were organic materials, readily available, possess similar particle size distributions and flowability characteristics to APIs and excipients used in pharmaceutical tablet manufacturing (Nordic Sugar, n.d.; Valves, n.d.; All-Fill, 2018) as shown in table 5.10. Material samples such as API's or excipients could not be obtained from GSK for health and safety reasons.

Characteristics	Coffee	Sugar
Particle Size (μm)	100 – 1000	450 – 650
Bulk Density (kg/m^3)	304	705
Flowability	Semi Free-Flowing	Free-Flowing

Table 5.9 Physical properties of test material

The following section outlines the techniques used in processing the NIR spectra and developing a predictive model based on the data that was used for further testing at a later point.

Engineering Specifications	NIRQuest512
Dimensions:	182 x 110 x 47 mm
Weight:	1.18 kg (without power supply)
Detector:	Hamamatsu G9204-512
	InGaAs linear array
Wavelength range:	900-1700 nm w/Grating NIR3
Integration time:	1 ms – 120 s
Dynamic range:	15 x 10 ⁶ (system);
	15000:1 for a single acquisition
Signal-to-noise ratio:	>15000:1 @ 100 ms integration;
	> 13000:1 @ 1000 ms integration
Dark noise:	6 RMS counts @100 ms;
	12 RMS counts @ 1000 ms
Grating – standard:	Grating NIR3, 150 l/mm, 900-1700 nm
Grating – custom:	NIR10, NIR11, NIR12, NIR13 and NIR14
Standard slit:	25 μm
Custom slits:	10 μm , 50 μm , 100 μm and 200 μm
	(or no slit)
Order-sorting:	OF1-RG830 long pass NIR filter (optional)
Optical resolution:	\sim 3.1 nm FWHM w/25 μm slit
Fiber optic connector:	SMA 905

Table 5.10 Ocean Optics NIR Specifications (NirQuest Near Infrared Spectrometers | Spectrecology - Spectroscopy & Optical Sensing Solutions, 2018)

NIR spectroscopy is widely used in the pharmaceutical industry for the measurement of chemical composition of a granulated material. NIR spectroscopy is a non-contact and non-destructive form of

measurement that requires no sample preparation and records a materials chemical or physical properties based on that materials absorbance, reflectance, emittance or scattering of light. The data produced by NIR spectrometers is presented in the form of a spectral waveform (as shown in figure 5.6) and reference spectra must undergo pre-processing for accurate interpretation of any test data.

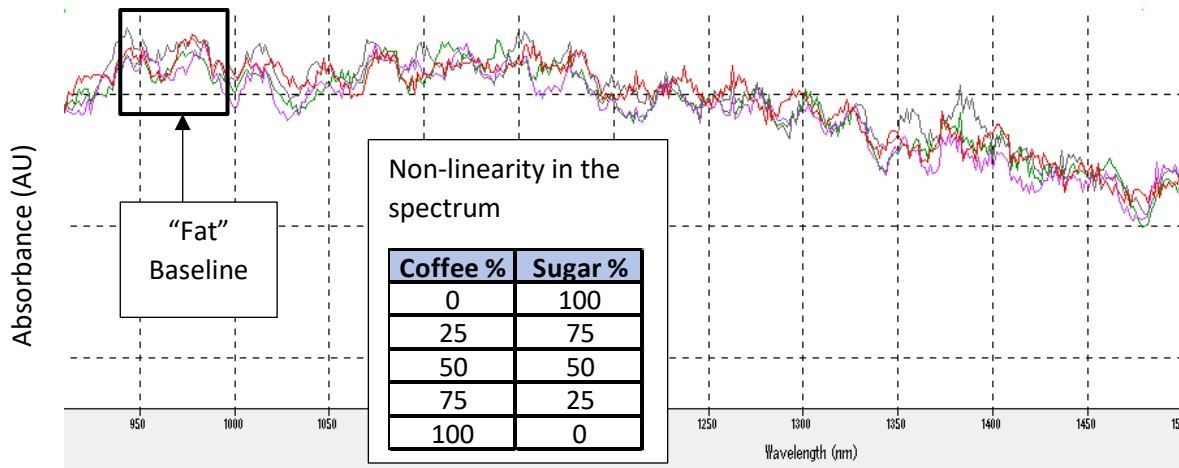


Figure 5.6 Raw NIR spectra from initial testing (Absorbance (AU) on Y axis, Wavelength (nm) on X axis)

The raw NIR reference spectra as shown in figure 5.6 depicts the spectral data of 4 blends of coffee and sugar at a mass ratio of 1:2:3:4 and shows a “fat” baseline and non-linearity in the spectrum despite the ratio of the granulated blend. The baseline in NIR spectra is used to determine subtle chemical variations in a material but can be masked due to the baseline shift, where the degree of influence is more pronounced in the longer wavelength of the spectrum. This phenomenon can alter the spectral measurements of samples that exhibit variable physical characteristics making them difficult to interpret correctly.

Further analysis of the above spectral data in figure 5.6 shows that at no point in the spectra, do all 4 samples have the same absorbance value nor is the space between each line equidistant despite the ratio of ingredients. Therefore, it is extremely difficult to determine the relationship between the variables of each sample without pre-processing of the reference spectral data.

5.2.2.1 NIR Pre-Processing and Analysis

Pre-processing of the NIR spectra was achieved through use of the CAMO Unscrambler X (Camo, 2004) multivariate analysis software package. Raw numerical NIR spectral data exported into the software, underwent Multiplicative Scatter Correction (MSC). MSC plots the raw spectra v the reference spectra and applies a best fit line according to regularized least squares regression (Labcognition, n.d.). This line provides the parameters that are used in the correction of the spectra as shown in figure 5.6 (corrected spectra shown in figure 5.7) based on the equation;

Equation 1. Multiplicative Scatter Correction (Labcognition, n.d.)

$$\text{Reference Spectra} = \frac{\text{Raw Spectra} - a}{b}$$

Where; a and b are the correction coefficients computed from the regression of each individual spectrum onto the average spectrum. Coefficient a is the intercept of the regression line, while coefficient b is the slope.

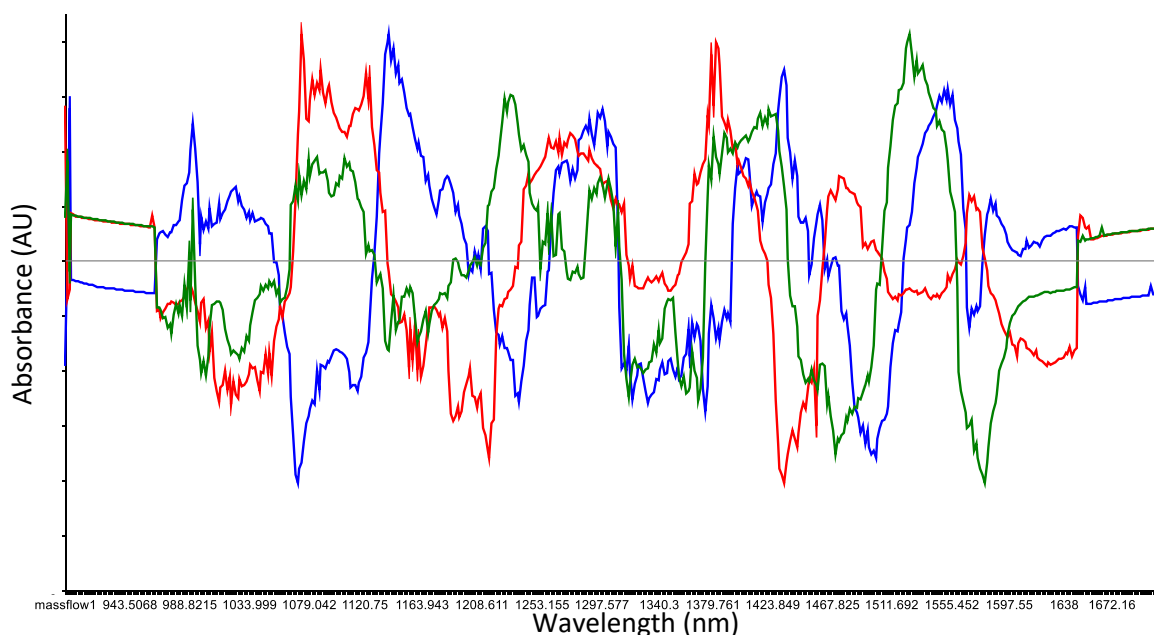


Figure 5.7 Pre-Processed Spectra of Coffee and Sugar NIR Data (Absorbance (Y) vs Wavelength (X))

A Partial Least Squares (PLS) Regression analysis was performed on the pre-processed data using the Unscrambler software to identify the relationship between variables. PLS is a statistical prediction tool that is used for data sets with a high quantity of variables that require dimensional reduction and works by “*successively extracting factors from both the X and Y such that covariance between the extracted factors is maximised*” (Maitra and Yan, 2008). PLS simultaneously models X and Y matrices to find latent variables in X that best predict latent variables in Y. These PLS components are similar to principle components but will be referred to as Factors from this point on.

Predictors with high collinearity are reduced to a smaller set of uncorrelated components and the resulting smaller set undergoes PLS regression to model the response variables in a multivariate fashion. The ability of PLS to fit multiple response variables into a single model allows for the explanation of the multifactorial relationships between process variables, hence its widespread use in the chemical and pharmaceutical industries. The resulting predictive model can then be employed to monitor or control in real-time, chemical and physical transformations of in-process material. This trait is aided by the computational speed at which PLS is performed which is due to the dimensional

reduction of the raw data set. Once the model is complete, a graphical overview of the analysed data is then outputted by the Unscrambler software to aid in the interpretation of the results which consists of the following;

1. Explained/Residual variance plots
2. Scores – Hotelling T^2 plots
3. XY-Loading plots
4. Predicted vs Reference plots

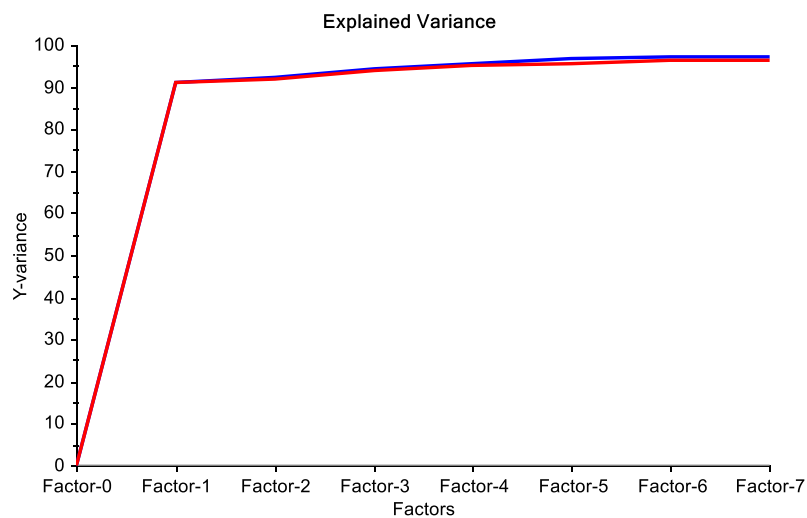


Figure 5.8 Graphical representation of Explained Variance

The explained variance plot (figure 5.8) explains how much of the Y variance is captured for each factor and determines a suitable number of factors to consider. Figure 5.8 shows that approximately, 90% of Y variance is captured in the first factor. In PLSR, latent variables are selected to provide maximum correlation with the dependent variables, thus, PLSR models contain the smallest number of factors possible. As factor numbers increase, the PLS model converges towards an ordinary multiple linear regression model (if one exists) (Tetko, I. V.; Gasteiger, J.; Todeschini, R.; Mauri, A.; Livingstone, D.; Ertl, P.; Palyulin, V. A.; Radchenko, E. V.; Zefirov, N. S.; Makarenko, A. S.; Tanchuk, V. Y.; Prokopenko, 2005).

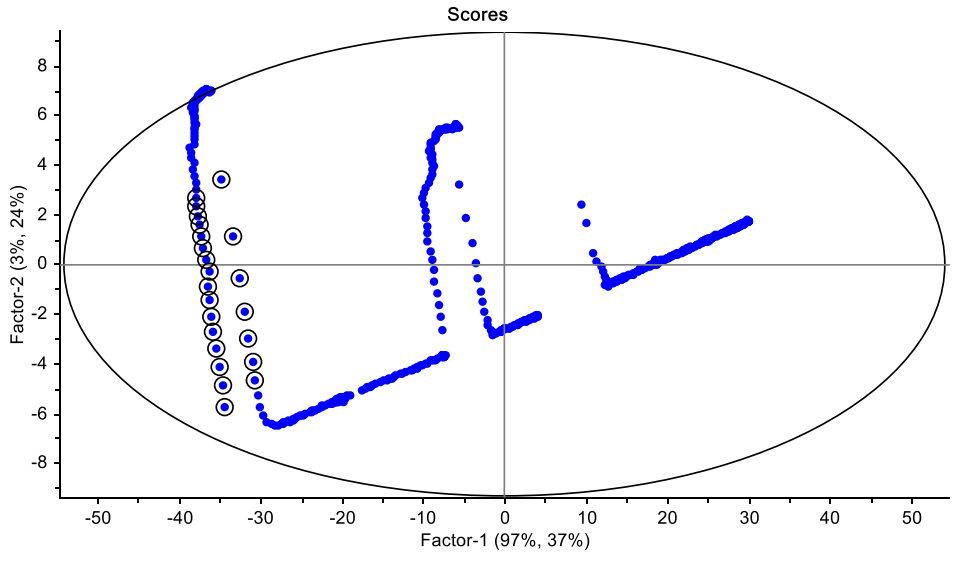


Figure 5.9 Scores – Hotelling T2 Plot

The Scores – Hotelling T^2 Plot (figure 5.9) is used to determine how well the data is distributed and the differences and similarities between sample data sets and is the multivariate extension of the Student's T^2 distribution (Tetko, I. V.; Gasteiger, J.; Todeschini, R.; Mauri, A.; Livingstone, D.; Ertl, P.; Palyulin, V. A.; Radchenko, E. V.; Zefirov, N. S.; Makarenko, A. S.; Tanchuk, V. Y.; Prokopenko, 2005). Under normal conditions 95% of the data should fall within the T^2 ellipse. The scores plot is most effective when used in tandem with a loadings plot. When the scores plot is used with its corresponding loadings plot it is possible to determine which of the variables are responsible for the differences in samples, for instance, samples to the right of the scores plot have large values for variables to the right of the loadings plot and small values to the left of the loadings plot.

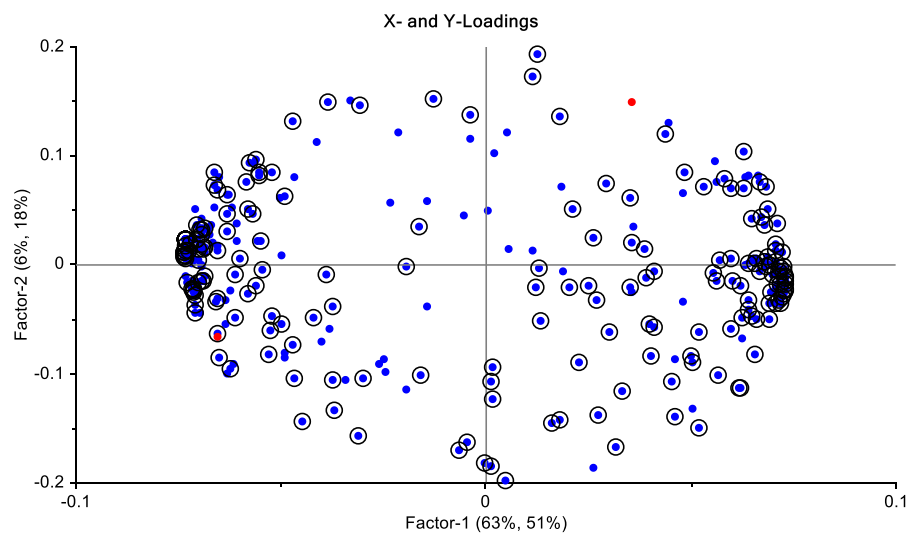


Figure 5.10 X-Y Loadings Plot

Figure 5.10 details the X-Y Loadings plot which is useful in determining the correlations between the independent and response variables while also indicating the % X variables that explain the % Y variables shown in brackets below the plot. If the value for the X variance is low and explains the majority % of the Y variance, this indicates that the number of input variables can be reduced to simplify the model. Figure 5.10 shows that 63% of X variance in the factor explains 51% of the Y variance.

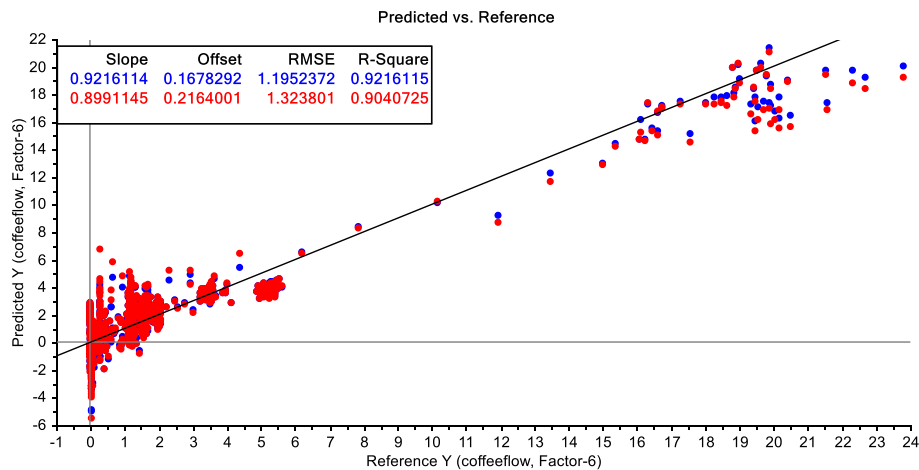


Figure 5.11 Predicted vs. Reference Plot

Figure 5.11 shows a predicted vs. reference plot from the results of a PLS model of coffee/sugar flow. The predicted vs. reference plot is used to determine the goodness of fit of the model to the data. If the plot shows points close to the straight line through the origin and with a slope value close to 1, the model is considered a good fit. The model also shows calibration results (red) and validation result (blue) that indicates how well the model fits the reference data and how well the fit of the model can be expected to perform for future predictions.

Statistical information such as RMSE and R-squared values for both the calibration and validation results is also displayed on the plot. The RMSE value shown in the above plot (figure 5.11) for the calibration and validation results is shown to be 1.195 and 1.32 respectively for a model containing 101 samples. RMSE is a measure (average of the squared errors) of the dispersion of these samples about the regression line, thus indicating the accuracy (approx. 99%) of the PLS regression models is satisfactory for both the reference data and future predictions. The R-squared value or the correlation coefficient of the PLS regression model also indicates the model performs well in handling new data sets.

The resultant plots from the PLS model provide an excellent graphical representation as to the models' performance in terms of the handling, processing and the predictive analysis of new data sets into the model. The numerical data of the model that is used to generate the plots can then be employed to

predict and control process variables in real-time. As new material is analysed by the model during normal production processes, the predictive values computed by the PLS model can be compared to predetermined reference values. The difference between these two values can then be employed as a response signal to the control systems of the plant equipment.

The overall accuracy of the model however, is entirely dependent on the quality of the original sample. Material contamination, poor material sampling and poor NIR set-up are just some of the many failure modes that could adversely affect the quality of the model. Models generated from contaminated samples can still yield favourable results as the contaminated sample is considered the reference, thus subsequent un-contaminated sample data from future testing would not be a good fit to the model resulting in poor predictability.

5.2.3 IR Temperature Sensor

For the non-contact measurement of a particulate mass, the ProPAT project team selected the Micro-Epsilon/ thermometer CT IR temperature smart sensor. The sensor was selected due to the high system accuracy of +/- 1%, repeatability of +/- 0.5%, its wide measurement range of -50°C - 600°C and its ability to accurately measure dynamic material flows (see table 5.12). The sensors form factor and signal processing capabilities were also advantageous in that its reduced size and separate optical probe allowed for simplistic integration into pipe systems via an M12 connection and sensor set-up times were minimal.

Micro-Epsilon/thermoMETER CT	
Material	Stainless Steel
Probe Dimensions	Ø14 x 24mm (M12 connection)
Temperature range	-50°C to 600°C
Spectral range	8 to 14µm
System accuracy	±1% or ±1°C
Repeatability	±0.5% or ±0.5°C
Temperature resolution	±0.1°C
Response time	150ms (95%)
Emissivity/gain (programmable)	0.100 to 1.100
Transmissivity/gain (programmable)	0.100 to 1.100
Environmental rating	IP 65 (NEMA-4)
Ambient temperature-sensor	-20°C to 130 or 180°C
Ambient temperature-controller	0 °C to 85°C
Relative humidity	10 - 95%, non-condensing
Vibration	IEC 68-2-6: 3 G, 11 to 200Hz, any axis
Shock	IEC 68-2-27: 50 G, 11ms, any axis
Signal processing	peak hold, valley hold, average; extended hold function with threshold and hysteresis
Certificate of calibration	Optional

Table 5.11 IR Temperature Sensor Specifications (Micro-Epsilon, 2016)

The Micro-Epsilon IR temperature sensor (figure 5.12) measures the surface temperature of a material or object through measuring the infrared radiation emitted from a material or object within the wavelength range of 8 - 14µm. Changes in surface temperature of a material results in changes in the intensity of emitted radiation and the intensity of the emitted radiation is dependent on the materials emissivity coefficient. Non-reflective dark bodied objects have high emissivity coefficients, whilst reflective or mirrored surfaces have low emissivity coefficients. The Micro-Epsilon IR temperature sensor software allows for the adjustment or calibration of the emissivity setting (defaulted to 0.95) to allow for the calibration of the sensor to different materials.



Figure 5.12 Micro-Epsilon (Micro-Epsilon, 2016)

This indicates that the sensor is only suited to applications involving homogenous powder blends as it is unable to distinguish between materials with differing emissivity values. Resultant values of the sensor when measuring a two-component mixture with respective high and low emissivity would result in excessively high or low temperature readings depending on the emissivity settings on the sensor. If emissivity is calibrated on the high end of the scale, the displayed temperature from the sensor would be lower than the actual surface temperature of the material and vice versa. However, with respect to the GSK application, the material will be sufficiently blended and homogenised prior to exposure to the sensors field of view, thus the sensor should be calibrated for a blended sample rather than individual ingredients. However, the inability of the sensor in distinguishing between differing material is not without its advantages. The emissivity settings allow the sensor to only focus on the material under process and exclude the temperature readings of housings, vessels and pipe systems, provided their respective emissivity values are not close to that of the material under test. To test the ability of the sensor to accurately measure the temperature of a blended sample, a coffee and sugar blend was formulated and the sensor was calibrated accordingly.

5.2.3.4 Sensor Calibration

A blend of 200g coffee and 200g sugar was formulated using water (300ml) as a binding agent to homogenise the mixture (similar to the granulation process of GSK's CTL) for the purpose of calibrating the IR temperature sensor to the emissivity of the test material. The "wet" mixture was placed into an oven at 40°C for a period of 24 hours to remove the moisture from the blend before the material was granulated as shown in figure 5.13. To ensure the complete removal of moisture from the blend, the material was weighed upon removal from the oven to confirm the total mass of the blend equated to 400g.



Figure 5.13 Granulated blend of 50% Coffee, 50% Sugar in baking tray after removal from oven

To calibrate the sensor to the blend, the mixture was again heated to 40°C and a thermocouple was inserted into the material to record the temperature of the blend. The IR temperature probe was then used to measure the temperature of the blend at the default emissivity setting of 0.95. The emissivity of the sensor was then adjusted until the temperature readout from the sensor equated to that of the thermocouple as shown in table 5.13.

Results from Sensor Calibration		
Sensor	Temperature	Emissivity
Thermocouple	37.7	N/A
IR Uncalibrated	23.2	0.95
IR Calibrated	37.4	0.68

Table 5.12 IR Temperature Sensor Calibration Results

A calibration accuracy of 99.2% of the reference thermocouple temperature was achieved through adjustments to the emissivity settings on the IR temperature sensor via the sensors software indicating the sensors suitability for the temperature measurement of a granulated blend of material.

The recorded emissivity value of the material (0.68), while lower than expected, is justified through comparison with the thermocouple readings. Emissivity values of most foods fall within the ranges of 0.85 – 1.00. The lower reading obtained from the calibration of the sensor could be due to the blending of the 2 materials. Reliable information on the emissivity values of a sugar/coffee blend could not be obtained and would require further investigation using specialised equipment to obtain the refractive index of the blended material. The refractive index of a material is a measure of the reduction of the speed of light inside the medium and is generally measured using a refractometer (in cases of liquids and gases). However, when dealing with fine powders, the refractive index of a material can be difficult to obtain accurately (PO-Laboratories, 2018).

5.3 Sensing Unit Mechanical Interface

For test purposes, it was necessary to house the selected suite of sensors in a single mechanical housing or interface to ensure that each sensor recorded the same material sample at simultaneously. It has been shown that the properties of a bulk solid mixture can be affected by changes in the particulate structure of a material i.e. size distribution, shape, texture (Allen, 2003b). Structural particle changes, particularly in pneumatic conveyance systems are caused through particle attrition which is the mechanical damage of particles during processing. Particle attrition occurs during the conveyance of material from one point to another. As material is travelling through, for instance a pipe system, the internal friction force on the pipe wall, particle impact and internal collisions wear down the material and can result in the alteration of particle size, shape and texture thus affecting the materials flowability, dissolution rates and potential for segregation (Pharmlabs, 2018).

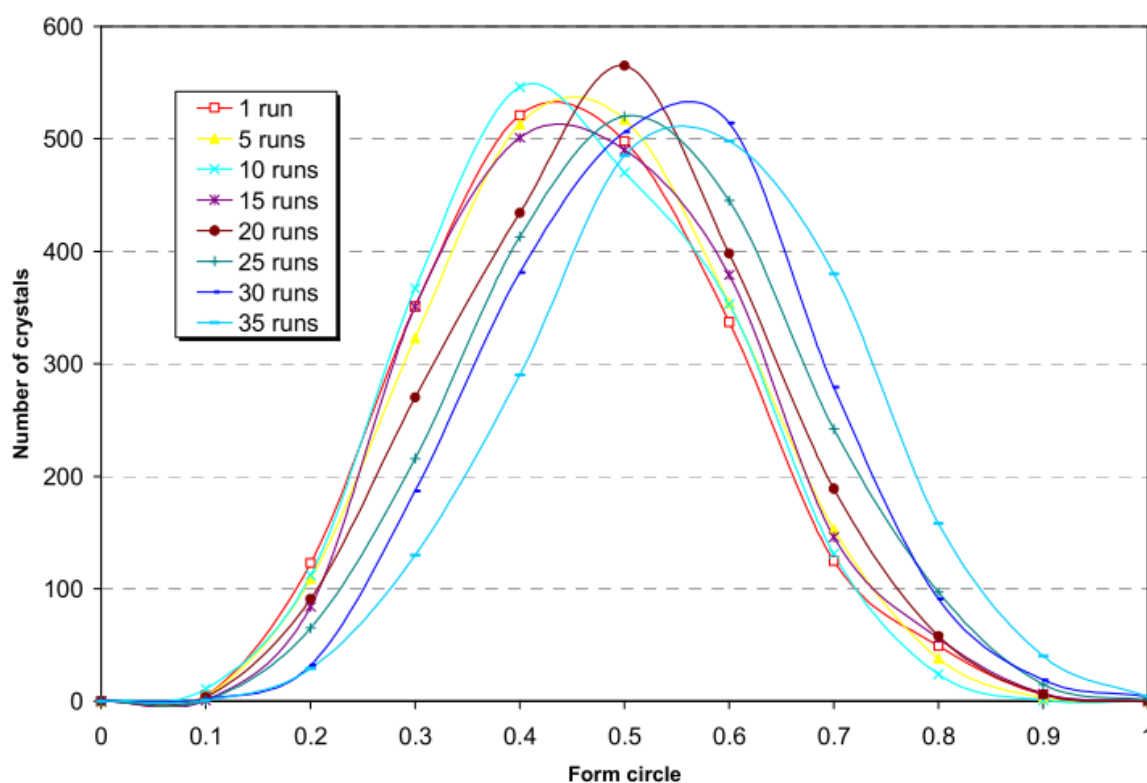


Figure 5.14 Analysis of Particle Attrition During Repetitive Cycling of Dextrose in a Pneumatically Conveyed System (Arakaki and Tel-tek, 2008)

The rate of particle attrition of a material is also dependant on the respective particle strength, the operational parameters i.e. velocity and the design of the conveyance system i.e. pipe material, no. of bends, radii and angle of bends. However, recent studies on the attrition of pneumatically conveyed dextrose through a pipe system (58mm pipe diameter) containing three 90° degree bends indicate that particle attrition occurs over a number of repetitive cycles (15 – 20) (Arakaki and Tel-tek, 2008). Figure 5.14 shows the cyclic conveyance of dextrose and its effect on the circularity of the particles

under test using number-weighted distributions constructed for the Feret ratio and the Form Circle factors. As can be seen in the figure 5.14, repetitive cycling of material does not significantly impact the circularity of the material until approx. 20 cycles. While dextrose and granulated sugar have similar physical properties, the inclusion of coffee adds an uncertainty as to the mechanical strength of the blend and so the levels of particle attrition could not be determined without particle imaging systems. Locating the chosen sensors in close proximity on a linear section of pipe would ensure that each sensor monitors the same sample of material, thus minimising the attrition or change of state in the material.

5.3.1 Modular Prototype Sensing Unit (MPSU) Design

In keeping with the standard pipe diameter of both GSK and MBN, a pipe system with an internal diameter of 50mm (stainless steel 304) was selected to convey the materials passed the field of view of the sensors. However, due to the internal curvature of the pipe wall and the dimensions of the selected sensors probes and sensing heads, it was not possible to locate the sensing heads flush to the internal pipe wall. Protruding sensor heads exposed to dynamic particle streams can cause a build-up of material in or near the sensing head. This material build up (shown in figure 5.15) can potentially obstruct the field of view of sensors or in some cases distort sensor readings resulting in inaccuracies.

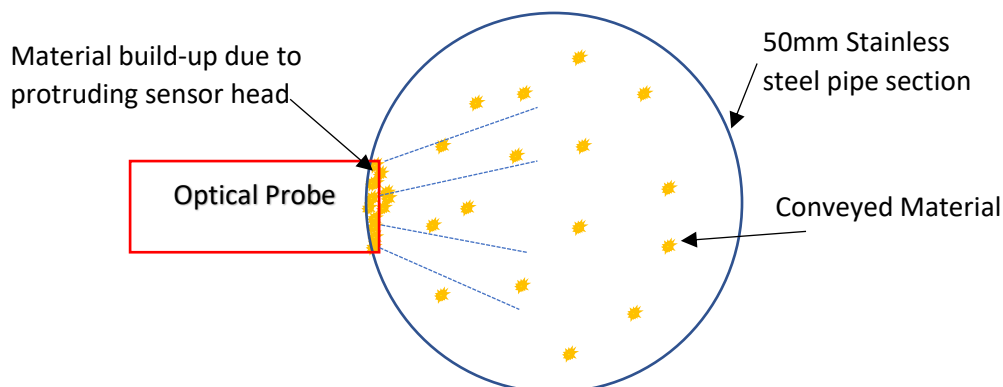


Figure 5.15 Schematic of Material Build-Up on Protruding Sensors

For the purposes of mounting the selected suite of sensors flush to the internal pipe wall to minimise particle build-up, a flat oval pipe section was proposed. However, as both GSK and MBN conveyance systems are comprised of 50mm round tubing, the flat oval section of the sensing unit would have to transition from round to oval to allow the system to be installed in the existing pipe systems. Consideration must also be given to the area of the pipe. Any change in the area of the pipe due to geometric transitions could incur pressure/velocity spikes or drops throughout the conveyance system that could negatively impact the flow of material, thus the area of the flat oval section must equate to that of the 50mm round tubing.

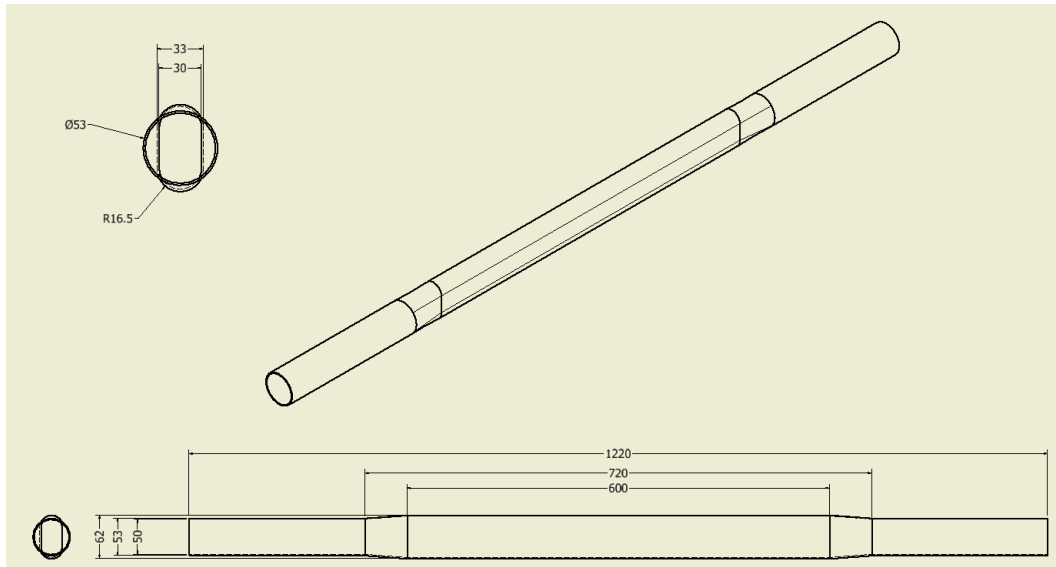


Figure 5.16 Sensing Unit Mechanical Interface Design

Figure 5.16 depicts the design for the mechanical interface to house the selected sensors and is comprised of a 50mm (internal diameter) stainless steel 304 tubing (250mm in length) at the inlet and outlet, a 60mm in length stainless steel 304 transition piece for round to flat oval coupling and 600mm stainless steel flat oval piece (59mm x 30mm internal dimensions). The purpose of the flat oval pipe section is to allow the probes from the selected sensors to be mounted flush with the internal wall of the pipe to reduce the potential for particle build-up around the sensing heads and to ensure minimal intrusion to the flow of material.

To reduce the influence of area change on the flow properties within the pipe system, a flat oval section with internal dimensions of 59mm x 30mm was sourced from Timeless Tubing (Timeless-Tube, 2017). This particular size was selected as the internal area of this section was the closest available in size to the internal area of the 50mm round pipe (as shown in the calculation below), however bespoke solutions were available at almost double the cost (depending on volumes).

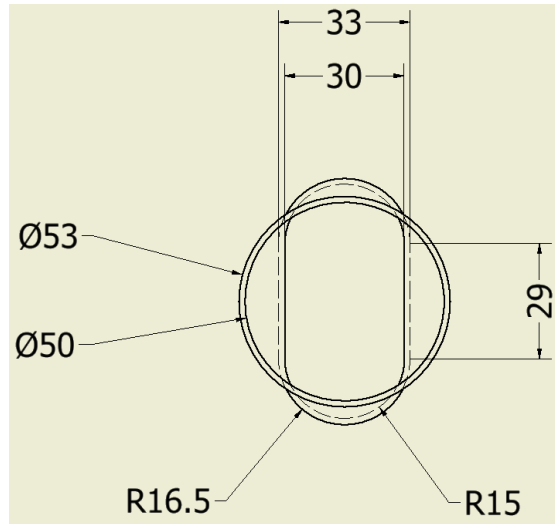


Figure 5.17 Dimensions for Calculation the Area of Round and Flat Oval Section

5.3.1.1 Calculations on the Effect of Geometrical Transitions on Internal Pressures and Velocities

Figure 5.18 depicts the Modular Prototype Sensing Unit (MPSU) housing and details the geometrical transitions that occur from inlet to outlet. Also specified in figure 5.18, is the air velocity at the inlet which was obtained from the end users during site visits to MBN Nanomaterialia. Under current MBN processing conditions, an airflow of 21.22m/s is employed as a method of pneumatically conveying materials through the manufacturing process so for the purposes of calculations and experimental tests, this airflow value is used.

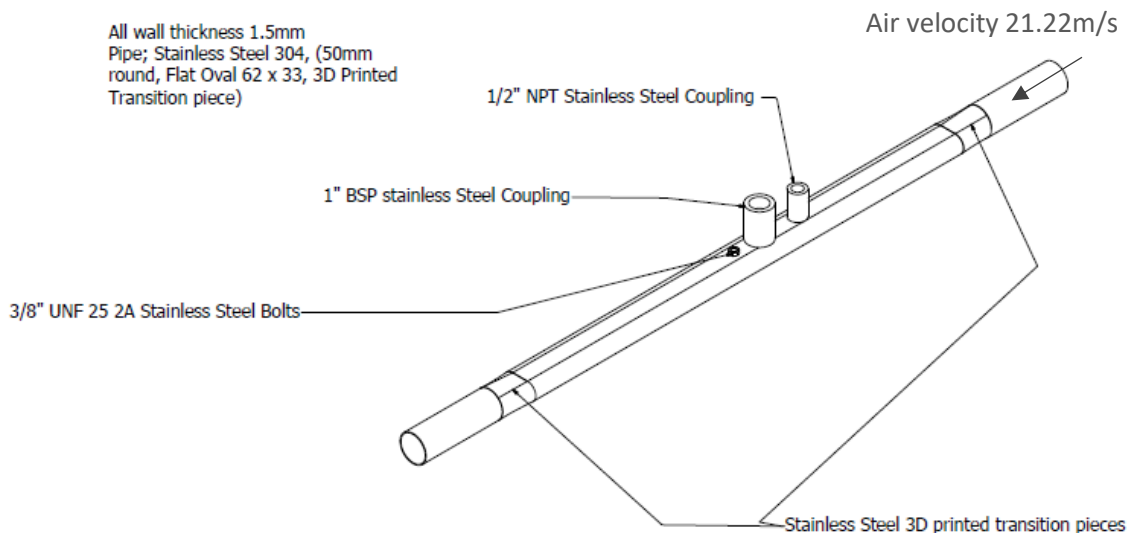


Figure 5.18 schematic of MPSU detailing initial air velocity at inlet

As the MPSU transitions from a conventional 50mm stainless steel round tube to a flat oval section as shown in figure 5.18, it is not known what affect this will have on the flow properties of the air and thus the material during testing. Area change within a pipe induces a velocity change on the conveyed

fluid and also impacts the pressure drop within the system. It is vital to ensure that the pressure drop within the system is not so severe as to impede the flow of material passed the field of view of the sensors. In order to determine the effect of area change within the MPSU on the flow conditions i.e. pressure drop and flow velocity, the following equations were employed.

1. Bernoulli Equation – relates the pressure, velocity, density and gravitational acceleration of an incompressible fluid. Assuming no friction. Used to determine the pressure drop across the area change within the MPSU i.e. round to flat oval transition section (Princeton.edu, 2018).
2. Equation of Continuity – describes how fluid conserves mass in its motion and provides useful information on the flow of fluids in a pipe (figure 5.19. Used to determine the velocity change in the MPSU (Engineering-Toolbox, 2018b).

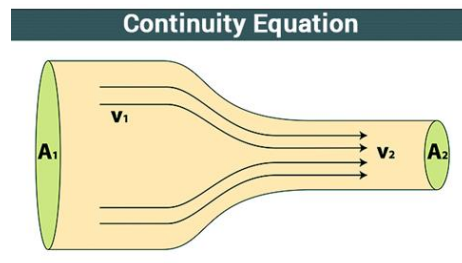


Figure 5.19 Equation of Continuity(Continuity Equation | Fluid Dynamics & Examples, 2018)

3. Darcy-Weisbach - is used to determine the pressure or head loss in a pipe due to frictional forces. This formula was used to determine the total pressure drop across the MPSU due to frictional forces (Darcy-Weisbach Pressure and Head Loss Equation, 2018).
4. Colebrook Equation – used to determine the pipe coefficient of friction (λ) (Engineering-Toolbox, 2018a)

Prior to the calculation of the above formulae, it was necessary to determine the CSA of both the round and flat oval pipe section as the area values are required for the equation of continuity.

Cross Sectional Area of 50mm round tube = $\pi R^2 \Rightarrow \pi 25^2 \Rightarrow \underline{1963\text{mm}^2}$

Cross Sectional Area of Flat Oval = $(H \times W) + \pi R^2$

Where;

H = Height of flat section = 29mm

W = Width (internal) = 30

R = Radius of the oval = 15

Thus, Cross Sectional Area of Flat Oval = $(29 \times 30) + \pi 15^2 = \underline{1577\text{mm}^2}$

The difference between respective areas = **386mm²**

Despite the area difference between the two sections, it was necessary to calculate the effect of this area reduction on the flow characteristics within the pipe system. This was achieved through use of the **Equation of Continuity** and the **Bernoulli Equation**.

Equation 2. Bernoulli Equation

$$P_1 + \frac{1}{2} \rho V_1^2 + \rho g Y_1 = P_2 + \frac{1}{2} \rho V_2^2 + \rho g Y_2$$

Where;

P_1 = Pressure (upstream) = ?, P_2 = Pressure (downstream) = ?

V_1 = Velocity (upstream) = 21.2m/s, V_2 = Velocity (downstream) = ?

Y_1 = Height (upstream), Y_2 = Height (downstream), (the unit is horizontal i.e. no change in height, thus Y_1 is assumed to equal Y_2)

ρ = Density of air at 20.2°C = 1.203kg/m³

g = acceleration due to gravity = 9.81 m/s²

As $Y_1 = Y_2$, the Bernoulli equation can be derived as; $P_1 + \frac{1}{2} \rho V_1^2 = P_2 + \frac{1}{2} \rho V_2^2$

And expressed in terms of $P_1 - P_2$ or $\Delta P = \frac{1}{2} \rho (V_1^2 - V_2^2)$

As the value of V_2 has not been determined, the equation of continuity must be employed;

Equation 3. Equation of Continuity

$$\rho_1 \cdot V_1 \cdot A_1 = \rho_2 \cdot V_2 \cdot A_2$$

As the density of air does not change in this system, the formula can be expressed as;

$$V_1 \cdot A_1 = V_2 \cdot A_2$$

Where ;

$V_1 = 21.22$ m/s, $V_2 = ?$

$A_1 = 1963\text{mm}^2$ or 0.001963m^2 , $A_2 = 1577\text{mm}^2$ or 0.001577m^2

$$\Rightarrow 21.22 \times 0.001963 = V_2 \times 0.001577$$

$$\Rightarrow V_2 = (21.22 \times 0.001963) / 0.001577$$

$$\Rightarrow \underline{\underline{V_2 = 26.4 \text{ m/s}}}$$

The equation of continuity calculates a velocity increase of approx. 5.2 m/s for V2 (26.4m/s) as the air is passed through the flat oval section and returning to 21.22m/s as it transitions back to the round section of the pipe system. Through substituting the calculated value for V2 into the **Bernoulli Equation**, it is possible to determine the ΔP that occurs due to the change in area as shown in the calculation below;

$$\Delta P = \frac{1}{2} \rho (V1^2 - V2^2) = \Delta P = \frac{1}{2} 1.203 (21.22^2 - 26.4^2) = \underline{\underline{-148.372 \text{ Pa}}}$$

At 148.4 Pa or 0.001484 bar (0.018% pressure drop from 8 bar inlet pressure), the pressure drop due to the area change within the pipe system would have a minimal impact on the flow properties within the pipe system. Pressure drop due to internal frictions are not considered in the above calculations but can be determined through use of the following **Darcy-Weisbach** formula.

Equation 4. Darcy-Weisbach Formula

$$\Delta P = \lambda \times \frac{L}{D} \times \frac{\rho}{2} \times \bar{w}^2$$

Where:

λ = Pipe Friction Co-efficient

L = Length of Pipe

D = Diameter (note: for non-circular pipes D_h (hydraulic diameter) is used)

ρ = Density

\bar{w} = Velocity

To solve for the above equation, the pipe co-efficient of friction (λ) must first be determined through use of the **Colebrook** equation and determining the **Reynolds** number for the flow conditions within the pipe.

Equation 5. Colebrook Equation

$$\frac{1}{\sqrt{\lambda}} = -2 \log \left[\frac{2.51}{RE \cdot \sqrt{\lambda}} + \frac{K}{D \cdot 3.7} \right]$$

Where;

RE = Reynold Number

K = Absolute Roughness of the Pipe = 0.015 for unpolished stainless steel (EnggCyclopedia, 2018)

As the friction co-efficient (λ) is involved on both sides of the equation, the **Colebrook equation** must be solved through iteration as it is not possible to solve through algebraic techniques. The **Reynolds number** must also be determined before solving the **Colebrook equation** and is calculated as follows.

$$RE = \frac{\bar{w} \times D}{\nu}$$

Where;

\bar{w} = Flow Velocity

D = Pipe Diameter

ν = Kinematic Viscosity = Dynamic viscosity/Density

Dynamic viscosity of air @ 20.2°C = 1.983 x 10⁻⁵N.s/m²

Density of Air @ 20.2°C = 1.203 kg/m³

$$\Rightarrow \nu = 1.983 \times 10^{-5} / 1.203 = 1.648 \times 10^{-5} \text{ m}^2/\text{s}$$

Thus, RE = (21.22 x 0.05) / 1.648 x 10⁻⁵ = 70358 (indicating turbulent flow)

The **Reynolds number** is a dimensionless number that is used to determine the flow state i.e. laminar or turbulent flow of a fluid in a pipe system. Fluid flow with a RE value of <2300 is considered to be laminar, while fluid flow with a RE value of >2600 (as in most cases) (Engineers-Edge, 2018) is considered turbulent. As shown in the above calculations, the fluid flow within the pipe system is considered turbulent. Turbulent air flow within the sensing unit will not impact the performance of the sensors as the material will still pass the field of view of the sensors.

Substituting the **Reynolds number** into the **Colebrook equation** now allows for the pipe friction coefficient (λ) to be determined.

$$\frac{1}{\sqrt{\lambda}} = -2\log\left[\frac{2.51}{70358 \cdot \sqrt{\lambda}} + \frac{0.015}{0.05 \cdot 3.7}\right]$$

As mentioned previously, the λ value is involved in both sides of the equation meaning the above formula must be solved through iterations. For efficiency and simplicity, the formula was solved using an online pipe friction co-efficient calculator (EnggCyclopedia, 2018) and yielded the following value for $\lambda = 0.08$. Substituting the λ value into the **Darcy-Weisbach formula** calculates the pressure loss due to friction for the 50mm pipe section (250mm in length).

Darcy-Weisbach Formula.

$$\Delta P = \lambda \times \frac{L}{D} \times \frac{\rho}{2} \times \bar{w}^2 = 0.08 \times \frac{0.25}{0.05} \times \frac{1.208}{2} \times 21.22^2 = \underline{\underline{108.8 \text{ pa}}}$$

When added to the pressure loss due to area change as per the **Bernoulli equation** (148.372 pa), the total loss from inlet to the flat oval section (as shown in figure 5.20) = **257.172 pa**. At **0.03%** of the inlet pressure, the resultant pressure drop is not considered large enough to negatively impact the performance of the sensing unit in terms of particle conveyance on sensor data acquisition. As the inlet pressure (P1) is regulated at **8 bar** or 80,000 Pa and the total loss in pressure = 257.172, this indicates that the pressure at P2 (flat oval section) = 79,742.828 Pa or **7.97 bar**. Furthermore, as the absolute roughness value (k) of the pipe (as used in the Colebrook equation) was given for unpolished stainless steel, the total pressure drop within the pipe is likely to be lower. Stainless steel pipe systems used in the pharmaceutical industry are required to be internally polished as standard to prevent material build up within the pipe. This also has the effect of reducing the frictional forces within the pipe resulting in a decreased pressure drop. This fact was considered when fabricating the MPSU and all pipe sections were both internally and externally polished.

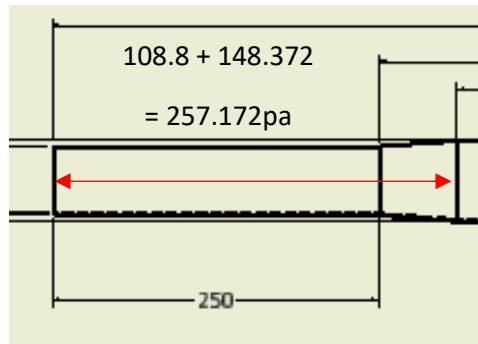


Figure 5.20 250mm, 50mm Diameter Pipe Section

Further in-depth calculations on the losses due to friction and area change are irrelevant as it has been shown that the flow conditions up to the flat oval section are not impeded sufficiently ($\Delta P = \sim 0.2\%$) to warrant further investigation and there exists sufficient pressure and particle velocity to convey the material passed the field of view of the sensors. Further confirmation is shown through basic Autodesk CFD simulations of the velocity profile and velocity XY plot of the sensing unit pipe system as shown in figure 5.21 and 5.22 respectively.

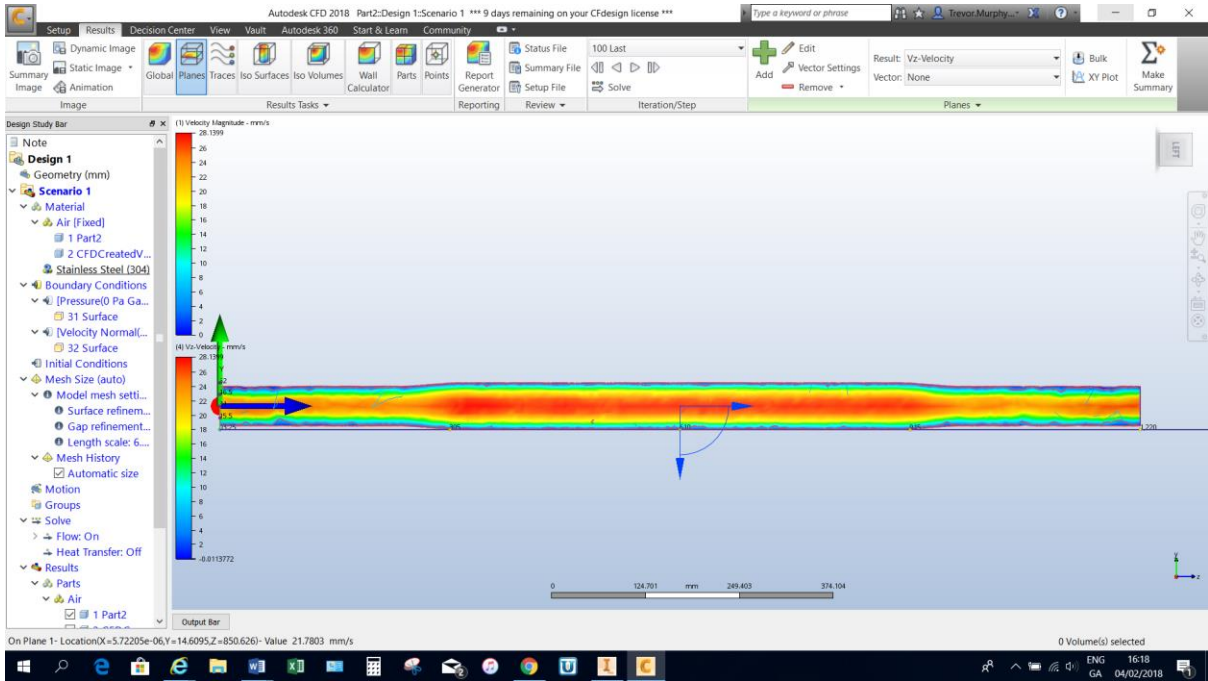


Figure 5.21 CFD Simulated Velocity Profile of the Sensing Unit Pipe System

Figure 5.21 details the velocity profile, denoted by the colour gradient and shows the increasing velocity as the flow transitions from round to flat oval at the inlet. As the flow is conveyed back to the round section at the outlet, the velocity is shown to decrease. An XY graph was plotted between the centre of the velocity profile from inlet to outlet to obtain numerical values for the above velocity profile and is depicted in figure 5.22.

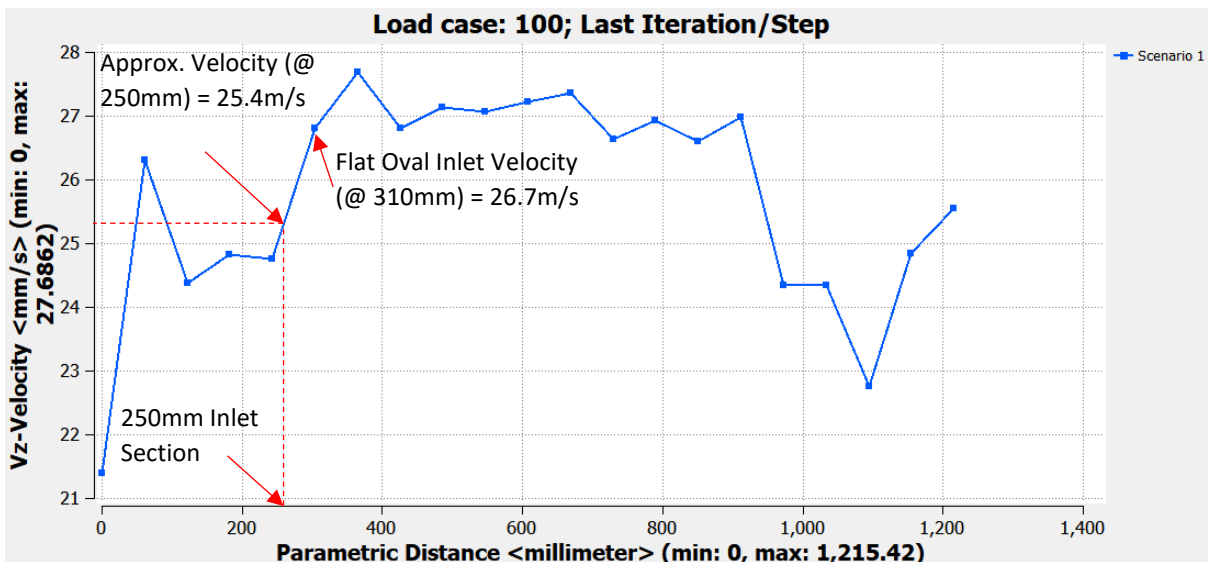


Figure 5.22 XY Plot of CFD Velocity Analysis

As shown above, the XY plot shows a sharp increase in velocity as the flow reaches the transition piece and is recorded in the above plot at approx. 25.4 m/s. Using the equation of continuity, the velocity

increase (V2) was calculated at 26.4 m/s indicating a difference of 3.8% between calculated and simulated results. This error is due to the 60mm transition piece that was not included in the calculations as the calculations assumed an abrupt transition from round to flat oval sections. A more accurate reflection of results can be seen if the point on the graph at which the completion of the transition from round to flat oval is taken i.e. at 310mm into the pipe section and is shown at 26.7m/s. The resultant % difference between the calculated value and that of the simulated value 310mm into the pipe section is then 1.1%.

5.3.1.2 Assembly and Sensor Integration

Assembly of the sensing unit housing was comprised, as per design, of a 250mm stainless steel round tubing at inlet and outlet, 2 x round to flat oval transition couplings and a 600mm length of 62mm x 33mm flat oval tubing. With respect to 50mm round and 62mm x 33mm flat oval tubing, these components were easily sourced from stainless steel suppliers (Timeless-Tube, 2017) as off the shelf stock items. The transition couplings however required fabrication. The most efficient and accurate method of fabricating the couplings was through additive manufacturing techniques such as laser sintering through U3Ds 3D printing facility (U3D, 2017) as shown in figure 5.23.

The cost of 3D printing the parts was significantly lower at €1,200 compared to the cost to fabricate the parts (€2,000) using conventional methods. Additionally, it was felt that the accuracy provided by the laser sintering process was advantageous.



Figure 5.23 3D Printed Transition Couplings

This method of fabrication however, was not without its drawbacks. Dimensional limitations of the 3D printer restricted the overall length of the parts to 60mm (which was accounted for in the original design). Preferably, the overall length of the transition couplings would exceed the 60mm of the 3D printed parts as the more abrupt the transition, the heavier the frictional losses, while more gradual

changes result in much lower pressure drops. “The degree of permanent pressure lost through a pipe size change is dependent on the geometry of the size change” (Neutrium, 2012). Surface finish on the transition couplings also required further work. Laser sintered parts have a granular finish caused through the fusion of (in this case) stainless steel 304 powder via high powered and concentrated lasers.



Figure 5.24 transition Pieces After Polishing process

Prior to use, the couplings underwent a polishing and grinding process to remove the granular surface resulting in a mirror finish on the finished couplings (figure 5.24). Aside from the aesthetics, the mirror finish, particularly internally, prevents material build up or agglomeration occurring within the granular or porous structure of the pieces.

Prior to the assembly of the components, consideration was given to each sensor mechanical requirements as shown in table 5.14.

Sensor	Requirements
IR Temperature Sensor	10mm bore in pipe wall
	Reflective surface (Metallic)
	M12 coupling (welded to test rig)
Microwave Mass Flow	1" NPT Coupling (welded to test rig)
	24mm bore in pipe wall
NIR Spectrometer	2 x 3/8"-24 UNF couplings (welded to pipe wall)
	2 x 9.5mm bores (directly opposite)

Table 5.13 Sensor Mechanical Interface Requirements

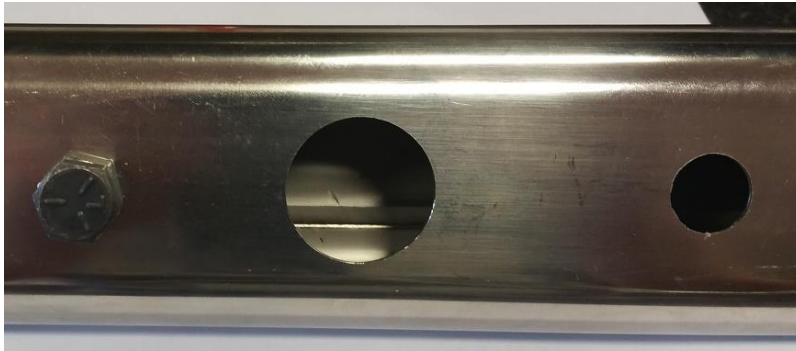


Figure 5.25 Sensor Location Points

To accommodate the sensor probes a series of holes drilled into the flat oval section in the centre line of the 600mm flat oval piece (figure 5.25). M12, 1" NPT and 2 x 3/8" UNF couplings were fused to the flat oval section to cover the holes and allow the respective probes to couple to the sensing unit. Modifications to the 1" NPT coupling, detailed in figure 5.26, were required to mate with the curvature of the flat oval section and ensure the unit is sealed adequately after assembly.



Figure 5.26 Modified NPT Coupling

Assembly of the sensing unit was achieved using tig welding to join the various components and was completed by DairyMaster welders at their facility in Causeway Co.Kerry (Dairymaster, 2018). Tig welding lends itself to applications requiring small intricate welds which made it the preferred choice to bond the couplings and bolts to the pipe wall while maintaining an air tight seal. Prior to welding the couplings and nuts onto the pipe wall, each component was located into position using threaded bar or bolts to lock them in place. Once secure, the edge of the coupling was welded to the external surface of the pipe wall resulting in a sealed and bonded weld.



Figure 5.27 Welded Transition Couplings

The next step of the assembly involved the welding of the transition pieces to the flat oval followed by the round tubing to the rounded end of the transition piece. Due to the high cost of the transition couplings and the potential for failure of the part through incorrect welding, care was taken during the welding of the components to prevent excessive arcing and pitting that could affect the performance of the sampling unit. The results of the welding operation are shown in figure 5.27.

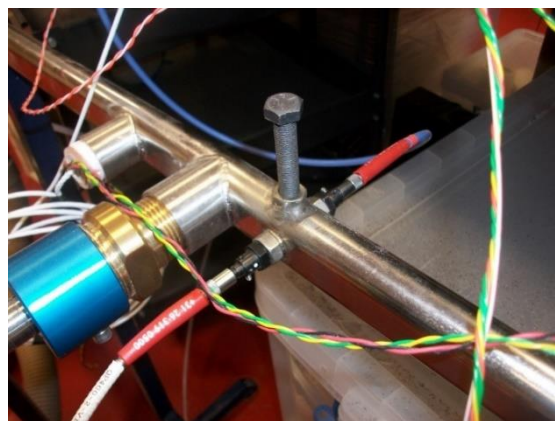


Figure 5.28 Sensors Mounted on Sensing Unit

Figure 5.28 depicts the sensors mounted onto the sensing unit in the locations depicted in figure 5.29. The location of the sensors was selected to ensure the light source from the IR and NIR sensors did not interfere with their respective measurements. NIR data was deemed to be most critical for the analysis of powder flow, thus was placed closer to the inlet and to ensure the probes from the microwave mass flow and IR temperature sensors did not affect the NIRs data acquisition. As the IR temperature sensor emitted an infrared light to measure the temperature of the dynamic material, it was decided to locate this sensor closer to the outlet and away from the NIR sensor. The microwave mass flow sensor is not affected by emitted light thus was located centrally with respect to the NIR and IR probes.

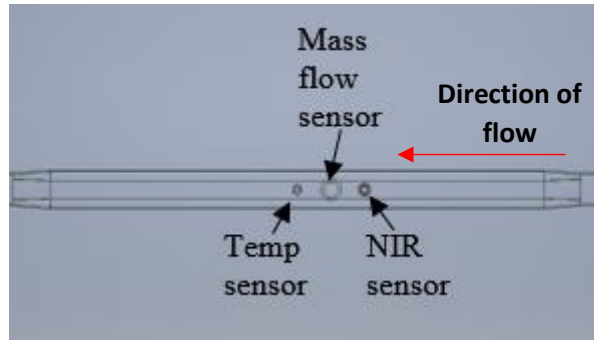


Figure 5.29 Sensor Locations

Finally, the sensing unit was mounted on trestles and connected to air and vacuum systems to produce the 21.22m/s air flow (as specified by end users) via the pressure regulator on the compressor. An air supply was placed into the sensing units inlet via a right-angle piece with attached funnel. The inserted air supply caused a displacement of air at the inlet funnel allowing material to be fed into the apparatus. Material fed into the sensing unit would then be conveyed passed the field of view of the sensors where it was then collected by the vacuum system as depicted in figure 5.30.

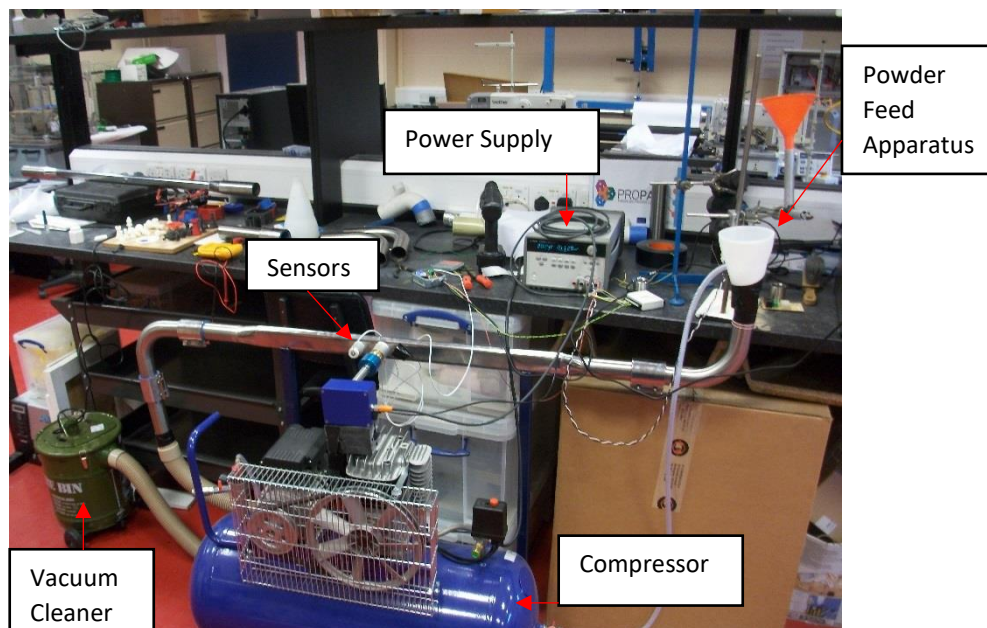


Figure 5.30 MPSU Test Rig

DC power supplies provided the operating voltage for the sensors and a PC with a connected data acquisition system recorded and monitored the resultant data in real time. A DC operated auger feeding system was also positioned above the funnel for later testing of the response signals and their ability to control the feed rate of incoming raw materials.

5.4 Conclusion

This chapter outlined the potential process improvements achievable through the implementation of PAT systems into existing manufacturing processes. The ability of a PAT system to retrofit state of the art smart sensors and process analysers into existing plant equipment minimises the risks associated with conventional plant upgrades such as the installation and commissioning of new production lines. New machinery and production lines undergo lengthy validation procedures whereas with an integrated PAT system, production lines can remain operational while the data undergoes the validation procedures.

Also highlighted in this chapter is the benefit of smart sensor technology. Calibration and set up procedures are efficiently completed and deliver accurate results while providing extreme flexibility through sensor software platforms. This fact is further highlighted when the set-up for the NIR spectrometer is considered. A significant amount of work was required to understand the mechanics of NIR spectroscopy prior to hardware set-up as any misunderstanding of the theory behind NIR spectroscopy can be reflected in the resultant NIR data and modelling. However, with NIR spectroscopy, the positive benefits far outweigh the negative. The data obtained from NIR analysis, particularly in the pharmaceutical industry can provide manufacturers with a higher level of process understanding while also lending itself to applications such as continuous process monitoring and control.

The next chapter will demonstrate the testing of the MPSU, designed to house the sensors and allow for simple process integration of sensors such as the microwave mass flow sensor, IR temperature sensor and NIR spectrometer into existing manufacturing processes. To ensure the MPSU did not adversely affect the flow conditions of existing process conditions, extensive calculations were performed (prior to fabrication) to ensure that the changes in pressure and flow velocity (as a result of area/geometry changes) would not restrict material flow between unit operations. Use of the continuity equation, Bernoulli equation, Colebrook equation and Darcy-Weisbach equation showed that the area changes and resultant pressure/velocity differences and frictional losses had minimal impact on the flow of material through the MPSU.

Chapter Six – ProPAT Sensing Unit Testing & Results

6.1 Introduction

One of the major objectives of this research was to determine the capability of smart sensors and process analysers (embedded into production processing equipment) to accurately measure and control process parameters in real time. Due to the complexity involved, significant work was required with respect to processing and analysing NIR data in comparison to smart sensor data. Smart sensor data is provided pre-processed and is easily calibrated through integrated software, whereas NIR data requires knowledge of multivariate analytics and strictly controlled test conditions to prevent sample contamination. This chapter details the initial work completed with respect to the understanding, testing and processing of NIR data prior to its inclusion in the sensing unit, such as collaborative NIR testing of a blend of Active Pharmaceutical Ingredient (API) and excipients through a twin-screw granulator for the determination of blend composition Particle Sizing Distribution (PSD) and segregation due to mixing. Further testing was completed on the back of the knowledge gained using the assembled sensing unit with embedded smart sensors and NIR spectrometers. A series of tests completed aimed to show the ability of NIR data to accurately measure and predict the blend composition of organic materials and the ability of smart sensors to control the processing parameters in real time.

6.2 NIR Analysis of Powder Blends using Collimating Lenses

6.2.1 Introduction

The following experiment tests the correct configuration of an NIR spectrometer and collimating lenses integrated onto the sensing unit to perform absorbance measurements on a dynamic stream of a bulk solid mixture. Earlier attempts of testing an NIR spectrometer for the measurement of chemical composition, via a collaborative effort between researchers at IT Tralee and UCC, were inconclusive due to incorrect NIR specification and configuration (see Appendix A-1). Detailed correspondence with Ocean Optics (OceanOptics, 2010) in conjunction with analysis of results from previous testing concluded that for an NIR spectrometer within the range of 900 – 1700nm was required along with collimating lenses (see appendix A-1).

The NIR spectrometer, with an operational path length of 30mm, was tested for a binary mixture of varying ratios to determine the ability of the NIR to measure the chemical composition of material conveyed through the pipeline of the sensing unit.

6.2.2 Aim

The aim of this experiment was to assess the accuracy of the collimating lens configuration when mounted onto the sensing unit (figure 6.1) for the determination of chemical composition of a binary mixture. The sensing unit provides an optical path length of 30mm between lenses that should provide

optimum conditions for monitoring the chemical composition or blend ratio of a coffee and sugar mixture.

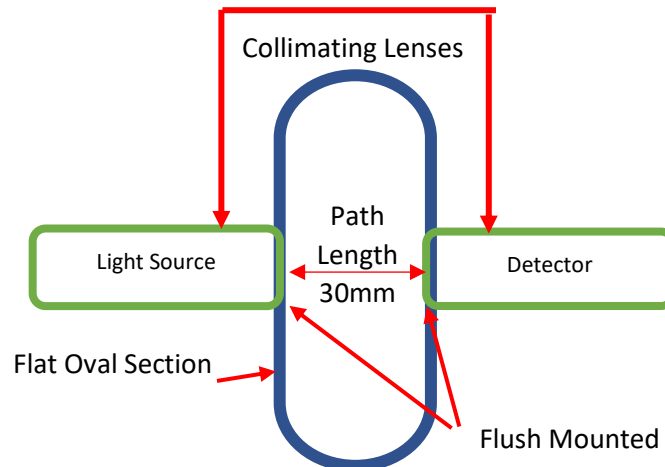


Figure 6.1 Experimental Set-Up of Collimating Lenses Mounted on Sensing Unit

6.2.3 Equipment & Materials Used

- Modular Prototype Sensing Unit (MPSU)
- Ocean Optics NIR Spectrometer (NIRQuest 512, Range 900 – 1700nm)
- Ocean Optics LS-1 tungsten halogen light source
- Ocean Optics Collimating Lenses (Ocean Optics, 2018)
- Ocean Optics Diffuse Reflectance Probe (Ocean Optics, 2013)
- Air Compressor
- Vacuum System
- Test Material (coffee, Sugar)

6.2.4 Methodology

As discussed in section 5.3.2, NIR reference spectra of the material is required prior to PLS model generation and testing. While NIR spectra from previous testing was obtained for the reference material, it was deemed necessary to obtain new reference spectra for each test. Reference spectra previously obtained from purchased material had since been used and contaminated as a result of testing (conveyance through vessels/pipe systems resulting in exposure to material tested previously), thus new material was obtained that could potentially differ from that of the reference material tested previously, thus affecting the results of the test. In addition, the reflective surface of the sensing unit must also be considered as light reflected from the pipe wall could also present as spectral anomalies in the resulting spectral data.

In order to identify and remove any anomalies on resultant waveforms (obtained during testing) caused through ambient or reflected light from the surface of the pipe, NIR dark (i.e. spectral measurement of material in the absence of ambient light) and reference measurements were required. Each individual component was placed into a sealed test tube and an NIR reflectance probe was then inserted into the material as shown in figure 6.2. NIR dark measurements were obtained through placing the test tube into a jig that sealed the material from ambient light and recording the resulting waveform. For the collection of NIR reference measurement, the tube was simply removed from the jig and the relevant spectral data was recorded.

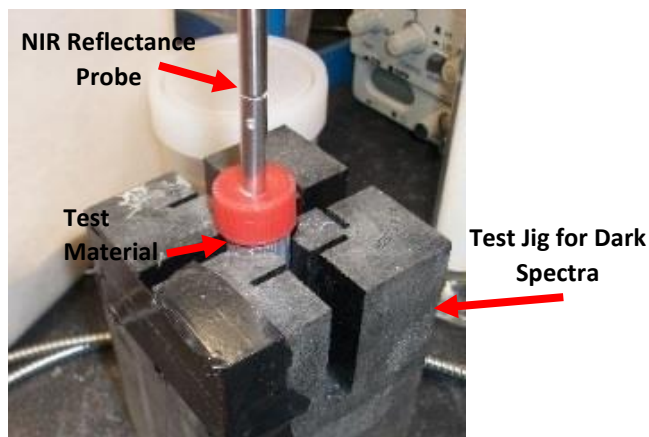


Figure 6.2 Dark NIR Data Acquisition

Several test runs of the material through the sensing unit were performed whilst varying the ingredient ratios of the material blend, as shown in table 6.1. The test material was carefully weighed and agitated to ensure the ratio of ingredients was accurate and the blend was mixed thoroughly prior to the placement of the material into a material feed hopper.

Material Blend Ratios	
Coffee%	Sugar%
100	0
90	10
80	20
70	30
60	40
50	50
40	60
30	70
20	80
10	90
0	100

Table 6.1 Blend Ratios of Test Material Through the Sensing Unit

The material feed hopper was situated directly over the inlet of the sensing unit and controlled using an auger mechanism to provide a regulated and uniform feed rate of the material into the sensing unit as depicted in figure 6.3. A steady 5v supply was directed to the auger feeder to maintain a uniform feed rate of the material as the rotational speed of the auger is proportional to the supply voltage. An air supply from the compressor was inserted into the inlet of the sensing unit and when initiated, caused a displacement of air at a velocity of 21.22 m/s from the inlet of the sensing unit to the outlet, effectively creating a vacuum at the material feed inlet below the hopper.

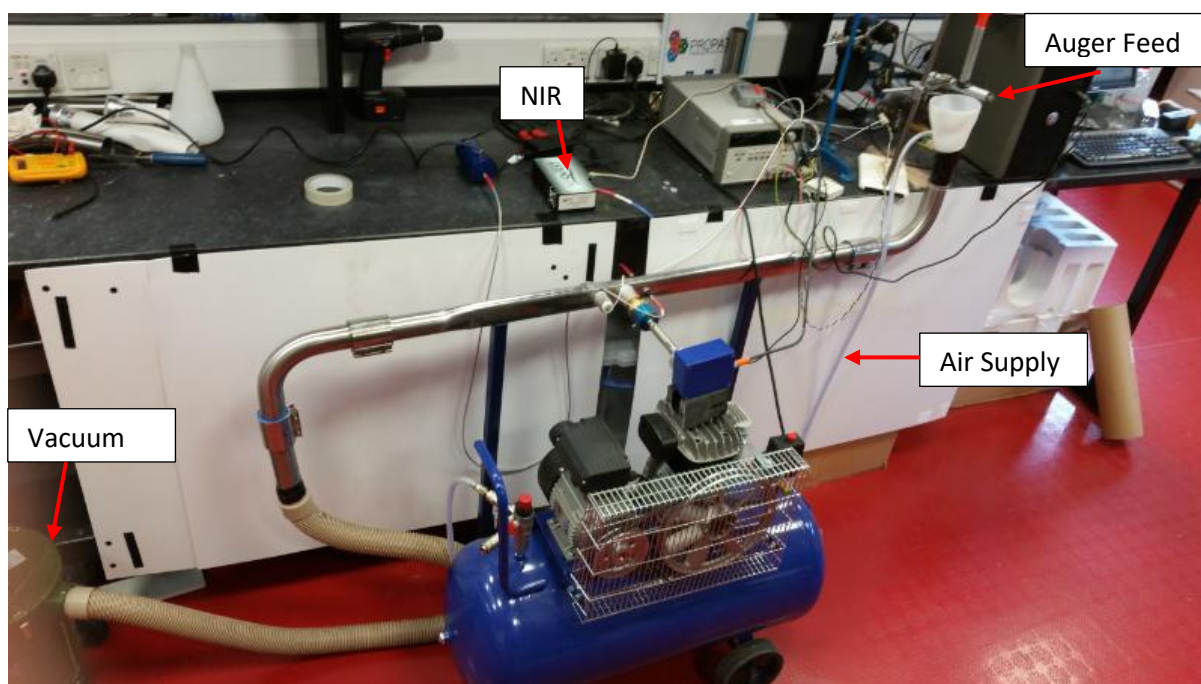


Figure 6.3 Experimental Set-up of NIR Spectrometer, Collimating Lenses and Sensing Unit

When the auger feeder was activated, material would flow from the hopper into the vacuum at the material inlet where it was then conveyed through the field of view of the NIR in the sensing unit. As the material was conveyed passed the collimating lenses, the spectral data for each blend ratio was recorded for later multivariate analysis and PLS model generation to determine the accuracy of this configuration in distinguishing between the varying blend ratios of a binary mixture. The recorded material blends were then collected through a vacuum system connected to the outlet of the sensing unit where it could be recycled for further testing.

In order to input material efficiently into the sensing unit, right angled bends were used to allow for vertical feeding of material into the sensing unit. The effect of the right-angle bends on the flow characteristics can be ignored due to the insertion of the air supply passed the right-angled bend as shown in figure 6.4. Losses due to friction or due to bend angle only effect the vacuum forces that are

generated by the displacement of air at the inlet of the sensing unit. The air supply situated after the bend remains unaffected.

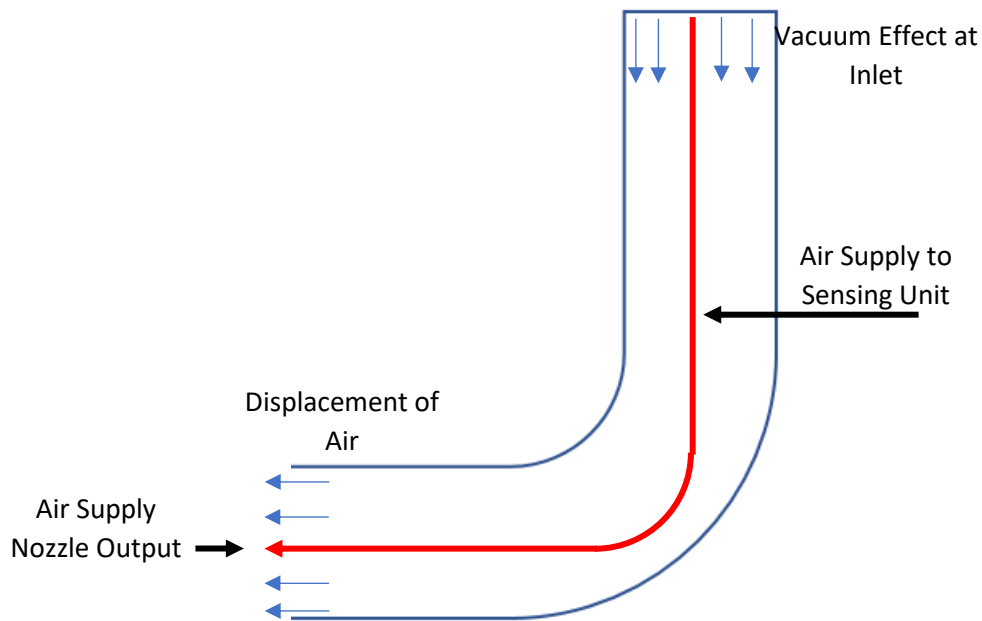


Figure 6.4 Air Supply Hose Inserted Into & Beyond the Bend

6.2.5 Results and Conclusions

A PLSR model was generated from the NIR test data for the prediction of chemical composition of a binary mixture of sugar and coffee and the model overview is shown in figure 6.5 The addition of the collimating lenses and the NIR spectrometer range of 900 – 1700 nm is shown to dramatically increase the quality and accuracy of the model. Typical explained variance of 90% for a 3-factor model indicates that the model is robust in terms of handling new data sets.

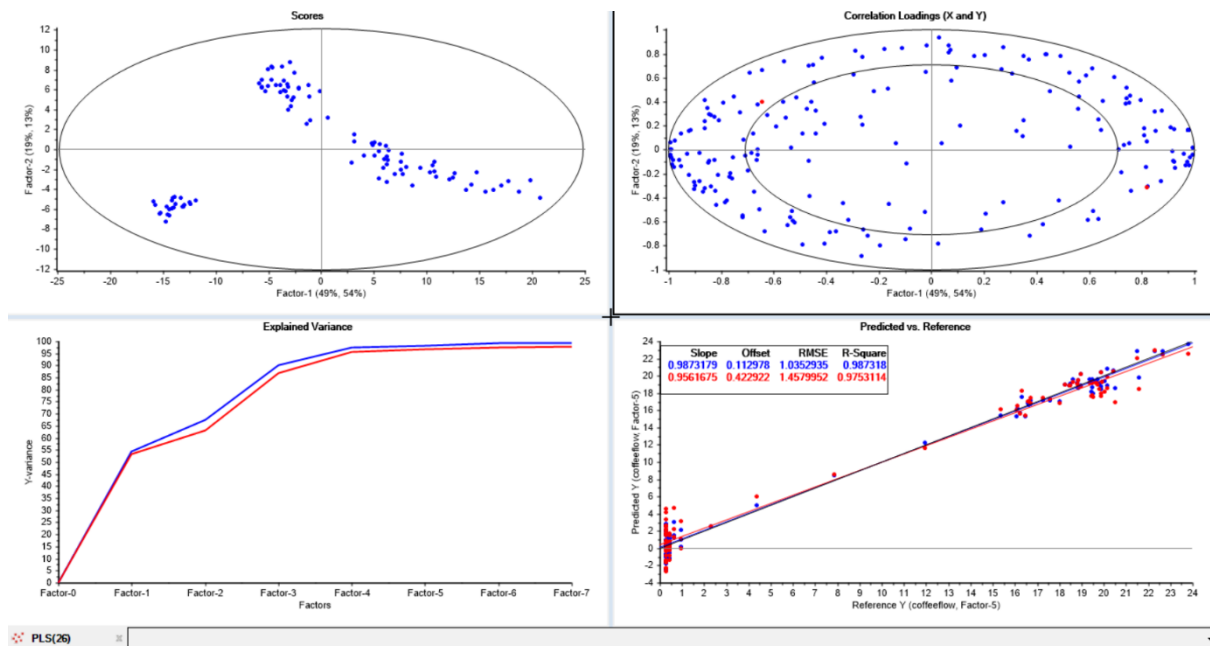


Figure 6.5 Multi-Variate Data Analysis Results of NIR Spectrometer with Collimating Lenses Mounted on the Sensing unit

Figure 6.5 also highlights the “goodness of fit” (R^2) value of the model at typically 0.97 with a RMSE of 1 - 1.5%. This is further highlighted through the position of the samples close to the regression line (bottom right) in both calibration and validation sample data.

The results of the above experiment as detailed in figure 6.5 show that NIR spectrometers can be used to accurately determine the chemical composition of an organic powder blend. This test also validates the inclusion of collimating lenses for the absorbance measurements of dynamic powder blends in a pipe system and highlights the importance of correct NIR set-up and wavelength range for the measurement of chemical composition.

During the testing of the varying material blends, the intensity of the NIR spectra was shown to be decreasing with every test run as can be seen in figure 6.6 (intensity Y-axis, wavelength (nm) X-axis).

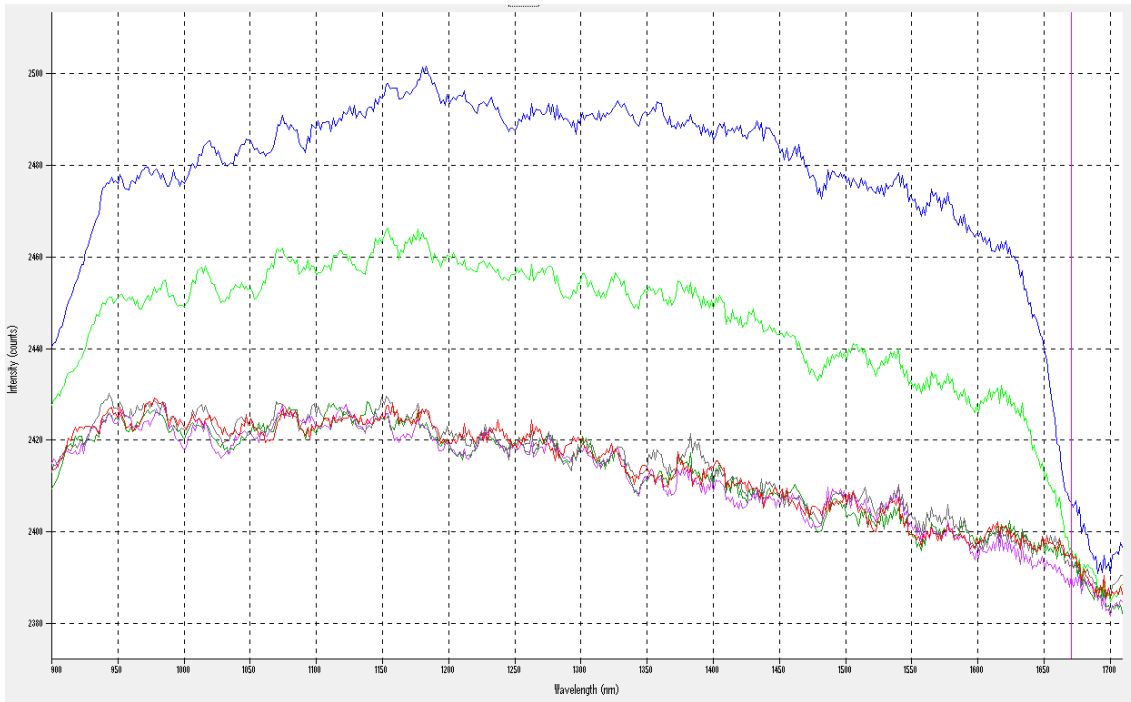


Figure 6.6 Effects of Lens Fouling on the intensity of the NIR data

The decreasing intensity was found to be caused by the build-up of material on the collimating lenses. This obstructed both the light source and the detector and resulted in a decreasing intensity of light. To address this issue efficiently, an access point to the collimating lenses was fabricated into the MPSU to allow for a periodic air purge of the lenses (figure 6.7).



Figure 6.7 Access point for lens purging during testing

While this had the desirable effect of cleaning the lenses and allowing for the continuation of testing, it also highlights the need for some form of automatic purging of lenses in between operations when under normal production conditions, as it is not feasible to manually purge optical lenses in between production processes.

6.3 Temperature Measurement Using the Modular Prototype Sensing Unit (MPSU)

6.3.1 Introduction

The following experiment is comprised of an IR temperature sensor integrated into the MPSU for the temperature measurement of a dynamic powder stream of varying temperatures. A PLS model will be generated from the test data to determine the accuracy of the model in predicting the temperature of the material during testing. The material under test is a granulated blend of coffee and sugar at a ratio of 1:1 and a mass of 300g, tested at the following temperatures; 0°C, 35°C, 70°C.

6.3.2 Aim

The aim of this experiment is to generate an accurate PLS model of the IR temperature sensor data through conveyance of material of varying temperatures within the MPSU. To assess the ability of the IR temperature sensor in providing real time data on dynamic powder blends.

6.3.3 Equipment & Materials Used

- Modular Prototype Sensing Unit (MPSU)
- IR Temperature Sensor (Micro-Epsilon, 2018b)
- Air Compressor
- Vacuum System
- Test Material (coffee, Sugar)
- Refrigeration unit
- Heat source (oven)
- Multi-Meter with attached Thermocouple

6.3.4 Methodology

To accurately test the IR temperature sensors ability to measure a moving particle stream of varying temperatures, sample material was heated/cooled prior to conveyance through the MPSU. 3 x 300g samples of granulated material (50% coffee, 50% sugar) were used in testing.

Sample 1 was placed in a refrigeration unit until a steady state temperature of 0°C was reached.

Sample 2 & 3 were placed in oven until a steady state temperature of 70°C was reached (figure 6.8), at which point, sample 2 was removed and allowed to cool until a temperature of 35°C was recorded using a thermocouple and multi-meter.



Figure 6.8 Granulated Material heated to 70°C

With each sample at the desired temperature, the material was then conveyed through the MPSU in the order of lowest to highest temperature (material was manually fed into the MPSU at random flowrates). A wait time of 5 minutes between tests ensured that any residual temperature from the previous material was dissipated and ensured each sample was exposed to the same test conditions. Upon completion of the test, the data was then exported to the CAMO software for analysis.

6.3.5 Results and Conclusions

As the IR temperature sensor is univariate in nature, the resultant PLS overview is easier to comprehend than that of the NIR data due to the significantly lower amounts of variables present in the model. Figure 6.9 details the results from the temperature measurement PLS modelling of the granulated coffee/sugar samples.

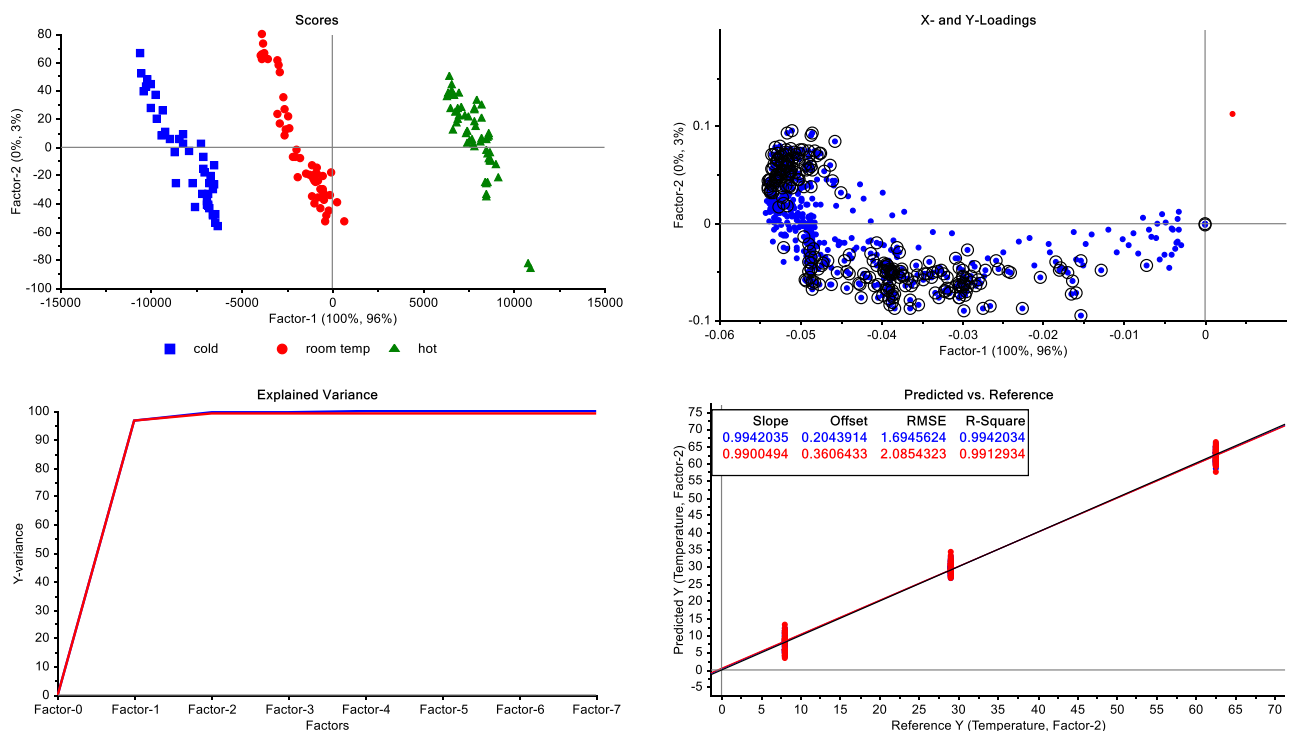


Figure 6.9 PLS Results from Temperature Measurement of Dynamic Powder Blend

Sample groupings distinguishing the varying temperatures in the scores plot (figure 6.9, top left) are clearly defined indicating that the IR temperature sensor was successful in measuring samples with varying temperatures and the resultant sensor data could then be used to generate a robust model. This is also denoted through the 95% explained variance in the single factor model as shown in figure 6.9 (bottom left).

While the predictive vs reference model is indicative of a good fit to the data ($R^2 = 0.99$, $RMSE = 1.7 - 2.1$), an increase/decrease in the material temperature can be seen (figure 6.9, bottom right). Material temperature measured pre-test at 0°C is recorded on the model at approx. 8°C, material temperature measured pre-test at 35°C is recorded on the model at approx. 28°C and material temperature measured pre-test at 70°C is recorded on the model at approx. 64°C and is further outlined in figure 6.10 and table 6.2.

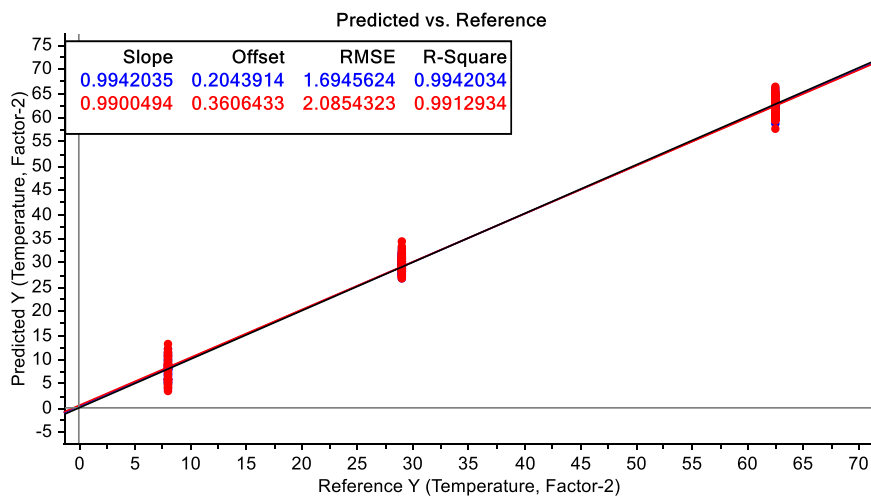


Figure 6.10 PLS Model Overview of IR Temperature Sensor Test

Pre-test Temperature (°C)	Recorded Temperature (°C)	Temperature Difference (°C)
0	8	8
35	28	-7
70	64	-6

Table 6.2 Temperature Change During Testing

The deviation in temperature between pre-test and post-test material can be attributed to the warming or cooling of the material when exposed to the airflow within the MPSU. As the material is conveyed through the MPSU, thermal transfer occurs between the material under test and the air within the test rig. Thermal transfer occurs in the direction of high temperature to low temperature as can be seen from the tabulated results in table 6.2. Material at 0°C, when exposed to the air temperature of the compressor 23°C approx. begins to rise in temperature due to the temperature

differential, whereas material at 70°C will begin to cool upon exposure to the same air temperature of the compressor. Ideal test conditions would incorporate a heated air supply too maintain the test temperature and reduce or eliminate the temperature differential recorded in the PLS model.

In conclusion, the experimental test of generating accurate PLS models from IR temperature sensor data was successful. Clearly defined sample groupings are shown for each temperature measurement of the sample material and strong correlation of the model to the test data is shown through the R^2 and RMSE values, 0.99 and 1.7 – 2.1 respectively. Furthermore, the ability of the model to record the changes in temperature from pre-test conditions to material conveyance indicate the suitability of this sensor for real-time data acquisition applications.

6.4 MPSU & Sensor Suite Measurement of Chemical Composition

6.4.1 Introduction

The following test incorporates the entire suite of sensors and process analysers integrated onto the MPSU. The inclusion of the smart sensors in conjunction with the NIR spectrometer will provide a new set of variables for the PLS model and allow for the assessment of their collective effect on the accuracy of the models' prediction of chemical composition of a material blend.

6.4.2 Aim

To analyse the combined data sets inputted from a suite of sensors integrated into the MPSU for the purposes of generating a predictive model on the chemical composition of a binary mixture of sugar and coffee.

6.4.3 Equipment & Materials Used

- Modular Prototype Sensing Unit (MPSU)
- Ocean Optics NIR Spectrometer (NIRQuest 512, Range 900 – 1700nm)
- Ocean Optics LS-1 tungsten halogen light source
- Ocean Optics Collimating Lenses (Ocean Optics, 2018)
- Ocean Optics Diffuse Reflectance Probe (Ocean Optics, 2013)
- Hense MIC Flowmeter (Hense, 2014)
- IR Temperature Sensor (Micro-Epsilon, 2018b)
- Air Compressor
- Vacuum System
- Test Material (coffee, Sugar)

6.4.4 Methodology

To accurately test the MPSU and integrated smart sensors and process analysers for the measurement of chemical composition of a binary mixture i.e. coffee and sugar, a series of sample blends of varying ratios were prepared.

Test No.	Coffee %	Sugar %
1	100	0
2	80	20
3	60	40
4	40	60
5	20	80
6	0	100

Table 6.3 Test Material Blend Ratios

Each material sample comprised of 300g of material at ambient temperature (25°C) and fed into the MPSU via an auger feeding system (figure 6.11) calibrated to 200g/min. The material under test was placed into a hopper system with a series of internal baffles used to ensure the material was adequately blended. The material was weighed before testing and after testing to ensure there was no residual moisture from the compressed air. Once activated, the auger would draw material through the hopper and into the MPSU via the vacuum generated from the air supply. The material was then conveyed passed the field of view of the sensors and process analysers and into the vacuum system for collection.

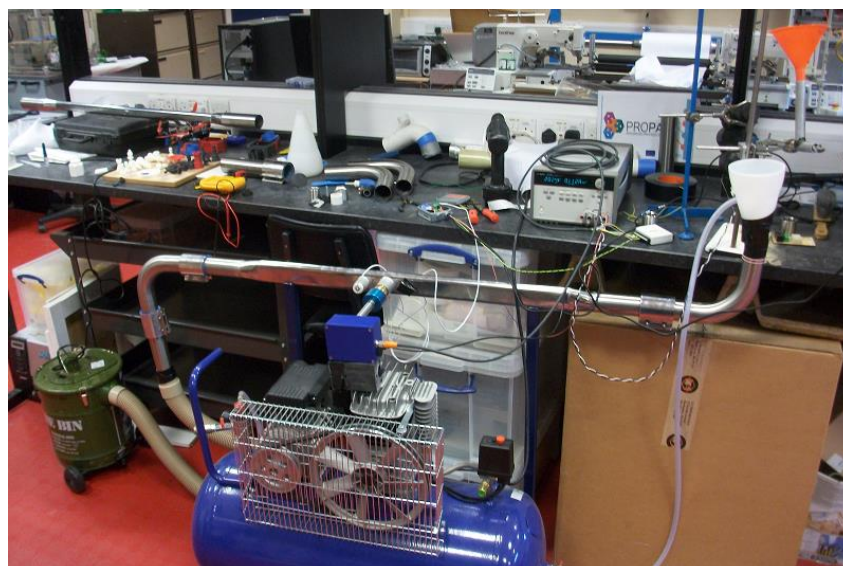


Figure 6.11 MPSU with Integrated Sensors and Feeding System

To prevent sample contamination, the system was purged between tests and the optical lenses of the IR temperature sensor and NIR spectrometer were cleaned to remove any build-up of material from

previous testing. This process was repeated for all 6 samples and the relevant data was recorded and uploaded into the CAMO unscrambler X software for analysis as shown figure 6.12 and 6.13 (test 1 and test 6 respectively).

results(1)(1)(%coffee	%sugar	coffeeflow	sugarflow	massflow1	temp	899.6781	901.3037	902.9
		1	2	3	4	5	6	7	8	
0.134	1	100.0000	0.0000	102.5677	0.0000	0.0086	25.3600	3541.0200	3598.6590	35
0.864	2	100.0000	0.0000	102.5677	0.0000	0.0086	25.4100	3527.3960	3596.5630	35
1.488	3	100.0000	0.0000	102.5677	0.0000	0.0086	25.0036	3537.8760	3592.3720	35
2.106	4	100.0000	0.0000	102.5677	0.0000	0.0086	24.0150	3539.9720	3600.7550	36
2.698	5	100.0000	0.0000	102.5677	0.0000	0.0086	24.5648	3542.0680	3609.1390	35
3.312	6	100.0000	0.0000	224.3595	0.0000	0.0187	24.6980	3537.8760	3596.5630	36
3.932	7	100.0000	0.0000	224.3595	0.0000	0.0187	24.9870	3544.1640	3604.9470	36
4.561	8	100.0000	0.0000	955.1104	0.0000	0.0798	25.3658	3535.7800	3607.0430	36
5.181	9	100.0000	0.0000	1929.4450	0.0000	0.1612	25.1458	3537.8760	3604.9470	36
5.793	10	100.0000	0.0000	3025.5710	0.0000	0.2528	25.4680	3539.9720	3600.7550	36

Figure 6.12 Raw Data from Test 1

results(1)(1)(%coffee	%sugar	coffeeflow	sugarflow	massflow1	temp	899.6781	901.3037	902.9292
		1	2	3	4	5	6	7	8	9
75.675	123	0.0000	100.0000	0.0000	198.2230	0.0086	25.6580	3504.3400	3563.0280	3563.0280
76.298	124	0.0000	100.0000	0.0000	198.2230	0.0086	25.1203	3502.2440	3560.9320	3560.9320
76.919	125	0.0000	100.0000	0.0000	198.2230	0.0086	24.9560	3486.5240	3554.6440	3555.6920
77.542	126	0.0000	100.0000	0.0000	198.2230	0.0086	24.5869	3487.5720	3546.2600	3553.5960
78.166	127	0.0000	100.0000	0.0000	198.2230	0.0086	25.4576	3482.3320	3563.0280	3546.2600
78.787	128	0.0000	100.0000	0.0000	198.2230	0.0086	25.4510	3477.0920	3554.6440	3530.5400
79.4	129	0.0000	100.0000	0.0000	198.2230	0.0086	25.0125	3488.6200	3548.3560	3544.1640
80.024	130	0.0000	100.0000	0.0000	198.2230	0.0086	25.6850	3486.5240	3529.4920	3529.4920
80.649	131	0.0000	100.0000	0.0000	904.3496	0.0391	25.7850	3474.9950	3543.1160	3533.6840
81.268	132	0.0000	100.0000	0.0000	3493.4800	0.1510	25.3250	3460.3230	3520.0600	3535.7800
81.877	133	0.0000	100.0000	0.0000	7494.8650	0.3240	25.6510	3456.1310	3512.7240	3514.8200

Figure 6.13 Raw Data from Test 6

6.4.5 Results and Conclusions

The inclusion of univariate sensors such as microwave mass flow and IR temperature sensors with the NIR spectrometer for the measurement of chemical composition of a binary mixture i.e. coffee and sugar through PLS modelling yielded favourable results. Figure 6.14 depicts the PLS model overview from the series of tests conducted on the material at varying blend ratios and uniform temperature and flow rates.

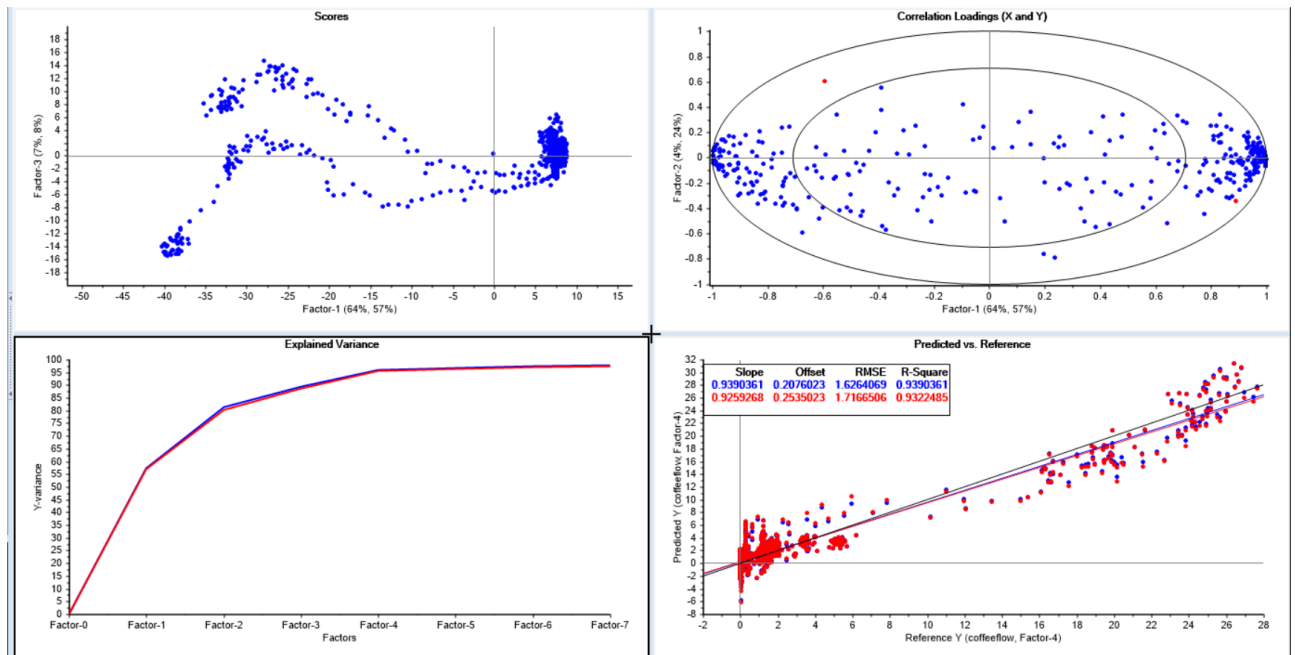


Figure 6.14 Results from PLS Model of MPSU and Sensor Suite

Segmented cross validation of the data results in a typical explained variance of 85% – 95% for a 3-factor model while predicted vs reference plot indicates a strong correlation of the model to the test data. The R^2 or “goodness of fit” value for the test data (at 0.93) in conjunction with a RMSE of 1.62 – 1.71 indicates the MPSU and the chosen sensors and process analysers are effective in distinguishing between varying blends of material. The above PLS results also indicate the systems suitability for real-time process monitoring and control applications. Suitable response signals can be extracted from the numerical data behind the PLS models (figure 6.14) and used to generate suitable response signals to control plant equipment in real time resulting in real time measurement and control of production processes.

6.5 Real-Time Process Control

6.6.1 Introduction

The following test details the collaborative work between this author and another member of the ProPAT team in IT Tralee Mr. Niall O’Mahony in the areas of process monitoring and process control respectively, using the MPSU and integrated smart sensors and process analysers to accurately control the feed rate of the material into MPSU.

This section focuses on highlighting how appropriate signals could be generated from in-process data while Mr. Niall O’Mahony focused on the data fusion and process control aspect of this project. The inclusion of this collaborative effort on process control at this point is thus warranted as it provides

clear proof of concept on the extraction of in-process data for real-time closed loop control of production processes.

6.5.2 Aim

The following tests the ability of NIR and microwave mass flow sensor data to accurately control the chemical composition of a binary mixture of Sugar (component 1) and Coffee (component 2) in real time.

6.5.3 Equipment & Materials Used

- Modular Prototype Sensing Unit (MPSU)
- Ocean Optics NIR Spectrometer (NIRQuest 512, Range 900 – 1700nm)
- Ocean Optics LS-1 tungsten halogen light source
- Ocean Optics Collimating Lenses (Ocean Optics, 2018)
- Ocean Optics Diffuse Reflectance Probe (Ocean Optics, 2013)
- Hense MIC Flowmeter (Hense, 2014)
- Air Compressor
- Vacuum System
- Test Material (coffee, Sugar)
- Auger Feed System
- PC with MatLab Software

6.5.4 Methodology

Testing the ability of the MPSU and integrated sensors to accurately control chemical composition was achieved through simultaneously feeding individual components into the MPSU for NIR and mass flow analysis and using the resultant data to control the material input of one component. Sugar (C1) and Coffee (C2) were loaded into separate auger feeding systems. Both the auger feeding system of C1 and C2 were controlled using sensor response signals, shown in figure 6.15, (routed through Matlab® System Identification tool and PID tuner) based on PLS modelling from the MPSU and integrated sensors and NIR data.

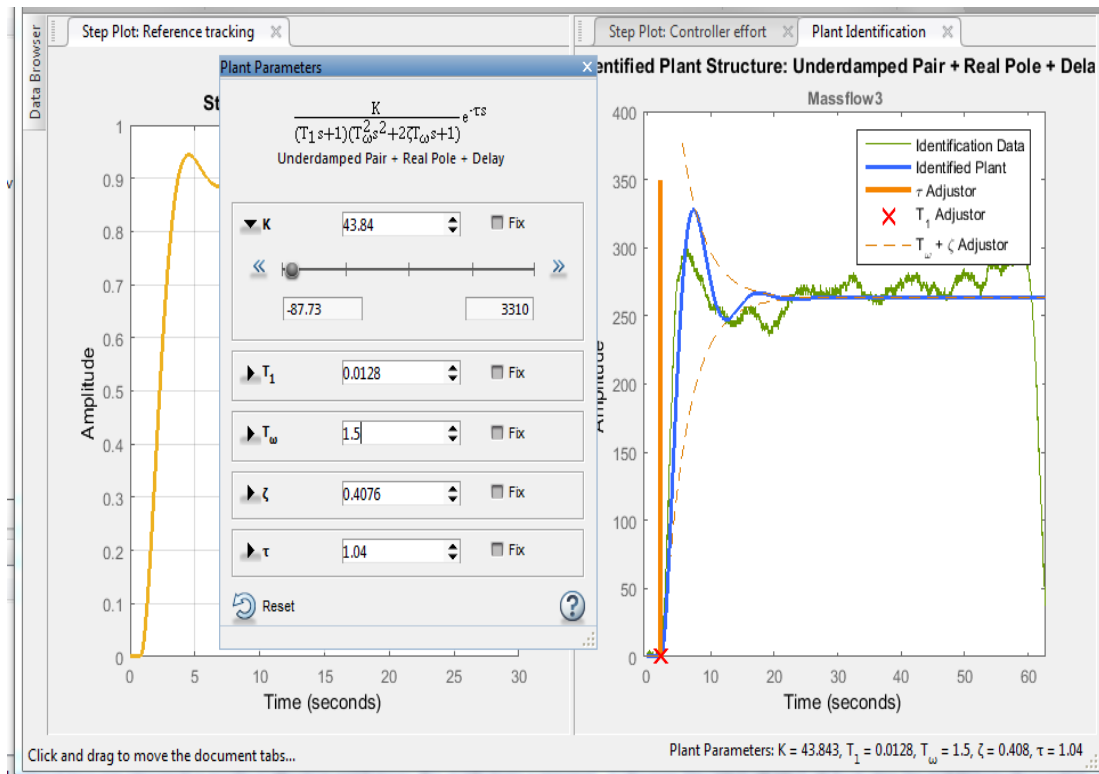


Figure 6.15 Auger Feeder Response Signals

Prior to initiating testing, point of 80% sugar, 20% Coffee was inputted into the system and the auger feeders of both components were activated. Material from both feeding systems was then conveyed through the MPSU and analysed by the integrated sensors and process analysers, which provided feedback for adjustments to the individual auger feeding systems

6.5.5 Results and Conclusions

Real-time feedback from MPSU sensors and analysers conditioned into appropriate response signals are shown to be effective in the closed loop control of process parameters. Figure 6.16 shows how effective control of individual component mass flow, and thus, chemical composition was achieved in real-time using in-process sensor data.

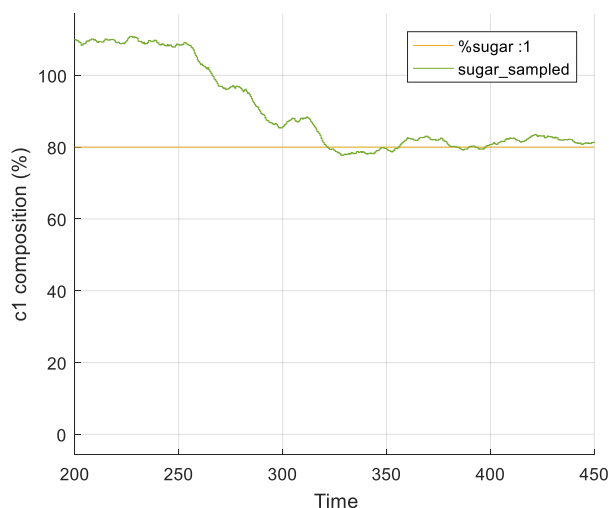


Figure 6.16 PID Control of Chemical Composition in Real time

The results from this test show the potential for PAT systems to provide accurate control of systems and processes with fast response times to deviations in product quality. Furthermore, the flexibility of this system, allows for adjustments to be made to plant equipment up/downstream along the process to ensure pre-determined levels of quality are reached.

6.6 Conclusions

This chapter focused on the series of tests conducted over the course of this research and highlighted the benefits of incorporating smart sensors and process analysers to provide real time information on the physical and chemical characteristics of in-process material. This chapter also outlined the ability of smart sensors and process analysers to be integrated seamlessly into existing material conveyance lines through use of a bespoke sensing units or through direct integration into plant equipment. The MPSU is shown to be capable of housing a diverse range of sensory options to analyse, monitor and control production processes in real-time.

Also outlined in this chapter is the benefits of utilising NIR spectroscopy for the measurement of chemical composition while also highlighting the importance of its configuration and data processing to ensure accuracy. Incorrect NIR configuration can result in significant noise that renders NIR data useless. This was evident in section 6.2, however correct specification and installation of NIR equipment provides valuable in-process data that can be utilised to develop an enhanced level of process understanding and control.

Further enhancement can be gained through the inclusion of appropriate non-contact smart sensors that minimise set-up and calibration times. In-built processors and optical probes and lenses lend themselves to applications where sensor integration into plant equipment can be complex due to processing conditions, environments and locations. This allows for the collection of valuable data that

when used in conjunction with NIR data can be analysed through multivariate data analytical tools to provide in-depth process knowledge and accurate response signals for closed loop control of plant equipment as was shown in this section.

Chapter 7 – Conclusion of Research & Future Work

7.1 Introduction

This chapter concludes the work undertaken as part of this research thesis, providing a summary of the findings from the in-depth research into Process Analytical Technology (PAT) and discusses the potential impact of these systems when implemented in the relevant industries. Investigations into the advancements in these areas is also outlined, showing how smart sensors and process analysers provide a window into the inner workings of the system while also highlighting their diverse application potential. Also included in this chapter are recommendations for future work and publications to date on the strength of this research.

7.1 Research, Methodology & Implementation Summary

This thesis has investigated key aspects of PAT systems and their potential impact on materials processing industries such as the pharmaceutical manufacturing industry. PAT systems allow for on/in-line process monitoring techniques that serve to significantly reduce cycle time and material sampling error through automatic sampling using the latest in embedded sensory and measurement technology.

Advancements in the areas of optical, non-contact sensing enable data capture in harsh or difficult to reach areas, thus protecting expensive measurement systems. With the Further emergence of smart sensor technologies, non-contact sensors are now available with in-built processers to condition output signals and significantly reducing set-up and calibration times. This thesis also focused on the area of Near Infrared Spectroscopy (NIR) and its deployment in the materials processing industries for the real-time and accurate measurement of chemical composition of a powder blend analysed using chemometric multivariate analytics.

The benefits of implementing PAT systems with embedded smart sensors and process analysers was outlined through an in depth live case study review of ProPAT end user (GlaxoSmithKline, MBN NanoMaterialia) manufacturing processes current state vs future state (PAT implementation) and showed expected improvements in areas such as product end quality and cycle time.

Also included in this thesis was the development of a Modular Prototype Sensing Unit (MPSU) that acted as a both housing for selected smart sensors and process analysers and a coupling for the unit to interface with existing end user material conveyance systems. This enabled for the simulation of end user process conditions and allowed for in-process data from embedded sensors and analysers to be collected, processed and interpreted using multivariate data analytics.

Significant knowledge was gained through investigations on NIR configurations and set-up that allowed for accurate material sample collection. Further knowledge was attained relating to the interpretation of the resultant data. This was achieved through multivariate data analytics of NIR spectral data using Partial Least Squares Regression (PLSR) techniques

7.2 Major Contributions

This project was successful in achieving the main aims and objectives as described in Chapter 1. The research carried out in this thesis defines PAT, its uses within industry and the associated benefits when compared to conventional batch manufacturing and off-line process analytical techniques. Experiments carried out during the course of this research further outline the potential for PAT to improve materials processing industries manufacturing methods through integrated smart sensors, spectroscopic equipment and multivariate data analytics.

7.2.1 Comparison of Conventional Material Processing vs PAT systems

Following an in-depth literature review, this thesis defined PAT and its suitability to industries such as pharmaceutical manufacturing through focusing on the key aspects and drivers of this system. Increasing demand on manufacturing supply chains in conjunction with the demise of the blockbuster drug models have highlighted the need for the pharmaceutical industry to adopt a more efficient approach to their manufacturing operations. Speed to market of newly developed product is critical in the pharmaceutical industry in particular and is traditionally dependant on production validation of drug formulations. Sample product batches from experimental production runs require rigorous validation through time and labour intensive off-line analytics as the production process is fine tuned to meet pre-determined levels of quality.

PAT systems dictate the levels of quality and make necessary adjustments to Critical Process Parameters (CPP) that affect the Critical to Quality Attributes (CQA). This is achieved through a suite of carefully selected and positioned measurement equipment i.e. smart sensors, optical sensor, spectroscopic sensor in key measurement locations. The collective data stream from the measurement equipment provides continuous real-time in process data of chemical and physical reactions that can be further employed in chemometric statistical modelling to allow for a continuous monitoring and control or closed loop system.

In-process PAT data significantly reduces the time required for off-line manual sampling while use of multivariate analytical software tools streamline the analysis, interpretation and reporting of the data

resulting in a product that is quicker to market and of a higher level of quality due to the increased level of process understanding.

7.2.2 Assessment & Selection of Measurement Solutions & Design of MPSU for ProPAT

This research focused on the assessment and selection of suitable measurement solutions to meet the requirement for ProPAT end user applications. Emphasis was placed on the use of non-contact smart sensors due to their ability to measure various characteristics of a dynamic particle stream through optical fibres coupled to conveyance pipe walls. The non-invasive nature of optical sensors ensured that minimal disruption to material flow during testing occurred thus protecting the sensing head from damage due to particle collision and ensuring unimpeded material flow and particle build up within conveyance lines. Coupling of optical fibres to conveyance pipes or existing equipment was also shown through this research to be achievable and outlines a major benefit of optical sensors for integration into areas within a production process that can be difficult to reach for conventional sensors such as thermocouples or volumetric flow metres.

The MPSU developed in this project highlighted the capabilities of housing a series of sensors to sample in-process material simultaneously with the ability to be retrofitted into standard size conveyance lines with minimal disruption to plant equipment or manufacturing operations. The MPSU can be designed for any pipe diameter/length and can be situated in many instances throughout a process to provide valuable information on the status of in-process material.

Several novel mass flow sensing methods were also investigated in this thesis and showed that in the case of mass flow measurement of a bulk solid, use of acoustics or inertial signals can, with significant development, yield an accurate and repeatable method of measurement of the mass flow of a dynamic powder stream.

7.2.3 Near Infrared Spectroscopy for Real-Time Measurement of Chemical Composition

This research highlighted the benefits of utilising spectroscopic techniques such as NIR for the measurement of chemical reactions and/or characteristics of in-process material. Advances in the field of spectroscopy has reduced both the physical size of spectrometers and their cost. When used in conjunction with chemometric statistical analysis tools, spectral data from in-process material can be used to generate predictive models using techniques such as Partial Least Squares Regression (PLSR). Predictive modelling of manufacturing processes can provide accurate closed loop control of the chemical composition of a pharmaceutical drug ensuring the content of Active Pharmaceutical Ingredient (API) does not deviate from pre-determined levels.

The predictive models generated in this thesis show that NIR is capable of accurate control of chemical composition through controlling or adjusting material feed rates of API's or excipients into a production process in real time. NIR data can be further enhanced through use of data fusion techniques that incorporate the amalgamated data sets of integrated smart sensors and process analysers into a single response signal that can be used to control the entire manufacturing stream.

7.2.4 Summary

This thesis, and the work undertaken as part of the ProPAT project, demonstrates the suitability of PAT systems to the materials processing industry while also highlighting its various favourable characteristics. PAT systems can be developed as modular systems that can be retrofitted into existing processes. The ability of PAT systems to incorporate bespoke sensor suites ensures that the vast majority of measurands can be accommodated to suit individual processes while also ensuring systems can be future proofed as advancement in the fields of smart and spectroscopic sensors continue. The use of multivariate statistical analysis is also shown to be fundamental to the accuracy of PAT and provides valuable information on process variables that can be further used as control signals to ensure optimum quality levels are obtained.

7.2.5 Publications

Inertia Sensing for Bulk Solid Measurement in Process Analytical Technology Systems

Authors: Trevor Murphy, Niall O'Mahony, Krishna Panduru, Daniel Riordan, Joseph Walsh
Conference: 2016 10th International Conference on Sensing Technology (ICST), At Nanjing, China, Volume: 1 (DOI: 10.1109/ICSensT.2016.7796245)

Acoustic and Optical Sensing Configurations for Bulk Solids Mass Flow Measurements

Authors: Niall O' Mahony, Trevor Murphy, Krishna Panduru, Daniel Riordan, Joseph Walsh
Conference: 2016 10th International Conference on Sensing Technology (ICST), At Nanjing, China (DOI: 10.1109/ICSensT.2016.7796229)

Computational Fluid Dynamics, Rapid Prototyping and Design of Materials Sampling Process for PATA

Authors: Trevor Murphy, Niall O'Mahony, Krishna Panduru, Daniel Riordan, Joseph Walsh
Conference: 33rd International Manufacturing Conference, At University of Limerick

Machine Learning Algorithms for Process Analytical Technology

Authors: Niall O'Mahony, Trevor Murphy, Krishna Panduru, Daniel Riordan, Joseph Walsh

Conference: World Congress on Industrial Control Systems Security (WCICSS-2017), At London, UK. (DOI: 10.1109/WCICSS.2016.7882607)

Fiber-optic Sensors for Process Analytical Technology

Authors: Niall O'Mahony, Trevor Murphy, Krishna Panduru, Daniel Riordan, Joseph Walsh

Conference: 33rd International Manufacturing Conference, At University of Limerick

Pharmaceutical manufacturing and the quality by design (QBD), process analytical technology (PAT) approach

Authors: Trevor Murphy, Niall O'Mahony, Krishna Panduru, Daniel Riordan, Joseph Walsh

Conference: 2016 27th Irish Signals and Systems Conference (ISSC)

Adaptive Process Control and Sensor Fusion for Process Analytical Technology

Authors: Niall O'Mahony, Trevor Murphy, Krishna Panduru, Daniel Riordan, Joseph Walsh

Conference: 2016 27th Irish Signals and Systems Conference (ISSC)

Smart sensors for process analytical technology

Authors: Niall O'Mahony, Trevor Murphy, Krishna Panduru, Daniel Riordan, Joseph Walsh

Conference: 2016 IEEE International Conference on Advanced Intelligent Mechatronics (AIM)
(DOI: 10.1109/AIM.2016.7576901)

7.3 Discussion

Advancements in areas such as sensor technology, computational power and data storage have given rise to a new era of "Big Data" which is the processing, analysis and interpretation of huge complex data sets for the purposes of statistical analytics and predictions. With the emergence of trends such as Industry 4.0 and increasing use of the Internet of Things (IoTs) platforms, more and more significance in being placed on the acquisition of real-time data for process understanding resulting in continued investment into sensor technology. These advancements are complimentary to PAT systems and are indicative of the future potential of this technology.

This is evident by the installation of PAT in many industrial facilities today such as GSK's continuous processing plants in Singapore and the advertisement of turnkey continuous equipment for common manufacturing processes such as tableting. While the challenges associated with PAT are many, so too are the benefits. PAT or continuous manufacturing systems are significantly smaller in size than their batch counterparts as they require significantly less in-process material to operate. This offers a

reduction in both energy costs and valuable floor space, while it also ensures that defective material or product is significantly more isolated than in batch systems resulting in reduced levels of waste.

7.4 Future Work

7.4.1. Regulatory Barriers

Regulatory barriers and a lack of incentives for manufacturing innovation in conjunction with the uncertainty surrounding validation of PAT systems are according to (Price, 2012, 2014; Li, 2014) breeding a reluctance within industry to abandon batch manufacturing for continuous PAT systems.

For PAT to progress, implementation strategies must be generated by the FDA and other regulatory bodies to ease the transition from batch manufacturing and to allay the fears of manufacturers. Incentives for developing PAT systems such as delayed patent release on products transitioning from batch to continuous would absorb some of the losses incurred through downtime during PAT upgrades to existing process lines.

7.4.2 Lens Fouling

Lens fouling of optical probes remains one of the biggest issues with fiber optic sensors as they can be prone to material build-up on the sensing head. During the testing of the MPSU, optical probes required air purging between tests to ensure accuracy of results. There exists a number of solutions to probe fouling such as automatic air purging and bevelled sensing heads to prevent material build-up, but each solution comes with some limitations depending on the application. Future work on lens fouling would involve a more robust solution to air/gas purging, such as the potential to use static electricity to deflect particles from the probe surface.

7.4.3 Development of Mass Flow Sensor

The success in the development of novel mass flow metering systems warrants further investigation into the use of inertia and acoustics for the measurement of mass flow of a bulk solid. Future work would involve the development of a series of prototypes for the mineral processing industries and increasing the accuracy of sensors through signal conditioning techniques.

7.4.4 Assessment of spectroscopic techniques

As the MPSU can accommodate a variety of sensors and analyser, future work would consist of replacing NIR spectroscopy with MIR spectroscopy for chemical composition and the use of Raman spectroscopy for the measurement of particle size.

Appendix

A-1 Analysis of the Effects of Granulation on Blend Uniformity and PSD Using NIR

A-1-1 Introduction

An opportunity arose during the course of this research, to take part in collaborative testing with Post-graduate researchers at the University College Cork (UCC) on a twin-screw granulator and its effects on the physical properties of a powder blend through NIR analysis. The testing took place at UCCs Analytical & Biological Chemistry Research Facility in Cork and was comprised of using IT Tralee's NIR Equipment to analyse granulated powder blends at the outlet of a Coperion K-Tron powder feeding system. The following details the test procedure and results of the collaborative effort.

A-1-2 Aim

The aim of this test was to determine the effects of twin screw granulation on blend homogeneity, PSD and segregation of a pharmaceutical grade powder blend through NIR spectroscopy in transmission mode.

A-1-3 Equipment & Materials Used

- Twin screw granulator powder feeding system – Coperion K-Tron loss-in-weight Micro-Ingredient Feeder (model K-CL-SFS-MT12) for dry or free flowing powder blends (figure A-1.1) (K-Tron, 2018).



Figure A-1.1 Experimental Set-Up of Collimating Lenses Mounted on Sensing Unit

- Hamamatsu RC-SW-NIR: C9408MA-SPL1 Spectrometer (640 – 1100nm) with SMA connectors (figure A-1.2)
- Ocean Optics LS-1 tungsten halogen light source (figure A-1.2) with Ocean Optics Fibre optic cable 600 μ m (Ocean Optics, 2013)



Figure A-1.2 Experimental Set-Up of Collimating Lenses Mounted on Sensing Unit

- API – Metoclopramide HCl Powder (ScienceLab.com, 2013)
- Excipient – Microcrystalline Cellulose(MCC) Binding agent (Foodchem, 2013)
- Excipient – Magnesium Stearate (MgSt) – Lubricant (Hardesty, 2015)

A-1-4 Methodology

The K-tron twin screw granulating feeder is generally used to convey and blend a bulk solid between unit operations. Typical applications of the K-tron include controlled feeding of jet mills or applications requiring accurate feeding of expensive micro-ingredients. The K-tron operates on the principle of co-rotating augers that intermesh to both mill and convey the bulk solid to the next unit operation as depicted in figure A-1.3.

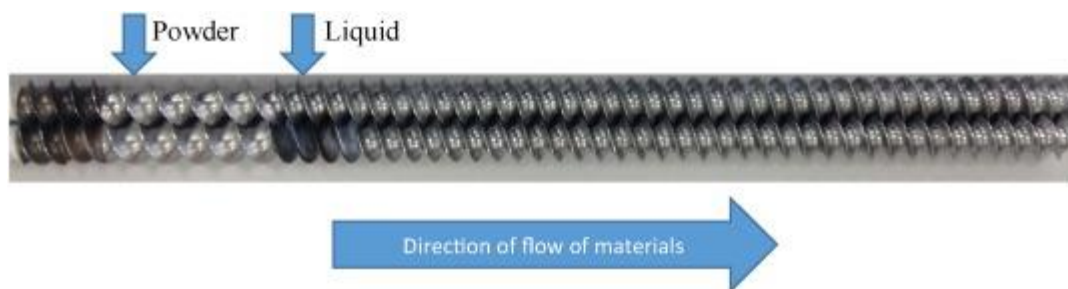


Figure A-1.3 Hamamatsu Spectrometer (left) & Ocean Optics Light Source (right)

The purpose of this test is to determine (through use of NIR data analysis), the effect twin screw granulation has on the flow properties of a pharmaceutical grade powder blend in terms of PSD, segregation and blend homogeneity. The most suitable position for NIR placement, was located at the outlet of the feeder which consisted of a 50mm downpipe. A Stainless-steel coupling was fabricated with the NIR sensor and light source in a fixed position opposite each other and positioned in an in-line configuration as shown in figure A-1.4.

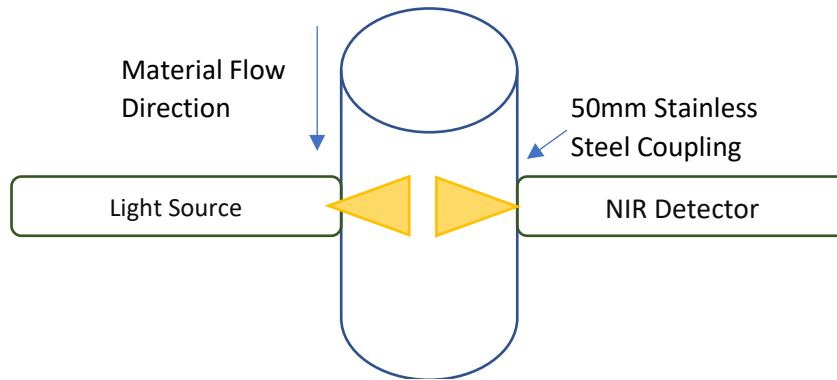


Figure A-1.4 Configuration of NIR/Light Source on Coupling

Prior to material testing, dark and reference measurements were collected for each material sample to allow for the interpretation of the subsequent NIR data. Several tests were then conducted on each material individually (for the purpose of identifying their respective spectral components) and a variety of blends and flow rates. After each test run, the feeder was stripped and cleaned to prevent any cross contamination from previously analysed blends and to maximise the accuracy of the test. The resultant data from the NIR sensor was recorded by UCC researchers for later analysis.

A-1-5 Results and Conclusions

Even though the collected NIR data was found to be unusable due to the limitations of the spectral range of the NIR spectrometer used in the test, the process followed and the consultation with Ocean Optics (during sourcing of the ocean optics NIR spectrometer) on the correct procedure was of great benefit. The Hamamatsu RC-SW-NIR spectral range of 640 – 1100nm was not suitable to the application of analysing a powder blend for PSD or chemical composition information such as segregation or blend homogeneity and the resultant data consisted mainly of noise. Spectrometers within the NIR range of 1300 – 2500nm are better suited to the analysis of chemical composition and PSD.

Furthermore, the correspondence with Ocean Optics revealed that collimating lenses were required to perform the absorbance measurements from the transmission measurements. Collimating lenses ensure that the light rays travel parallel to each other and do not disperse in unwanted directions. As path length must be constant in order to calculate absorbance from transmittance measurements, use of the Ocean Optics 600µm optical cable would have yielded similar results i.e. noise, if used with a spectrometer within the favourable range of 1300 – 2500nm for this application. This established the correct procedure to use for NIR testing with powders in this thesis.

B-1 Appendix PLSR results from material sampling chamber testing

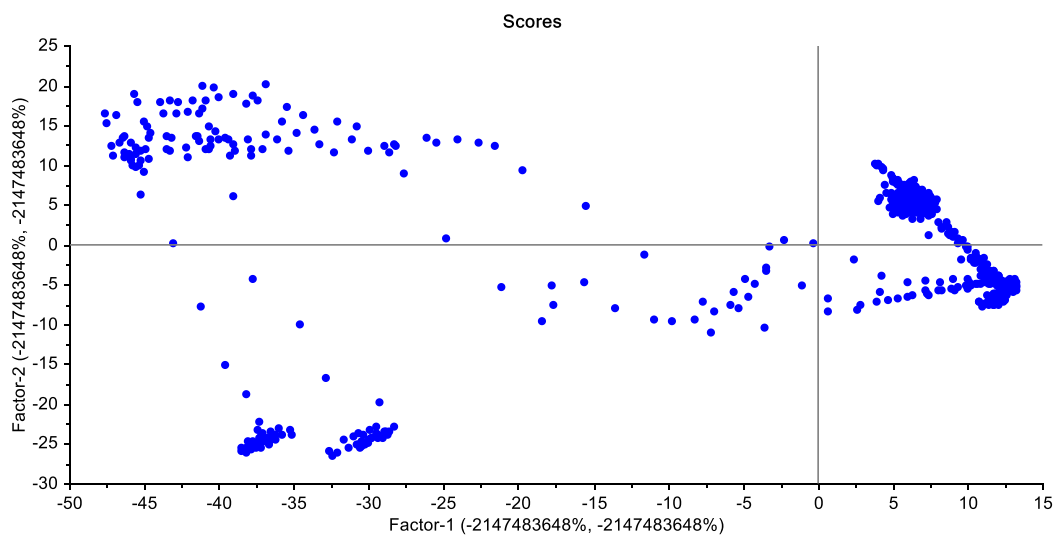


Figure B-1.1 Results from test 1 PLSR of coffee and sugar

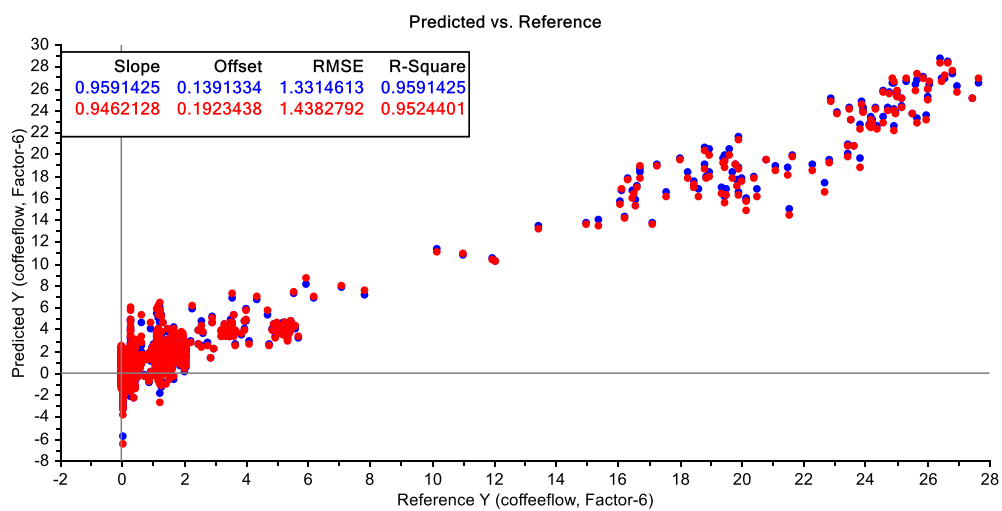


Figure B-1.2 Results from test 2 PLSR of coffee and sugar

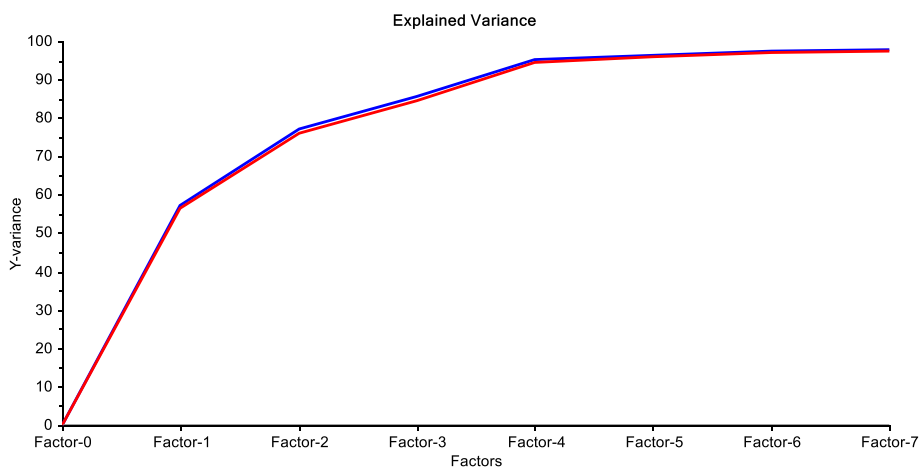


Figure B-1.3 Explained variance graph from test 2 PLSR of coffee and sugar

B-2 Appendix PLSR results from material sampling chamber testing

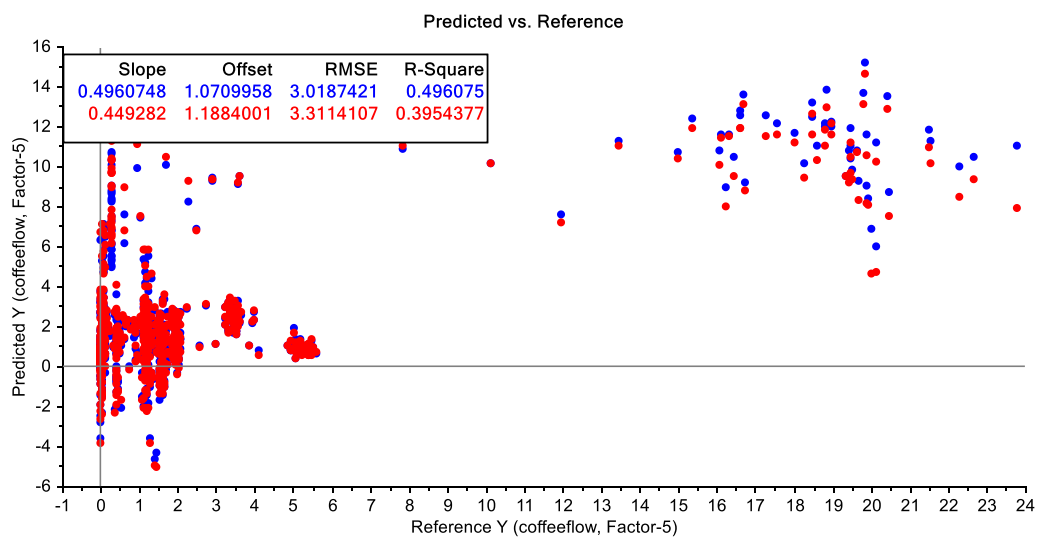


Figure B-2.1 Figure B-4 Results from test 3 PLSR of coffee and sugar

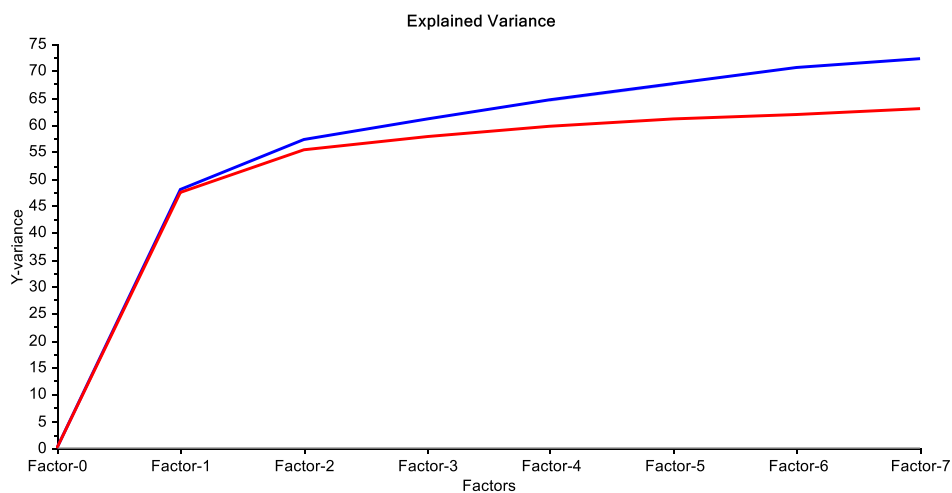


Figure B-2.2 Figure A-2.2 Explained variance graph from test 3 PLSR of coffee and sugar

B-3 Appendix PLSR results from material sampling chamber testing

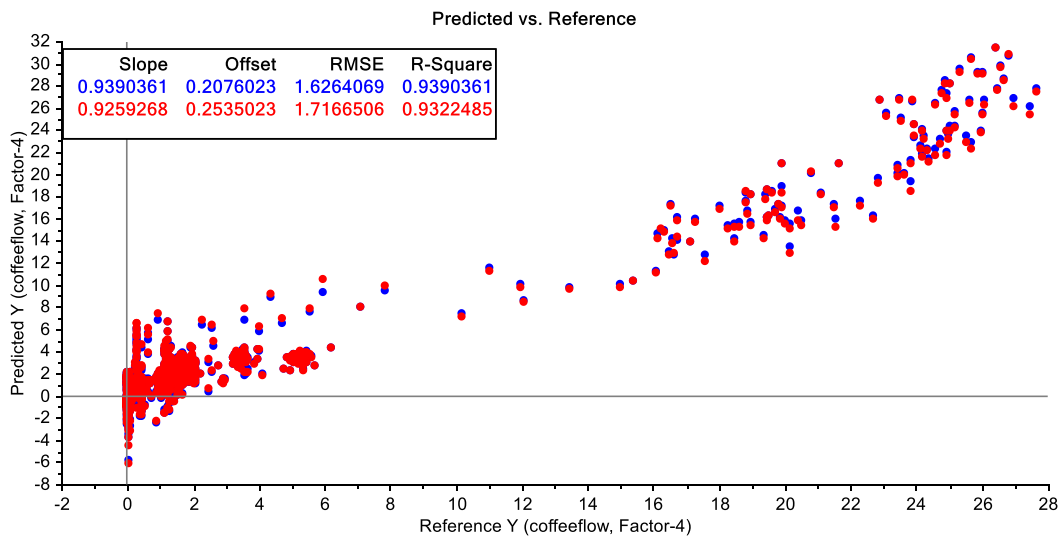


Figure B-3.1 Results from test 4 PLSR of coffee and sugar

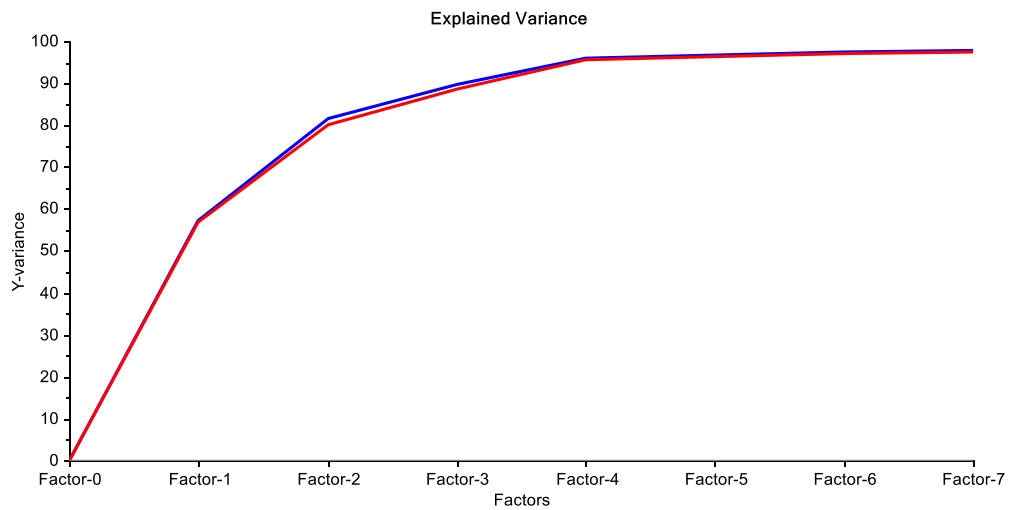


Figure B-3.2 Explained variance graph from test 4 PLSR of coffee and sugar

B-4 Appendix PLSR results from material sampling chamber testing

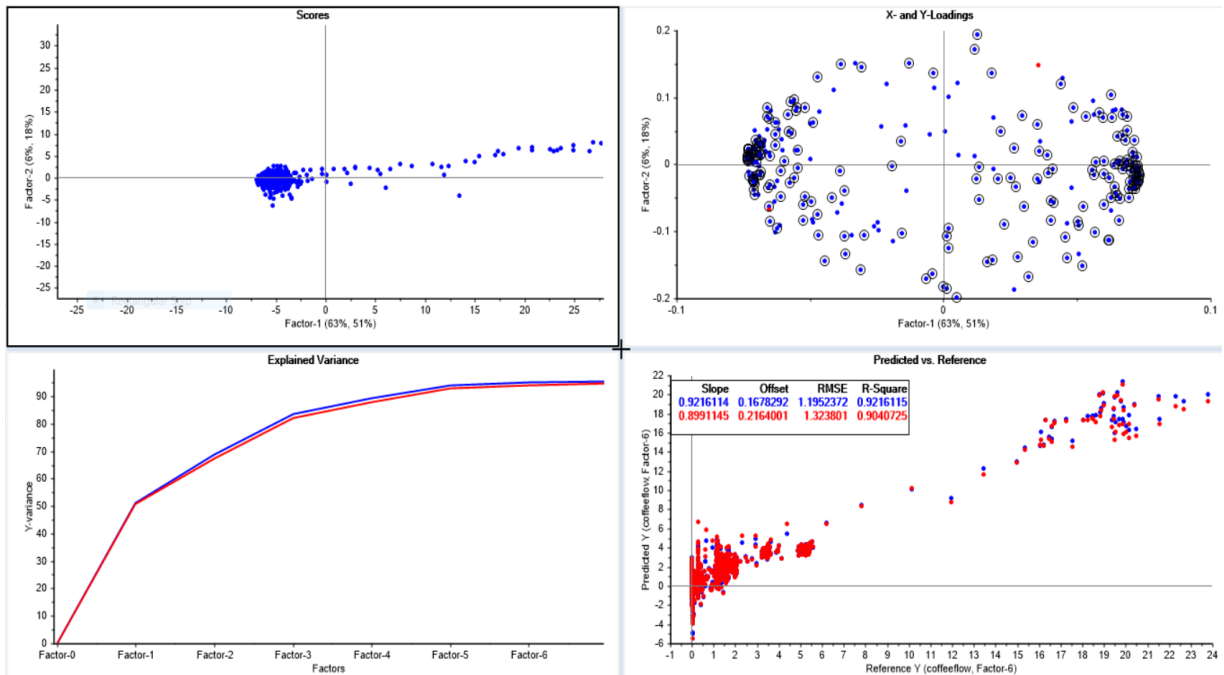


Figure B-4.1 Figure A-4.1 Results from test 5 PLSR of coffee and sugar

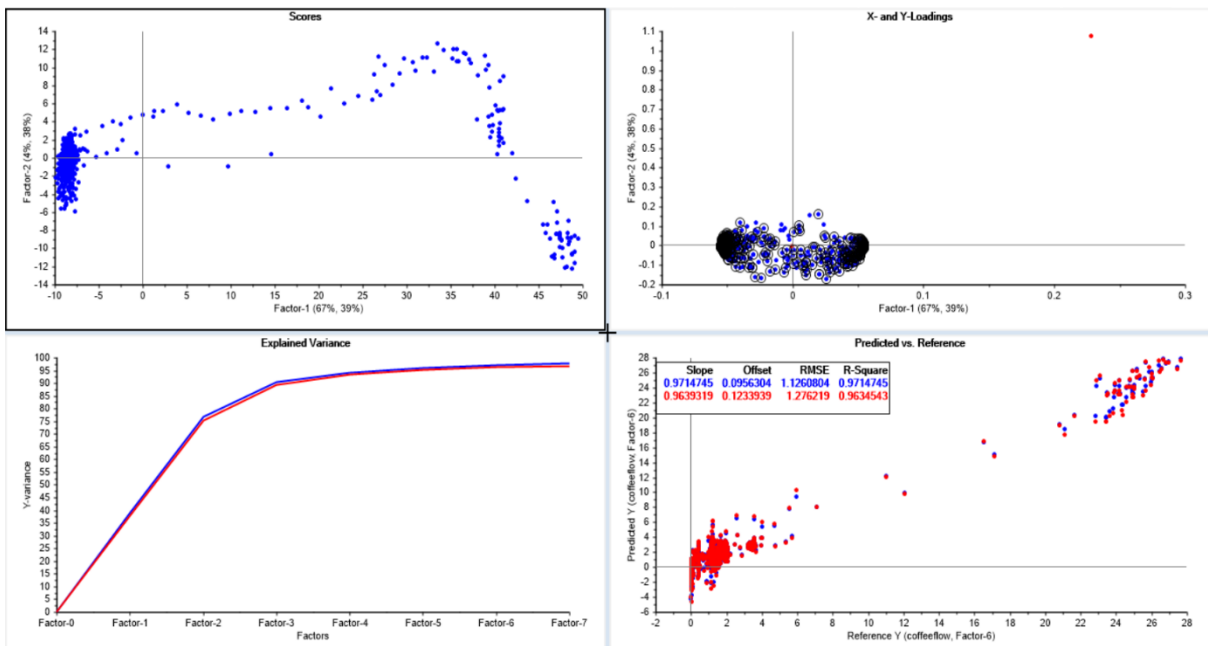


Figure B-4.2 Figure A-4.2 Results from test 6 PLSR of coffee and sugar

B-5 Appendix PLSR results from material sampling chamber testing

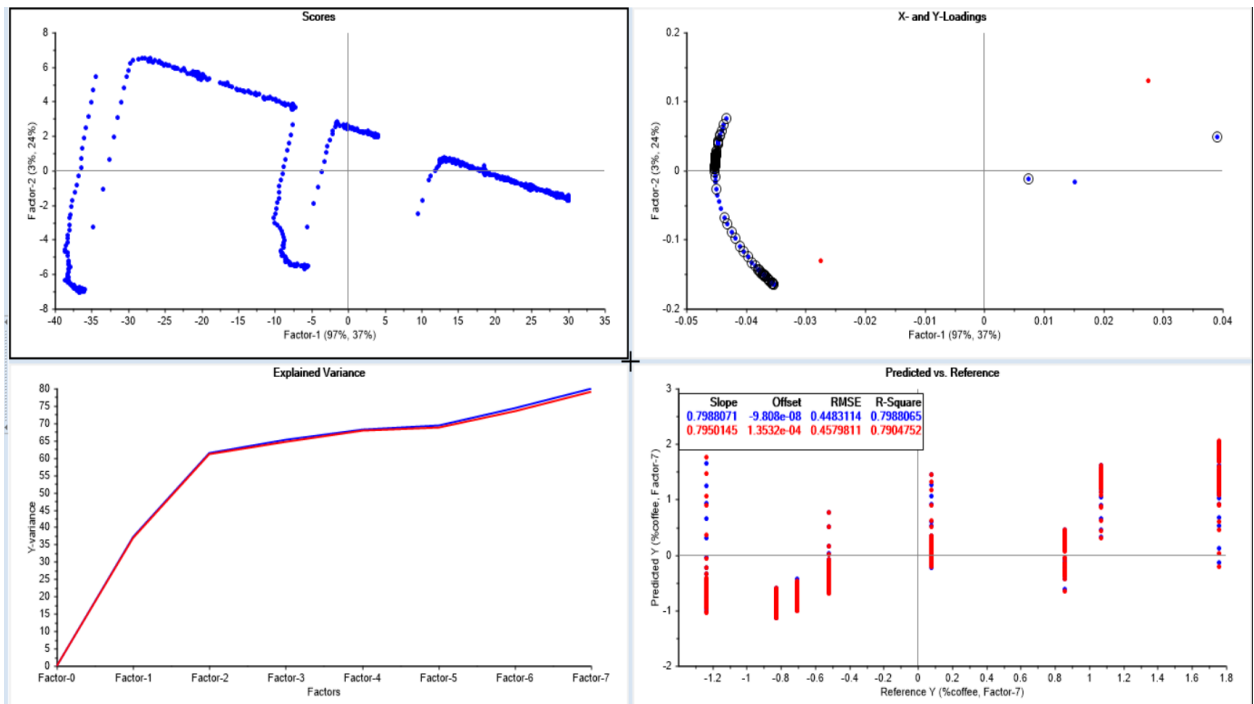


Figure B-5.1 Results from test 7 PLSR of coffee and sugar

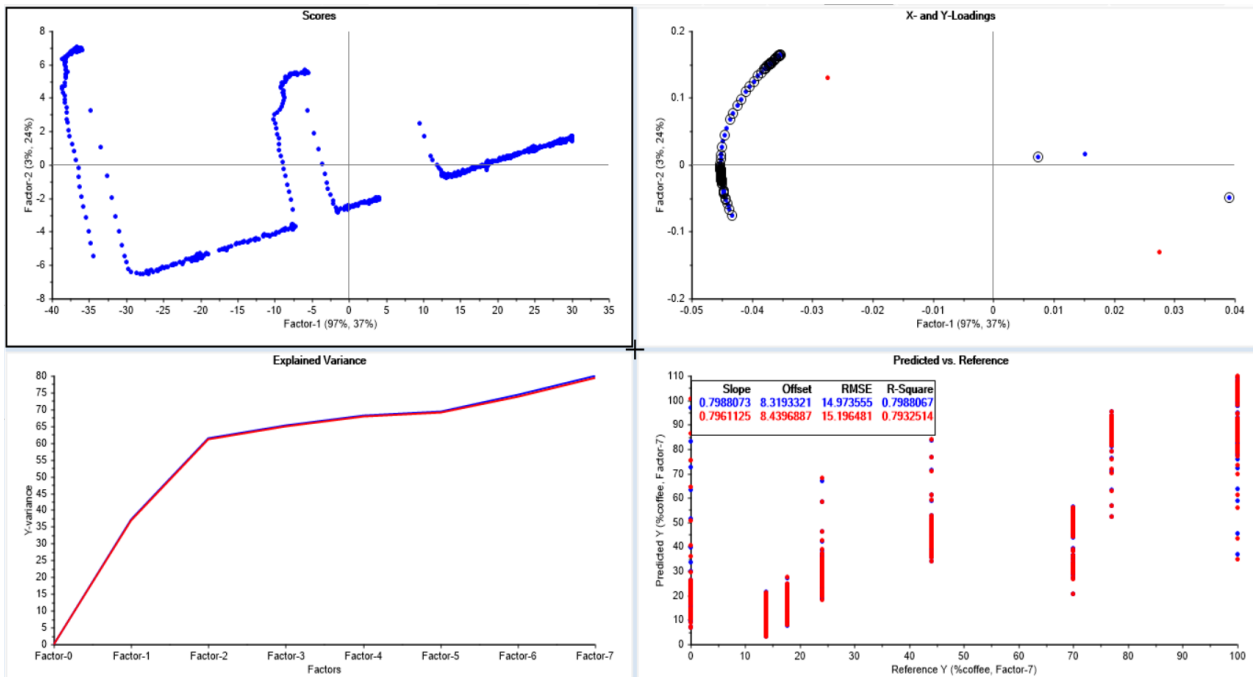


Figure B-5.2 Results from test 8 PLSR of coffee and sugar

C-1 Appendix NIR reference spectra

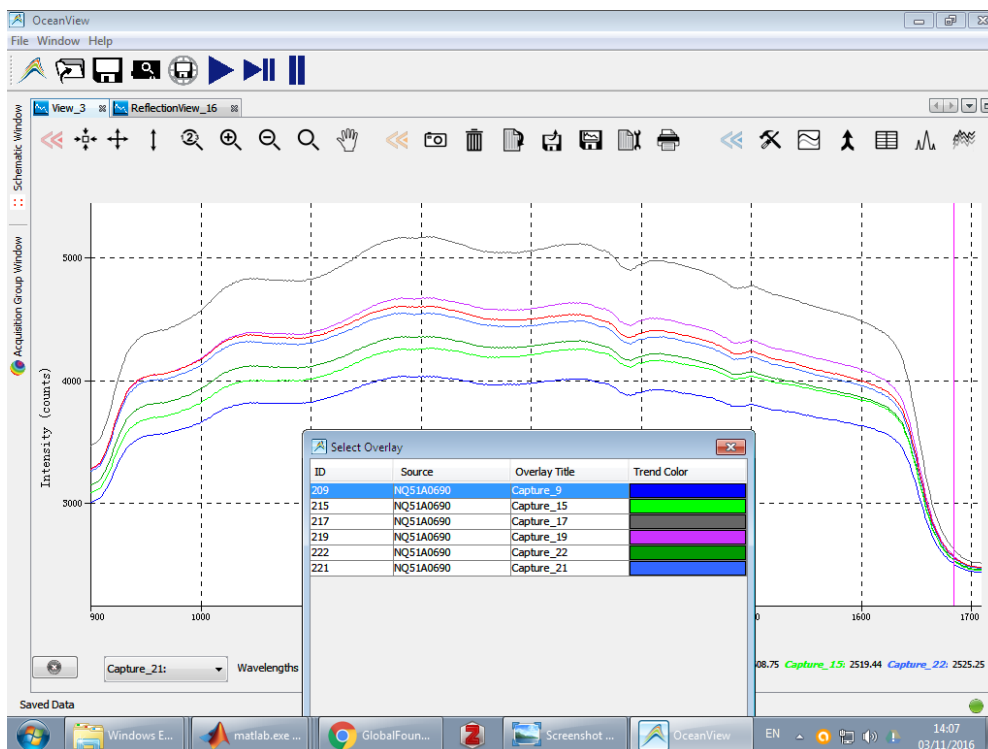


Figure C-1.1 Reference spectral data from NIR sensor for coffee

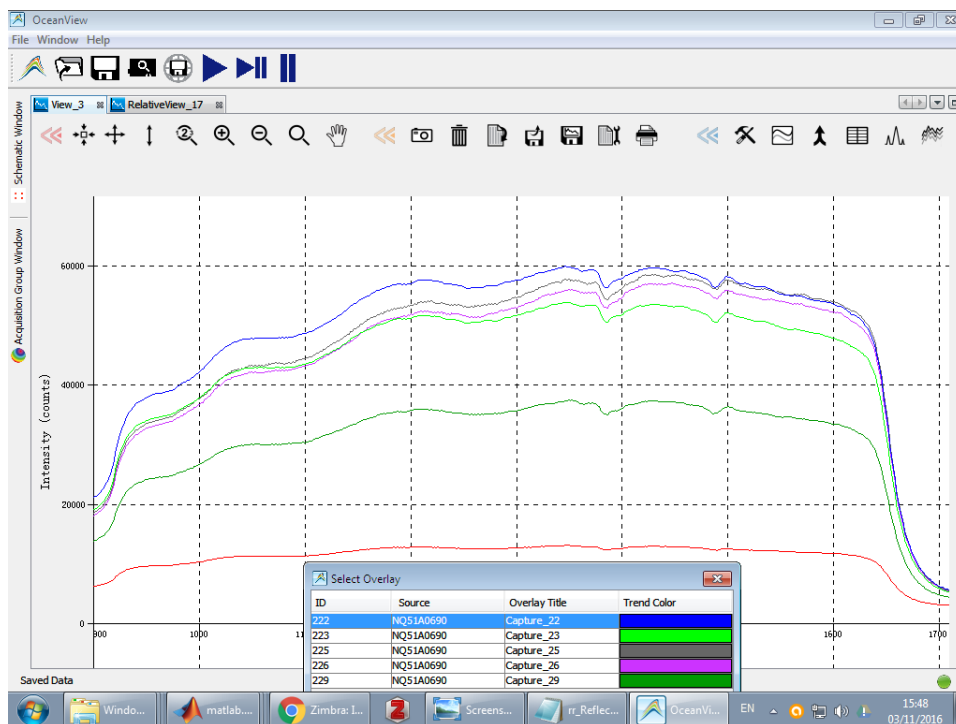


Figure C-1.2 Reference spectral data from NIR sensor for sugar

D-1 Appendix raw data from NIR

sensor_data	(λ)	massflow1	temp	dp	899.6781	901.3037	902.9292	904.5544	906.1796	907.8044	909.4291	911.0537	912.678	914.3022	915.9263	917.55	919.1737
		1	2	3	4	5	6	7	8	9	10	11	12	13	14	15	16
0.134	1	-1.1208	-2.4363	1.2863	1.5940	1.5851	1.5510	1.5729	1.6169	1.6099	1.5688	1.6834	1.5813	1.6130	1.5751	1.6966	1.6320
0.864	2	-1.1208	-2.4363	1.0124	1.5537	1.5791	1.5510	1.5902	1.5993	1.6042	1.5549	1.6778	1.5733	1.6025	1.5674	1.6456	1.6003
1.488	3	-1.1208	-2.3122	0.1908	1.5847	1.5671	1.5274	1.5729	1.5935	1.5817	1.6049	1.6553	1.5679	1.5814	1.5700	1.6100	1.5588
2.106	4	-1.1208	-2.4363	1.2863	1.5909	1.5910	1.5746	1.5700	1.6052	1.5986	1.5771	1.6525	1.6107	1.5814	1.5674	1.6100	1.5490
2.698	5	-1.1208	-2.4363	1.6970	1.5971	1.6150	1.5628	1.6105	1.6461	1.5817	1.5910	1.6497	1.5519	1.6077	1.5570	1.5998	1.5343
3.312	6	-1.0950	-2.4363	1.5601	1.5847	1.5791	1.5687	1.6134	1.6285	1.6071	1.6022	1.6778	1.5947	1.5762	1.5881	1.5489	1.5197
3.932	7	-1.0950	-2.4363	0.6016	1.6033	1.6030	1.5687	1.5989	1.6227	1.6268	1.5827	1.6778	1.5920	1.6025	1.5777	1.5438	1.5245
4.561	8	-0.9399	-2.4363	1.0124	1.5785	1.6090	1.5863	1.6220	1.6256	1.6099	1.5855	1.6722	1.5519	1.5867	1.5312	1.5438	1.4903
5.181	9	-0.7332	-2.3122	0.4647	1.5847	1.6030	1.5746	1.5902	1.6256	1.6212	1.5855	1.6412	1.5412	1.6130	1.5156	1.5642	1.4415
5.793	10	-0.5007	-2.1880	0.3278	1.5909	1.5910	1.5863	1.6105	1.6169	1.6381	1.6077	1.6469	1.5945	1.6051	1.5208	1.5285	1.4757
6.415	11	-0.4232	-2.1880	1.0124	1.5723	1.6090	1.5746	1.6018	1.6227	1.6268	1.5938	1.6609	1.5947	1.5867	1.5518	1.5540	1.4708
7.045	12	-0.5007	-2.1880	0.3278	1.6405	1.5791	1.6276	1.5613	1.6440	1.5901	1.5799	1.6609	1.6000	1.5867	1.5415	1.5540	1.4708
7.665	13	-0.7332	-2.3122	1.2863	1.6281	1.6269	1.6099	1.6307	1.6344	1.6183	1.5966	1.6159	1.6268	1.5867	1.5622	1.5489	1.4708
8.284	14	-0.8883	-2.1880	1.4232	1.6715	1.5970	1.6158	1.6018	1.6169	1.6409	1.6299	1.6497	1.5947	1.6183	1.5777	1.5591	1.4855
8.894	15	-0.9916	-2.3122	1.9709	1.6343	1.6509	1.6335	1.6336	1.6402	1.6663	1.6133	1.6412	1.5947	1.6393	1.5518	1.5642	1.4610
9.521	16	-1.0433	-2.1880	0.0539	1.6343	1.6389	1.6158	1.6278	1.6110	1.6889	1.5966	1.6750	1.5840	1.5972	1.5518	1.5438	1.4659
10.141	17	-1.0691	-2.1880	1.2863	1.6033	1.6150	1.6040	1.6191	1.6110	1.5996	1.6522	1.6103	1.6000	1.5814	1.5467	1.5183	1.4561
10.735	18	-1.1208	-2.1880	1.5601	1.6281	1.6210	1.5804	1.6481	1.5877	1.6607	1.5744	1.6187	1.5893	1.5920	1.5518	1.5132	1.4586
11.357	19	-1.1208	-2.3122	1.6970	1.6281	1.6269	1.6040	1.6249	1.6402	1.6268	1.6244	1.6103	1.6161	1.5972	1.5596	1.4980	1.4610
11.965	20	-1.0691	-2.1880	0.7386	1.6405	1.6210	1.6099	1.6336	1.6169	1.6268	1.6077	1.6440	1.5759	1.6235	1.5415	1.4980	1.4366
12.577	21	-0.9399	-2.3122	0.6016	1.6219	1.6389	1.6099	1.6625	1.6023	1.6776	1.6022	1.5990	1.5893	1.5972	1.5674	1.4980	1.4561
13.202	22	-0.7849	-2.3122	-0.4938	1.6281	1.5970	1.6217	1.6394	1.6461	1.6437	1.6244	1.6046	1.6161	1.5814	1.5518	1.4827	1.4610
13.826	23	-0.7332	-2.1880	-0.2199	1.6374	1.6269	1.6335	1.6365	1.5993	1.6889	1.5938	1.5934	1.6107	1.5867	1.5674	1.5132	1.4561
14.452	24	-0.8883	-2.1880	-0.6307	1.6591	1.6449	1.6541	1.6654	1.6315	1.6268	1.6355	1.5934	1.6589	1.5867	1.6165	1.4954	1.4464
15.072	25	-0.9658	-2.3122	-2.1369	1.6033	1.6269	1.6276	1.6249	1.6081	1.6325	1.5855	1.5990	1.5813	1.5893	1.5363	1.4725	1.4513
15.679	26	-0.7332	-2.0639	-2.2738	1.6219	1.6030	1.6452	1.5960	1.6519	1.5873	1.6411	1.5540	1.5947	1.5920	1.5622	1.4725	1.4366
16.272	27	-0.3715	-2.3122	0.3278	1.6467	1.5910	1.6511	1.5931	1.6519	1.5986	1.6022	1.5709	1.6161	1.5788	1.5777	1.4929	1.4464
16.863	28	0.0419	-2.1880	-1.7261	1.6281	1.6210	1.6099	1.6336	1.6110	1.6155	1.6299	1.5765	1.6161	1.5604	1.5518	1.4827	1.4219
17.511	29	0.3778	-2.0639	-0.6307	1.6281	1.6269	1.6335	1.6134	1.5935	1.6212	1.6383	1.5652	1.6161	1.5972	1.5570	1.4700	1.4855
18.128	30	0.4036	-2.0639	-1.7261	1.5909	1.6150	1.6217	1.6191	1.5760	1.6042	1.6299	1.5596	1.6000	1.5867	1.5622	1.4598	1.4317
18.736	31	0.5070	-2.1880	-1.3154	1.6033	1.5552	1.6570	1.5844	1.6198	1.5704	1.6216	1.5315	1.6000	1.5920	1.5570	1.4572	1.4415
19.354	32	0.5328	-2.1880	-0.6307	1.6095	1.6269	1.5981	1.5989	1.5993	1.5901	1.6133	1.5624	1.6348	1.5867	1.5415	1.4572	1.4513
19.973	33	0.6362	-2.3122	-0.4938	1.5971	1.6150	1.6276	1.6134	1.6081	1.6099	1.6411	1.5455	1.6241	1.5814	1.5674	1.4623	1.4464
20.598	34	0.5328	-2.1880	-3.7800	1.6343	1.6269	1.6276	1.6076	1.5935	1.5901	1.6744	1.5174	1.6054	1.5657	1.5441	1.4470	1.4366
21.217	35	0.5587	-2.3122	-0.9046	1.5909	1.6210	1.6099	1.6567	1.5701	1.5873	1.6411	1.5512	1.6268	1.5709	1.5570	1.4572	1.4659
21.811	36	0.5070	-2.3122	-0.3569	1.6219	1.6150	1.6452	1.6134	1.6023	1.5986	1.6466	1.5343	1.6348	1.5657	1.5932	1.4369	1.4464
22.42	37	0.5328	-2.3122	-0.6307	1.5909	1.5791	1.6452	1.5931	1.5935	1.6155	1.6411	1.5512	1.6080	1.5920	1.5674	1.4521	1.4415
23.044	38	0.5328	-2.0639	-0.7676	1.6157	1.6150	1.6335	1.6076	1.5993	1.6212	1.6244	1.5343	1.6241	1.5814	1.5518	1.4623	1.4366

Figure D.1.1 Raw NIR data from NIR spectrometer

D-2 Appendix PLS model

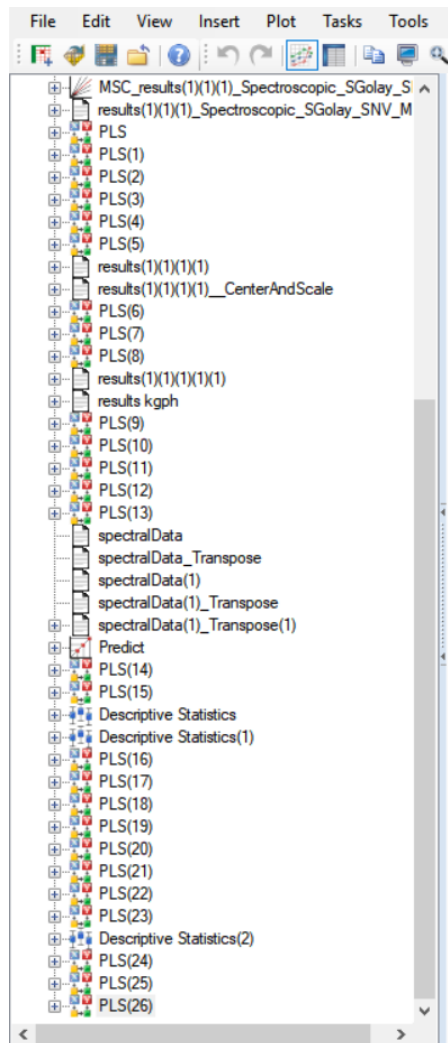


Figure D.2.1 Highlights the number of PLS tests conducted during the generation of PLS model

References

- Ahlawat, N., 2014. Raman Spectroscopy: A Review. *International Journal of Computer Science and Mobile Computing*, 3(11), pp.680–685.
- Ahuja, D. and Parande, D., 2012. Optical sensors and their applications. *Journal of Scientific Research and Reviews*, [online] 1(5), pp.60–68. Available at: <<http://www.wudpeckerresearchjournals.org>>.
- All-Fill, 2018. *Common Powder Groups - All Fill*. [online] Available at: <<http://www.allfill.co.uk/faq/common-powder-groups/>> [Accessed 15 Feb. 2018].
- Allen, T., 2003a. *Powder Sampling and Particle Size Determination*. [online] *Powder Sampling and Particle Size Determination*. Elsevier. Available at: <<http://www.sciencedirect.com/science/article/pii/B9780444515643500036>> [Accessed 26 Nov. 2015].
- Allen, T., 2003b. *Powder Sampling and Particle Size Determination*. [online] *Powder Sampling and Particle Size Determination*. Elsevier. Available at: <<http://www.sciencedirect.com/science/article/pii/B9780444515643500115>> [Accessed 10 Dec. 2015].
- Andor, 2017. *What is ATR Spectroscopy? | Andor*. [online] Available at: <<http://www.andor.com/learning-academy/absorption-transmission-reflection-spectroscopy-an-introduction-to-absorption-transmission-reflection-spectroscopy>> [Accessed 15 Oct. 2017].
- Arakaki, C. and Tel-tek, C.R., 2008. Changes in Particle Size and Shape in Pneumatic Conveying of dextrose. (February 2015).
- Bakeev, K.A., 2004. Near-Infrared Spectroscopy as a Process Analytical Tool. *Spectroscopy*, 19(1), pp.39–42.
- Barnam, R.A. and Prescott, J.K., 2011. *Considerations for Steering Particle Size*. [online] Pharmpro. Available at: <<http://www.pharmpro.com/article/2011/04/considerations-steering-particle-size>> [Accessed 6 Dec. 2016].
- Barron, W.R., 1992. Principles of Infrared Thermometry. *Sensors Magazine*, 9, p.10.
- Bhuyan, M., 2010. *Intelligent Instrumentation: Principles and Applications*. CRC Press.
- Bio-Thermal-Energy, 2018. *RayMas® Non-contact Solids Flow Meter | Bio-Thermal-Energy, Inc.* [online] Available at: <<http://b-t-einc.com/raymas.htm>> [Accessed 15 Feb. 2018].
- Bourgeois, J. and Goldstein, S.C., 2015. Distributed Intelligent MEMS: Progresses and Perspectives. *IEEE Systems Journal*, 9(3), pp.1057–1068.
- Breede, J., 2015. The effects of improved calibration. *Fire and Safety Magazine*, pp.56–59.
- Brittain, H.G., 2002. Particle-Size Distribution II : Powdered Solids of sampling powdered solids. *Pharmaceutical physics*, 2(July), pp.1–5.
- Broadcast, C., 2006. Guidance for Industry Guidance for Industry. *Centre for drug evaluation and research*, [online] 1(August), p.14. Available at: <<http://www.fda.gov/downloads/Drugs/.../Guidances/ucm070287.pdf>>.
- Bu, D., 2007. Chemometric Analysis for Spectroscopy. *Tech Flash*.
- Byjus.com, 2018. *Continuity Equation | Fluid Dynamics & Examples*. [online] Available at: <<https://byjus.com/physics/continuity-equation/>> [Accessed 16 Feb. 2018].

Camo, 2004. Multivariate Data Analysis for Biotechnology and Bio-processing. *Camo*. [online] Available at: <<http://www.camo.com>>.

Camo, 2016. *Chemometrics intro*. [online] Available at: <<http://www.camo.com/rt/Resources/chemometrics.html>> [Accessed 2 Mar. 2016].

Camo, 2018. *The Unscrambler® X, Leading Multivariate Data Analysis & Design of Experiments software*. [online] Available at: <<http://www.camo.com/rt/Products/Unscrambler/unscrambler.html>> [Accessed 25 Feb. 2018].

Carillo, D., 2002. *Contact Sensors Loosing the Battle against Non-Contact Sensors*. [online] Available at: <<https://www.frost.com/prod/servlet/market-insight-print.pag?docid=JEVS-5N2H2L>> [Accessed 23 Oct. 2017].

Choudhary, A., 2011. *Pharmaceutical Guidelines*. [online] Pharma Guideline. Available at: <<http://www.pharmaguideline.com/2016/02/principle-of-tablet-compression-machine.html>> [Accessed 5 Dec. 2016].

Cie, 2004. The evaluation of whiteness. *Colorimetry, 3rd Edition*, [online] 552, p.24. Available at: <http://div1.cie.co.at/?i_ca_id=551&pubid=23>.

Cohen, O. and Edan, Y., 2008. A sensor fusion framework for online sensor and algorithm selection. *Robotics and Autonomous Systems*, 56(9), pp.762–776.

Dairymaster, 2018. *Milking Parlours Milking Machines, Heat detection, Scrapers, Feeders, Milk Cooling - Dairymaster*. [online] Available at: <<http://www.dairymaster.com/>> [Accessed 16 Feb. 2018].

Demand-Solutions, 2017. *critical process parameters*. [online] Available at: <<http://www.demandsolutions.com/resource-center/supply-chain-glossary/supply-chain-glossary-c/critical-process-parameters.html>> [Accessed 5 Apr. 2017].

Department of Energy Office of Science, 2000. Scientific Discovery through Advanced Computing. *Office of Science, U.S. Department of Energy*, p.28.

DeWitt, D.P. and Nutter, G.D. eds., 1988. *Theory and practice of radiation thermometry*. New York: Wiley.

Digby, C. (IRIS), 2014. Horizon 2020 Call : H2020-MG-2014 _ TwoStages Type of action : RIA Proposal number : SEP-210144595 Proposal acronym : SuperMoBike. pp.1–40.

Dippel, B., 2016. *Pros and Cons of Raman spectroscopy*. [online] Available at: <<http://www.raman.de/htmlEN/home/advantageEn.html>> [Accessed 3 Mar. 2016].

DPT, 2013. What is quality by design (QbD) – and why should you care? *DPT Thought Leadership*, 1(11).

Eastern-Instruments, 2017. *Solids Mass Flow Meter | Powder/Bulk Solids*. [online] Available at: <<http://www.powderbulksolids.com/article/Solids-Mass-Flow-Meter-10-19-2016>> [Accessed 19 Oct. 2017].

Easternn-Instruments, 2017. *Solids Flow Meters, Feeders and Fillers - EI Mass Flow Meters*. [online] Available at: <<https://easterninstruments.com/Solids Flow Measurement.html>> [Accessed 19 Oct. 2017].

Edmund-Optics, 2017. *Infrared Fresnel Lenses – IR Fresnel Lenses*. [online] Available at: <<https://www.edmundoptics.com/optics/optical-lenses/fresnel-lenses/infrared-ir-fresnel-lenses/>> [Accessed 8 Oct. 2017].

- Elmenreich, W., 2002. *Sensor Fusion in Time-Triggered Systems*. [online] Technischen Universität Wien. Available at: <https://www.researchgate.net/publication/215499135_Sensor_Fusion_in_Time-Triggered_Systems>.
- EnggCyclopedia, 2018. *Absolute Pipe Roughness*. [online] Available at: <<http://www.enggcyclopedia.com/2011/09/absolute-roughness/>> [Accessed 4 Feb. 2018].
- Engineering-Toolbox, 2018a. *Colebrook Equation*. [online] Available at: <https://www.engineeringtoolbox.com/colebrook-equation-d_1031.html> [Accessed 16 Mar. 2018].
- Engineering-Toolbox, 2018b. *Equation of Continuity*. [online] Available at: <https://www.engineeringtoolbox.com/equation-continuity-d_180.html> [Accessed 16 Mar. 2018].
- Engineers-Edge, 2018. *Pressure Drop Along Pipe Length - Fluid Flow Hydraulic and Pneumatic, Engineers Edge*. [online] Available at: <https://www.engineersedge.com/fluid_flow/pressure_drop/pressure_drop.htm> [Accessed 4 Feb. 2018].
- Envea, 2018. *Ultrasonic flow meter / mass / for solids / ultra-compact - Solidflow 2.0 - Environnement S.A.* [online] Available at: <<http://www.directindustry.com/prod/environnement-sa/product-23554-1814367.html>> [Accessed 15 Feb. 2018].
- Escubed, 2015. *Sampling Techniques*. [online] Escubed Ltd. Available at: <[http://www.escubed.co.uk/sites/default/files/particle_size_analysis_\(an003\)_sampling_techniques.pdf](http://www.escubed.co.uk/sites/default/files/particle_size_analysis_(an003)_sampling_techniques.pdf)> [Accessed 11 Oct. 2015].
- Evitherm, 2018. *Influencing Factors of Emissivity*. [online] Available at: <<http://www.evitherm.org/default.asp?ID=216>> [Accessed 13 Aug. 2018].
- Fauchais, P., Montavon, G. and Bertrand, G., 2010. From powders to thermally sprayed coatings. *Journal of Thermal Spray Technology*, 19(1–2), pp.56–80.
- FDA, 2004a. Pharmaceutical CGMPs for the 21s Century - A risk-based approach. [online] (September), p.32. Available at: <<http://www.fda.gov/Drugs/DevelopmentApprovalProcess/Manufacturing/QuestionsandAnsweronCurrentGoodManufacturingPracticescGMPforDrugs/UCM071836>>.
- FDA, U.S.D. of H. and H.S., 2004b. Guidance for Industry PAT — A Framework for Innovative Pharmaceutical Development, Manufacturing, and Quality Assurance. [online] (September), p.16. Available at: <<http://www.fda.gov/downloads/Drugs/GuidanceComplianceRegulatoryInformation/Guidances/ucm070305.pdf>>.
- Fedder, G.K., Howe, R.T., Liu, T.-J.K. and Quevy, E.P., 2008. Technologies for Cofabricating MEMS and Electronics. *Proceedings of the IEEE*, 96(2), pp.306–322.
- Foodchem, 2013. Microcrystalline Cellulose MSDS. (Mcc), pp.6–7.
- Frank, R., 2013. *Understanding Smart Sensors (3rd Edition)*. Norwood, MA, USA: Artech House.
- Friend, S., Arlington, S., Marshall, J. and Bailey, W., 2011. Pharma 2020: Supplying the Future. [online] p.36. Available at: <www.pwc.com/pharma2020>.
- Fukui, J., Osanai, M., Mizoroke, S. and Khorram, H.R., 2015. MEMS manufacturing solutions. In: *Advanced Semiconductor Manufacturing Conference (ASMC), 2015 26th Annual SEMI*. pp.356–361.
- Gaura, E. and Newman, R.M., 2004. Smart, intelligent and cogent MEMS based sensors. In:

Proceedings of the 2004 IEEE International Symposium on Intelligent Control, 2004. IEEE, pp.431–436.

Gea, 2017. *Volumetric and Gravimetric Feeder*. [online] Available at: <<http://www.gea.com/en/products/gea-volumetric-feeder.jsp>> [Accessed 19 Oct. 2017].

Global-Spec, 2017. *Solids Flow Meters Information | Engineering360*. [online] Available at: <http://www.globalspec.com/learnmore/sensors_transducers_detectors/flow_sensing/flowmeters_solids> [Accessed 20 Oct. 2017].

GMPUA, 2017. *Process Analytical Technology (PAT)*. [online] Available at: <<http://www.gmpua.com/World/Manu/07/j.htm>> [Accessed 26 Oct. 2017].

GSK, 2017. *Barnard Castle | GSK UK*. [online] Available at: <<http://uk.gsk.com/en-gb/about-us/uk-locations/barnard-castle/>> [Accessed 30 Oct. 2017].

GSK, 2018. *Home | GSK*. [online] Available at: <<https://www.gsk.com/>> [Accessed 16 Mar. 2018].

Happel, J., 2015. *Case Study Flow Measurement in Dense Phase Applications*.

Hardesty, 2015. *Magnesium Stearate NF Powder MSDS*.

Harun, S.W.; Yasin, M.; Yang, H.Z.; Ahmad, H., 2010. Fiber Optic Displacement Sensors and Their Applications. *Fiber Optic Sensors*, p.359.

Hayes, M. (Leo P., 2009. *Right-First-Time Project*. [online] PharmaChem Skillnet. Available at: <<http://www.pharmachemskillnet.ie/index.cfm/page/presentations>> [Accessed 18 Feb. 2016].

Hense, 2014. *MIC-SMART*. Brilon.

Hense, 2017a. *MIC-Flowmeter | Solid flow meters | Products | Hense Wägetechnik GmbH*. [online] Available at: <<https://hense-waetechnik.de/en/solid-flow-meters/mic-smart-microwave-meter/>> [Accessed 30 Oct. 2017].

Hense, 2018b. *MIC-Flowmeter | Solid flow meters | Products | Hense Wägetechnik GmbH*. [online] Available at: <<https://hense-waetechnik.de/en/solid-flow-meters/mic-smart-microwave-meter/>> [Accessed 21 Jan. 2018].

Hense, 2018c. *MIC-Flowmeter | Solid flow meters | Products | Hense Wägetechnik GmbH*. [online] Available at: <<https://hense-waetechnik.de/en/solid-flow-meters/mic-smart-microwave-meter/>> [Accessed 16 Mar. 2018].

Hense, n.d. *Type 'MIC- Flow Meter' for Solids | MIC-Flowmeter | Solid Flow Measurement | Products | Hense Wägetechnik GmbH*.

Horiba, 2016a. *Pharmaceutical Particle Size, Shape, Surface Area and Stability - HORIBA*. [online] Horiba Scientific. Available at: <<http://www.horiba.com/scientific/products/particle-characterization/applications/pharmaceuticals/>> [Accessed 1 Dec. 2016].

Horiba, 2016b. *What are the most common applications of Raman spectroscopy?* [online] Available at: <<http://www.horiba.com/scientific/products/raman-spectroscopy/raman-academy/raman-faqs/what-are-the-most-common-applications-of-raman-spectroscopy/>> [Accessed 2 Mar. 2016].

ICH Expert Working Group, 2009. *Pharmaceutical Development Q8. ICH Harmonised Tripartite Guideline*, 8(August), pp.1–28.

li, W.N.P., 2014. *Generic Entry Jujitsu: Innovation and Quality in Drug Manufacturing*. 4(1).

Imko, 2018. *IMKO Moisture Measurement*. [online] Available at:

<<https://imko.de/enn/products/industrial-moisture/sonovario/standard>> [Accessed 11 Jan. 2018].

Iso, 1999. ISO 2859-1 Sampling procedures for inspection by attributes: Part 1 - Sampling schemes indexed by acceptance quality limit (AQL) for lot-by-lot inspection. *Iso*, 2nd editio, p.94.

Jagtap, M. and Karekar, P., 2016. A BRIEF REVIEW ON PROCESS ANALYTICAL TECHNOLOGY (PAT). *Internationa Journal of Current Pharmaceutical Research*, 8(1).

Jensis, K., 2013. *What accuracy can color sensors and mini spectrometers achieve*. MAZeT GMBH.

Jeon, D. and Eun, Y., 2014. Distributed asynchronous multiple sensor fusion with nonlinear multiple models. *Aerospace Science and Technology*, (Journal Article).

Johanson, J.R., 1988. Segregation mechanisms. [online] (August), pp.13–18. Available at: <http://www.powderbulk.com/wp-content/uploads/pdf/pbe_19880801_13.pdf>.

K-Tron, 2018. *MT12 Datasheet -- Coperion K-Tron -- Micro-Ingredient Feeder | Engineering360*. [online] Available at: <<http://datasheets.globalspec.com/ds/2896/CoperionKtron/F335EE28-DD88-42FF-9E41-A88A4EBFBC80>> [Accessed 5 Feb. 2018].

Kaminska, J. and Danko, J., 2011. Analysis of the Granulation Process Mechanism –. *Metallurgy and Foundry engineering*, 37(1), p.7.

Kemtrak, 2017. *Kemtrak DCP007 Photometer (UV-VIS-NIR) - Industrial in-line analyzer for concentration and color control*. [online] Available at: <http://www.kemtrak.com/products_DCP007.html> [Accessed 8 Oct. 2017].

Keyence, 2017a. *What is a Fiber Optic Sensor? | Sensor Basics: Introductory Guide to Sensors | KEYENCE*. [online] Available at: <<https://www.keyence.com/ss/products/sensor/sensorbasics/fiber/info/>> [Accessed 27 Oct. 2017].

Keyence, 2018b. *Digital Infrared Temperature Sensor - FT series | KEYENCE America*. [online] Available at: <<https://www.keyence.com/products/process/temperature/ft/index.jsp>> [Accessed 15 Feb. 2018].

King, R.J., King, K.V. and Woo, K., 1992. Microwave moisture measurement of grains. *IEEE Transactions on Instrumentation and Measurement*, 41(1), pp.111–115.

Kinjal G, S. and Ketan V, S., 2014. Process Analytical Technique. *Pharma Science Monitor*, 5(2), pp.21–38.

Krohn, D., MacDougall, T. and Mendez, A., 2014. *Fiber Optic Sensors - Fundamentals and Applications*.

Labcognition, n.d. *Multiplicative Scatter Correction*. [online] Available at: <http://www.labcognition.com/onlinehelp/en/multiplicative_scatter_correction.htm>.

Lean-Manufacturing-Tools, 2017. *Value Add vs Non-Value Adding Processes*. [online] Available at: <<http://leanmanufacturingtools.org/89/value-add-vs-non-value-adding-processes/>> [Accessed 5 Apr. 2017].

Lettieri, P. and Macrì, D., 2016. Effect of process conditions on fluidization. *KONA Powder and Particle Journal*, 2016(33), pp.86–108.

Lewis, D, C., 2016. *Accurately Measuring Dry Bulk Solids*. [online] Powder Bulk Solids. Available at: <<http://www.powderbulksolids.com/article/Accurately-Measuring-Dry-Bulk-Solids-01-04-2016>> [Accessed 20 Oct. 2017].

Li, H., 2007. PAT – Practical Approaches to Implement Text NIR in Pharmaceutical Processes Process

- Analytical Technology (PAT) Typical Pharma Manufacturing Unit Operations and PAT. pp.1–29.
- Liiprott, D., 2017. *Metering Screw Feeding*. [online] Agg-Net. Available at: <<https://www.agg-net.com/resources/articles/concrete/metering-screw-feeding>> [Accessed 19 Oct. 2017].
- LLC, 2017. *An Introduction to Fiber-Optic Sensors | Sensors Magazine*. [online] Available at: <<http://www.sensormag.com/components/introduction-to-fiber-optic-sensors>> [Accessed 8 Oct. 2017].
- Luna, n.d. Fiber optic sensing 1. [online] pp.1–8. Available at: <www.lunainc.com>.
- Luo, R.C. and Pan, Y.-L., 2007. Rapid Manufacturing of Intelligent Mold With Embedded Microsensors. *IEEE/ASME Transactions on Mechatronics*, 12(2), pp.190–197.
- Macri, D., Poletto, M., Barletta, D., Sutcliffe, S. and Lettieri, P., 2017. Analysis of industrial reactive powders flow properties at high temperature. *Powder Technology*, [online] 316, pp.131–138. Available at: <<http://dx.doi.org/10.1016/j.powtec.2016.10.064>>.
- Magnesite, G., 2017a. *Profile | grecianmagnesite*. [online] Available at: <<http://www.grecianmagnesite.com/>> [Accessed 4 Nov. 2017].
- Magnesite, G., 2018b. *Profile | grecianmagnesite*. [online] Available at: <<http://www.grecianmagnesite.com/>> [Accessed 16 Mar. 2018].
- Maguire, J. and Peng, D., 2015. How to Identify Critical Quality Attributes. pp.1–40.
- Mahony, N.O., Murphy, T., Mahony, N.O., Murphy, T., Panduru, K., Riordan, D. and Walsh, J., 2016a. Adaptive process control and sensor fusion for process analytical technology. *2016 27th Irish Signals and Systems Conference (ISSC)*, (June).
- Mahony, N.O., Murphy, T., Panduru, K., Riordan, D. and Walsh, J., 2016b. Adaptive process control and sensor fusion for process analytical technology. *2016 27th Irish Signals and Systems Conference (ISSC)*.
- Mahony, N.O., Murphy, T., Panduru, K., Riordan, D. and Walsh, J., 2016c. Smart Sensors for Process Analytical Technology. *2016 IEEE International Conference on Advanced Intelligent Mechatronics (AIM)*, 2020(637232).
- Maitra, S. and Yan, J., 2008. Principle Component Analysis and Partial Least Squares : *Not A Paper*, pp.79–90.
- Majors, R.E., 2013. *Sampling Preparation Fundamentals For Chromatography*. 1st ed. Agilent Technologies.
- Malar, K. and Kamaraj, N., 2014. Development of smart transducers with IEEE 1451.4 standard for Industrial automation. In: *2014 IEEE International Conference on Advanced Communications, Control and Computing Technologies*. IEEE, pp.111–114.
- Malvern-Panalytical, 2017. *Malvern Mastersizer 2000 particle size analyzer*. [online] Available at: <<https://www.malvern.com/en/support/product-support/mastersizer-range/mastersizer-2000>> [Accessed 14 Nov. 2017].
- Maslaton, R., 2012. Resource Scheduling in QC Laboratories. 32(5), pp.1–5.
- MBN, 2017a. *MBN Nanomaterialia | Materials for Industry, Research and innovation*. [online] Available at: <<http://www.mbn.it/eng/>> [Accessed 30 Oct. 2017].
- MBN, 2018b. *MBN Nanomaterialia | Materials for Industry, Research and innovation*. [online] Available at: <<http://www.mbn.it/eng/>> [Accessed 16 Mar. 2018].

MCB University Press., 1981. *Sensor review*. [online] MCB University Press. Available at: <<http://www.ingentaconnect.com/content/mcb/087/2002/00000022/00000004>> [Accessed 4 Sep. 2018].

Mccarthy, W.J., Magnuson, E.J., Nicolet, T. and Solutions, I., n.d. Measurement of samples by Transmission Spectroscopy with the Antaris FT-NIR Analyzer. (Figure 4), pp.4–5.

Measurement, F., 2000. Flow measurement. *Source*, pp.47–59.

Megara, 2017a. *Megara Resins | A diversified manufacturer of chemical raw materials*. [online] Available at: <<http://www.megararesins.com/>> [Accessed 4 Nov. 2017].

Megara, 2018b. *Megara Resins | A diversified manufacturer of chemical raw materials*. [online] Available at: <<http://www.megararesins.com/>> [Accessed 16 Mar. 2018].

Meier, R., Salomatin, J., Happel, J., Korblein, G., Schlothauer, M. and Kleinebudde, P., 2016. Monitoring of continuous powder feeding by a microwave sensor - tackling problems of gravimetric feeders. *10th World Meeting on Pharmaceuticals, Biopharmaceuticals and Pharmaceutical Technology, Glasgow, 2016*.

MIC, 2015. *M2 - MassFlowmeter*.

MIC, 2017. *Flowmeter*. [online] Available at: <<http://www.mic-worldwide.com/en/products/non-coal/massflow.html>> [Accessed 19 Oct. 2017].

Micro-Epsilon, 2016. Instruction Manual thermoMETER CT. *Micro-Epsilon*.

Micro-Epsilon, 2017a. *Color measurement of tablets in pharmaceutical production*. [online] Available at: <http://www.micro-epsilon.com/applications/branch/medizintechnik/Farbmessung_von_Tabletten/?sLang=en> [Accessed 8 Oct. 2017].

Micro-Epsilon, 2018b. *Infrared sensors for non-contact temperature measurement | Micro-Epsilon America*. [online] Available at: <<https://www.micro-epsilon.com/temperature-sensors/>> [Accessed 16 Feb. 2018].

Misra, N.N., Sullivan, C. and Cullen, P.J., 2015. Process Analytical Technology (PAT) and Multivariate Methods for Downstream Processes. *Current Biochemical Engineering*, 2, pp.4–16.

Mohankumar, D., 2017. *Photodiode Design Note*. [online] Available at: <<http://www.electroschematics.com/4129/photodiode-design-note/>> [Accessed 15 Oct. 2017].

Morrissey, M., n.d. *Can you go with the Flow? Solids Flowmeters for Industrial Applications | bulk solids handling*. [online] Available at: <<https://pdfs.semanticscholar.org/d7e8/bb19ea454432b239897f218843877113678e.pdf>>.

Murphy, T., Mahony, N.O., Panduru, K., Riordan, D. and Walsh, J., 2016a. Inertia Sensing for Bulk Solid Measurement in Process Analytical Technology Systems. *International Control Systems Technology ICST China 2016*, 1(1), pp.1–6.

Murphy, T., O' Mahony, N., Panduru, K., Riordan, D. and Walsh, J., 2016b. Pharmaceutical manufacturing and the quality by design (QBD), process analytical technology (PAT) approach. *Irish Systems and Signals Conference 2016*, pp.1–7.

Narayanan, H., Product, S. and Spectroscopy, M., n.d. The Versatility of Fiber Optic Probes for Polymer Production Process Monitoring Advantages of Fiber Optic Probes Types of NIR Probes.

Nave, R., 2017. *Total Internal Reflection*. [online] Available at: <<http://hyperphysics.phy->

astr.gsu.edu/hbase/phyopt/totint.html> [Accessed 8 Oct. 2017].

Nestler, M., Demmler, M., Dunger, T., Rost, D. and Zeuner, M., 2011. Yield improvement by localized trimming in semiconductor and MEMS manufacturing. In: *Semiconductor Conference Dresden (SCD), 2011*. pp.1–4.

Neutrium, 2012. *Pressure Loss from Fittings*. [online] Fluid Flow. Available at: <https://neutrium.net/fluid_flow/pressure-loss-from-fittings-expansion-and-reduction-in-pipe-size/> [Accessed 4 Feb. 2018].

Nordic Sugar, n.d. A world of sugar.

O'Mahony, N., Murphy, T., Panduru, K., Riordan, D. and Walsh, J., 2016a. Acoustic and Optical Sensing Configurations for Bulk Solids Mass Flow Measurements. *International Control Systems Technology ICST China 2016, 2020*(637232), pp.1–6.

O'Mahony, N., Murphy, T., Panduru, K., Riordan, D. and Walsh, J., 2016b. Fibre-optic sensors for Process Analytical Technology. In: *33rd International Manufacturing Conference*. [online] Limerick: IMC33 University of Limerick. Available at: <http://ulsites.ul.ie/imc33/sites/default/files/IMC33_Conference_Programme.pdf>.

Ocean-Optics, 2018. *Ocean FX Spectrometers for High Speed Acquisition - Ocean Optics*. [online] Available at: <https://oceanoptics.com/ocean-fx-spectrometer-high-speed-acquisition/?gclid=EAlalQobChMlglfChnN_L2AIVxLftCh1fQwylEAAAYASAAEgJ_ePD_BwE> [Accessed 9 Jan. 2018].

Ocean Optics, 2013. Fibers and Probes.

Ocean Optics, 2018. *74-series Collimating Lenses - Ocean Optics*. [online] Available at: <<https://oceanoptics.com/product/collimating-lens-74-series/>> [Accessed 11 Feb. 2018].

OceanOptics, 2010. NIRQuest - Installation and Operation Manual. [online] Available at: <www.oceanoptics.com>.

Omega, 2018. *Fixed Infrared Temperature Sensor | Fixed Infrared Transmitter | Temperature Sensor | Omega*. [online] Available at: <<https://www.omega.com/pptst/OS212.html#order>> [Accessed 15 Feb. 2018].

Opitz, S., 2014a. *SPIRE 1 – 2014 – Integrated Process Control Title : Robust and affordable process control technologies for improving standards and optimising industrial operations Acronym : ProPAT Grant Agreement No : 637232*. Leeds.

Opitz, S., 2014b. *SPIRE 1 – 2014 – Integrated Process Control Title : Robust and affordable process control technologies for improving standards and optimising industrial operations Acronym : ProPAT Grant Agreement No : 637232*. 1, pp.1–52.

Optics, M., 2013. Optical Fiber Sensors Guide.

Palmer, E., 2014. *FiercePharma Manufacturing*. [online] Supply Chain. Available at: <<http://www.fiercepharmamanufacturing.com/story/amgen-opens-200m-continuous-purification-plant-singapore/2014-11-20>> [Accessed 16 Jan. 2016].

Palmer, E., 2016. *FiercePharma Manufacturing*. [online] Fiercepharma. Available at: <<http://www.fiercepharmamanufacturing.com/story/gsk-doubles-down-singapore-continuous-processing-plant/2015-06-29>> [Accessed 16 Jan. 2016].

Particle-Sciences, 2012. Process Analytical Technology (PAT). 7.

- Particle Sciences, 2011. Sampling of Powders. *Technical Brief 2011*, [online] 5. Available at: <http://www.particlesciences.com/docs/technical_briefs/TB_2011_5.pdf>.
- Pasquini, C., 2003. Near infrared spectroscopy: Fundamentals, practical aspects and analytical applications. *Journal of the Brazilian Chemical Society*, 14(2), pp.198–219.
- Peeran, M., 2005. *Comparison of Raman and IR Spectroscopy*. [online] Chemvista.org. Available at: <<http://www.chemvista.org/ramanIR4.html>> [Accessed 3 Mar. 2016].
- Penirschke, A., Puentes, M., Maune, H., Schussler, M., Gaebler, A. and Jakoby, R., 2009. Microwave mass flow meter for pneumatic conveyed particulate solids. In: *IEEE Instrumentation and Measurement Technology Conference, 2009. I2MTC '09*. pp.583–588.
- Pharmlabs, 2018. *The Compounding Lab*. [online] Available at: <<https://pharmlabs.unc.edu/labs/powders/properties.htm>> [Accessed 3 Feb. 2018].
- Piriou, J., Elissondo, B., Hertschuh, M. and Ollivier, R., 2012. Control Strategy as the Keystone of the Product Lifecycle , from Product / Process Understanding to Continuous Process Verification and Improvement. *Pharmaceutical Engineering*, 32(1), p.8.
- PO-Laboratories, 2018. *Refractive Index of Powders*. [online] Available at: <https://www.po-labs.com/main/page_facilities_refractive_index_of_powders.html> [Accessed 28 Aug. 2018].
- Polytech, 2007. Process Control Using NIR Spectroscopy. *Polytech*, pp.1–4.
- Portoghese, F., Berruti, F. and Briens, C., 2008. Continuous on-line measurement of solid moisture content during fluidized bed drying using triboelectric probes. *Powder Technology*, 181(2), pp.169–177.
- Price, W., 2012. Problems of Innovation-Deficient Pharmaceutical Manufacturing. pp.1–3.
- Price, W., 2014. Making Do in Making Drugs: Innovation Policy and Pharmaceutical Manufacturing. *Boston College Law Review*, [online] 55(2), p.491. Available at: <<http://lawdigitalcommons.bc.edu/bclr/vol55/iss2/5%5Cnhttp://lawdigitalcommons.bc.edu/bclr/vol55/iss2/5/>>.
- Princeton.edu, 2018. *Bernoulli's Equation*. [online] Available at: <https://www.princeton.edu/~asmits/Bicycle_web/Bernoulli.html> [Accessed 16 Mar. 2018].
- ProPAT, 2017. *PROPAT – INTEGRATED PROCESS CONTROL*. [online] Available at: <<http://pro-pat.eu/>> [Accessed 1 Apr. 2017].
- Prosys.ie, 2017. *Top Powder Sampler - ProSys*. [online] Available at: <<http://www.prosys.ie/sampling-systems/top-powder-sampler/>> [Accessed 2 Jan. 2017].
- PSG, 2017. *Volumetric and Gravimetric Feeding - Powder Process-Solutions*. [online] Available at: <<https://www.powder-solutions.com/processing/main/process-designs/volumetric-and-gravimetric-feeding/>> [Accessed 19 Oct. 2017].
- Purutyan, H. and Carson, J., 2006. Predicting, diagnosing, and solving mixture segregation problems. *Powder and Bulk Engineering*. [online] Available at: <http://www.powderbulk.com/enews/sponsor_whitepaper/jenike.pdf>.
- Quadro, 2017. Comil Pharmaceutical Applications. *Engineering*, [online] pp.1–4. Available at: <https://www.quadro.com/sites/quadro/files/Comil_Pharm_Applications.PDF>.
- Raytek, 2017. Raytek Infrared Sensor.
- Reich, G., 2005. Near-infrared spectroscopy and imaging: Basic principles and pharmaceutical

applications. *Advanced Drug Delivery Reviews*, 57(8), pp.1109–1143.

Ritchie, G., 2017. *General Chapters: NEAR-INFRARED SPECTROPHOTOMETRY*. [online] Available at: <http://www.pharmacopeia.cn/v29240/usp29nf24s0_c1119.html> [Accessed 15 Oct. 2017].

Romero-Torres, S., Huang, J. and Hernandez-Abad, P.E., 2009. *Practical Considerations on PAT Analyzer Selection - Raman vs. NIR Spectroscopy* |. [online] American Pharmaceutical Review - The Review of American Pharmaceutical Business & Technology. Available at: <<http://www.americanpharmaceuticalreview.com/Featured-Articles/117780-Practical-Considerations-on-PAT-Analyzer-Selection-Raman-vs-NIR-Spectroscopy/>> [Accessed 3 Mar. 2016].

Sampling-Systems, 2017. *Sampling Systems - In-Line Samplers*. [online] Available at: <http://www.sampling.com/in_line_samplers.html> [Accessed 2 Jan. 2017].

Sampling.UK, 2018. *Sampling Systems News February 2013 - sterile Food Scoops*. [online] Available at: <https://www.sampling.co.uk/news_1302a.html> [Accessed 3 Sep. 2018].

Schanda, J., Eppeldauer, G. and Sauter, G., n.d. Tristimulus Color Measurement of Self-Luminous Sources. In: *Colorimetry*. [online] Hoboken, NJ, USA: John Wiley & Sons, Inc., pp.135–157. Available at: <<http://doi.wiley.com/10.1002/9780470175637.ch6>> [Accessed 4 Sep. 2018].

ScienceLab.com, 2013. Metoclopramide HCl Material Safety Data Sheet. *Science Lab*, pp.1–5.

Sensuron, 2016. Introduction to Fiber Optic Sensing. pp.1–39.

Sentry, 2017a. *Powder sampler / for solids / for granule / automatic - HPR - Sentry Equipment Corp.* [online] Available at: <http://www.directindustry.com/prod/sentry-equipment-corp/product-11839-1805864.html?utm_source=ProductDetail&utm_medium=Web&utm_content=SimilarProduct&utm_campaign=CA> [Accessed 2 Jan. 2017].

Sentry, 2017b. *Samplers | Powder/Bulk Solids*. [online] Available at: <<http://www.powderbulksolids.com/article/samplers>> [Accessed 2 Jan. 2017].

Shrestha, B., Basnett, H. and Raj, P., 2009. Process Analytical Technology: A Quality Assurance Tool. *Research J. Pharm. and Technology*, [online] 2(2), pp.225–227. Available at: <[http://rjptonline.org/RJPT_2\(2\)_2009/2-183.pdf](http://rjptonline.org/RJPT_2(2)_2009/2-183.pdf)>.

Siemens, n.d. Solids Flow Meters - Weighing and Batching Systems - Siemens. [online] Available at: <<http://w3.siemens.com/mcms/sensor-systems/en/weighing-systems/solids-flow-meters/Pages/solids-flow-meters.aspx#w2gHTM-990x1400-https://webservices.siemens.com/guidedselection/powcms/?cmd=productoverview&lang=en&pid=f5893259-088a-4bea-91b7-8392e56febc6>> [Accessed 20 Oct. 2017].

Spectroscopy, N.I.R., 2013. NIR Spectroscopy : A guide to near-infrared spectroscopic analysis of industrial manufacturing processes. *Metrohm AG*, pp.1–46.

Status, C., Guidelines, D., Tech-, P.A. and Space, D., 2012. Quality by Design. 8.

Stellarnet, 2018. *Raman Spectrometers, Lasers, and Probes* | *StellarNet.us*. [online] Available at: <http://www.stellarnet.us/systems/raman-spectrometers-lasers-and-probes/?gclid=EAlaQobChMIklyFw-DL2AIVIRbTCh35oAovEAAAYASAAEgK6lvD_BwE> [Accessed 9 Jan. 2018].

Stone, K., 2018. *API (Active Pharmaceutical Ingredient)*. [online] What is an Active Pharmaceutical Ingredient. Available at: <<https://www.thebalance.com/what-is-api-active-pharmaceutical-ingredient-2663020>> [Accessed 5 Apr. 2017].

Strother, T., 2009. NIR and Raman : Complementary Techniques for Raw Material Identification.

Thermo Scientific.

Tecdas, 2018. *Sono Vario LD | Sensor Radar para humedad y temperatura en materiales con mediana densidad - IMKO - Humedad en Granos y Semillas*. [online] Available at: <<https://www.tecdas.com.bo/divisiones/caudal-nivel-presion-humedad-y-pesaje/humedad-1/humedad-en-granos-y-semillas/sono-vario-ld-sensor-radar-para-humedad-y-temperatura-en-materiales-con-mediana-densidad>> [Accessed 14 Feb. 2018].

Tetko, I. V.; Gasteiger, J.; Todeschini, R.; Mauri, A.; Livingstone, D.; Ertl, P.; Palyulin, V. A.; Radchenko, E. V.; Zefirov, N. S.; Makarenko, A. S.; Tanchuk, V. Y.; Prokopenko, V. V., 2005. *Partial Least Squares Program - Method Description*. [online] Virtual computational chemistry laboratory - design and description. Available at: <http://www.vcclab.org/lab/pls/m_description.html> [Accessed 25 Mar. 2018].

Thayer, 2017. *Thayer Powder Feeder™ Model PF-S-4 – Thayer Scale*. [online] Available at: <<http://www.thayerscale.com/product/pfs4/>> [Accessed 19 Oct. 2017].

Timeless-Tube, 2017. *Timeless Tube – Timeless Tube*. [online] Available at: <<http://www.timelesstube.com/>> [Accessed 12 Jan. 2017].

Tollifson, T., n.d. Online Reaction Monitoring of In-Process Manufacturing Samples by UPLC. pp.1–5.

Tongue, A., 2017. *Extrinsic vs Intrinsic Fiber Optic Sensors - Sensuron*. [online] Available at: <<http://www.sensuron.com/industry-news/extrinsic-vs-intrinsic-fiber-optic-sensors/>> [Accessed 8 Oct. 2017].

Tuchin, V. V, Chiou, A. and Heinemann, S., 2012. Part One Process Control and Quality Assurance. 3.

U3D, 2017. *U3D » Equipment*. [online] Available at: <https://umg.ucd.ie/u3d/?page_id=6> [Accessed 5 Mar. 2017].

Valves, A., n.d. Bulk Density Chart.

Weber, G., 2012. Influence of Temperature on the Compaction and Strength of Some Pharmaceutical Excipients. *Unknown*, pp.1–12.

Wei, J., Zhang, N., Wang, N., Lenhert, D., Neilsen, M. and Mizuno, M., 2005. Use of the “smart transducer” concept and IEEE 1451 standards in system integration for precision agriculture. *Computers and Electronics in Agriculture*, 48(3), pp.245–255.

WestPharma, 2016. *Posts about QTPP on westpharma*. [online] Available at: <<https://westpharma.wordpress.com/tag/qtpp/>> [Accessed 4 Mar. 2016].

Wilks, P., 2007. NIR vs Mid-IR – How to choose. *Spectroscopy*, 4, pp.32–34.

Willis, R.C., 2004. Process Analytical Technology. *Process Analytical Technology PAT regs are expected to help maximize drugmakers' efficiencies and profits.*, [online] (1), pp.21–22. Available at: <<http://pubs.acs.org/subscribe/archive/tcaw/13/i02/pdf/204regulations.pdf>>.

Wilson, D.H., 2001. How to troubleshoot and maintain your feeder. (December).

Wirth, T., Berlenbach, R., Zimmer, H.-E. and Brudel, M., 2009. Optimisation of Drying Processes in the Pharmaceutical Industry. *Apact 09*, (May), pp.1–4.

Wu, H., White, M. and Khan, M.A., 2011. Quality-by-Design (QbD): An integrated process analytical technology (PAT) approach for a dynamic pharmaceutical co-precipitation process characterization and process design space development☆. *International Journal of Pharmaceutics*, [online] 405(1–2), pp.63–78. Available at: <<http://linkinghub.elsevier.com/retrieve/pii/S037851731000894X>>.

Xi, F., He, J. and Liu, Z., 2010. Adaptive fast consensus algorithm for distributed sensor fusion. *Signal Processing*, 90(5), pp.1693–1699.

Yan, Y., 1996. Mass flow measurement of bulk solids in pneumatic pipelines. *Measurement Science and Technology*, 7(12), pp.1687–1706.

Yu, F. and Yin, S., 2002. Fiber optic sensors. 2(6), p.Chapter 2.